

Wearable and Flexible Electronics

1 ORGANIC ELECTRONICS

1.1	Conjugated polymers.....	4
1.2	Atomic Orbitals.....	7
1.3	Chemical Bonds	9
1.4	Molecular orbitals	10
1.5	The Carbon Atom.....	15
1.6	Resonance and delocalization.....	19
1.7	The Band Gap in conjugated molecules.....	22
2	Materials.....	28
2.1	Oligomers vs Polymers	28
2.2	Pentacene.....	28
2.3	Tetracene	29
2.4	6,13-Bis(triisopropylsilylethynyl)pentacene TIPS Pentacene	30
2.5	α -sexithiophene (α -6T)	30
2.6	α,ω -dihexylsexithiophene (α,ω -DH6T).....	31
2.7	Fullerene - C ₆₀	32
2.8	poly (3-hexylthiophene) P3HT	32
2.9	PEDOT:PSS.....	35
3	Doping in Organic Materials.....	39
3.1	Free charge carriers in conjugated polymers.....	41
3.2	The Polaron	45
3.3	Charge transport in organic materials: Inorganic vs Organic.....	47
3.4	A consideration on charge carriers in organic semiconductors.....	50
3.5	Charge Transport Models	51
3.5.1	The small polaron model.....	51
3.5.2	Hopping Transport.....	53
3.5.3	Multiple Trapping and Thermal Release (MTR).....	56
4	Charge injection into organic semiconductor	60
4.1	Mott-schottky model and deviations	60
4.2	Strong Electron Acceptors	71
4.3	The case of conductive polymers	72

5	Organic Field Effect Transistors (OFETs).....	76
5.1	OFET Model.....	76
5.2	Output and transfer characteristics.....	82
5.3	Typical OFETs electrical parametrs	85
5.4	The role of OH groups.....	86
5.5	using SAM for tuning the OFETs threshold voltage	87
5.6	Non idealities in OFETs.....	89
5.6.1	Charge trapping.....	89
5.6.2	Contact Resistance	93
5.6.3	The effect of moisture on OFET performance	96
5.6.4	The effect of oxygen	98
5.7	OFETs architectures.....	99
5.8	Deposition Techniques in Organic Electronics.....	100
5.8.1	Spin Coating.....	101
5.8.2	Thermal Evaporation.....	101
5.8.3	Patterning of the electrodes.....	102
5.8.4	Photolithography.....	103
5.8.5	Soft Lithography: Overview.....	105
5.9	Contact printing techniques.....	110
5.10	Non-contact printing techniques.....	113
5.11	Inkjet printing technique.....	115
6	Low Voltage Organic Transistors	118
6.1	The Organic Electrochemical Transistor.....	123
6.1.1	PEDOT:PSS based electrochemical transistors	124
6.2	Electrolyte-Gated Organic Field Effect Transistor (EGOFET).....	127
6.2.1	Ionic Conductivity and Transport.....	130
6.2.2	Electric Double Layers	131
6.2.3	EGOFET Principle of Operation.....	132
6.2.4	Polyelectrolyte-Gated OFET Characteristics.....	133
7	The Organic Charge-Modulated Field-Effect Transistor.....	135
7.1	DNA sensing	137
7.2	Cellular electrical and pH sensing.....	138
7.3	Pressure and temperature sensing – Artificial Skin.....	142
8	Effect of mechanical deformation in Organic FETs.....	144

9	Solar Cells.....	151
9.1	Crystalline and multicrystalline silicon	151
9.2	Inorganic thin film.....	152
9.3	Emerging technologies	152
9.4	Working Principle.....	154
9.5	Open-circuit voltage	158
9.6	Short-circuit current.....	158
9.7	Fill-factor	159
9.8	Power conversion efficiency	160
9.9	Spectral response.....	161
9.10	External quantum efficiency	162
10	Organic Solar Cells.....	164
10.1	Photon absorption.....	166
10.2	Exciton diffusion.....	167
10.3	Charge separation.....	168
10.4	Charge transport.....	168
10.5	Charge collection.....	169
10.6	Architectures for Organic Solar Cells.....	170

1. Organic Electronics

In the late 70's (1977) a group of researchers, Heeger, MacDiarmid, and Shirakawa discovered the conducting properties of polymers. They demonstrated that it is possible to obtain a conducting polymer by doping polyacetylene with arsenic pentafluoride (AsF_5). This discovery, which earned them the Nobel Prize in chemistry, paved the way for the new field of Organic Electronics. Intrinsic conducting and semiconducting plastic materials, either electrons (n-type) or holes (p-type) transport with band like structure, can now be made. The main advantages of employing this new generation of materials for electronics applications lie in the possibility of being processed with very easy and low cost techniques. Indeed, organic materials, either oligomers or polymers, can be deposited by various methods such as thermal evaporation in vacuum, molecular beam deposition, spin coating, and patterned with very low cost techniques as photolithography, screen printing, inkjet printing and soft lithography suitable for mass production over a very large scale of Plastic Electronics devices. Moreover, due to their intrinsic mechanical properties they opened the way for unusual applications. In fact, organic semiconductors, being plastic materials, are very flexible; they can be easily deposited on unusual substrates such as paper, fabric or 3D structures which are not suitable for the most common inorganic materials as silicon. The possibility of fabricating flexible electronics is now a reality; flexible smart tags, displays, integrated circuits solar cells etc...are now available at the state of the art.

1.1 CONJUGATED POLYMERS

Let's make a little flash back about chemistry, valence Electrons are the electrons which are placed in the outer shell of an atom, and determine the properties of that element.

Number of electrons in the outer shell \rightarrow valence of the element

The periodic table is characterized by 7 rows, each row starts with an element having 1 valence electron and ends up with an element having its outer shell full. For instance, hydrogen has only one electron, whereas helium has two electrons. In all chemical

reactions an atom tends to acquire or to give electrons in order to give rise to a more stable structure (molecule).

- Electropositive elements use to give electrons → up to 4 valence electrons
- Electronegative elements hav from 4 to 8 valence electrons they want to acquire electrons.

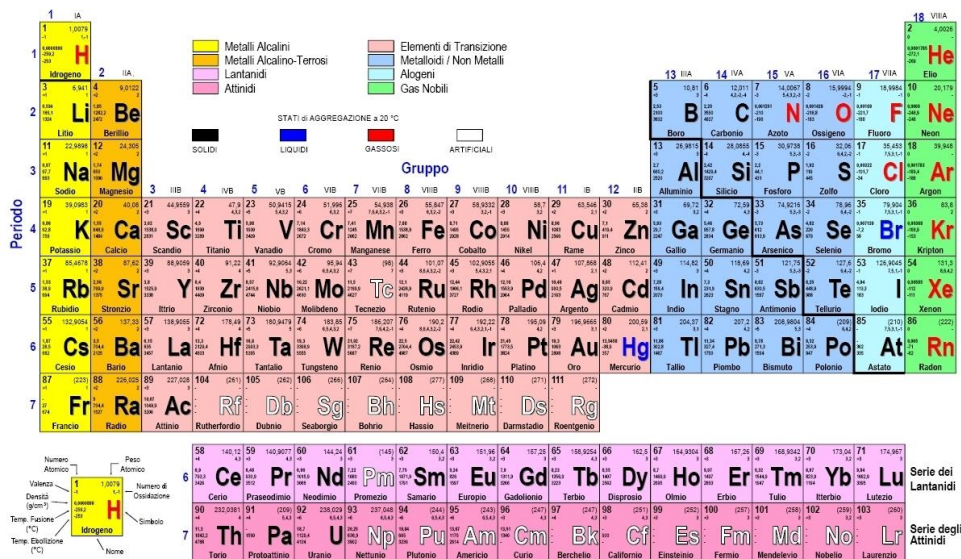


Figure 1.1: the table of elements

The solution of the radial part of the Schrodinger equation for the hydrogen atom allowed us to obtain the possible energies.

We have introduced two integer numbers

$$n = 1, 2, 3, \dots$$

$$l = 0, 1, 2, \dots, n - 1$$

For the fundamental state ($n = 1$), there will be only one l value, and the energy will be -13.6 eV (ionization energy for hydrogen). The first excited state ($n = 2$) will give place to two l values ($l = 0$ ed $l = 1$), but only one energetic level (in E_n depends only on n).

Degenerate energy levels have same energy but different wave functions!

The angular part solution of Schrodinger equation led us to a third quantic number called $m = -l, -l+1, \dots, 0, \dots, l-1, l$ (magnetic momentum number).

Therefore:

Given a certain n , there will be a single energetic level, but n different l values and $2l+1$ different m values

Moreover, we also have the spin number that can acquire only two values $+1/2$ e $-1/2$.

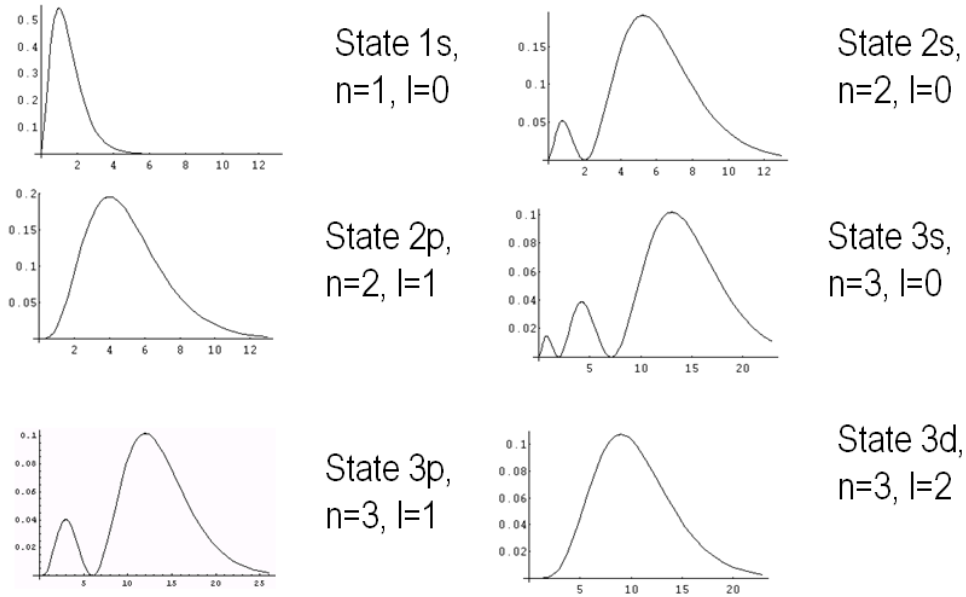


Figure 1.2: wavefuntions of different orbitals

Orbital wave functions

$l=0 \rightarrow$ s states ($m=2l+1=1$) number of s type orbitals

$l=1 \rightarrow$ p states $\rightarrow m= 3$ number of p type orbitals

$l=2 \rightarrow$ d states $\rightarrow m= 5$ number of d type orbitals

$l=3 \rightarrow$ f states $\rightarrow m= 7$ number of f type orbitals

Summarizing:

- n defines the energy (shell)
- l defines the geometry of the orbital (s, p, d, f)
- m defines its spatial position: only one s orbital, 3 different p orbitals, 5 d orbitals and 7 f orbitals
- s defines the spin momentum

•

Aufbau rules

1) Principle of minimum energy

Electrons tends to occupy a free orbital with the lowest energy

2) Pauli exclusion principle

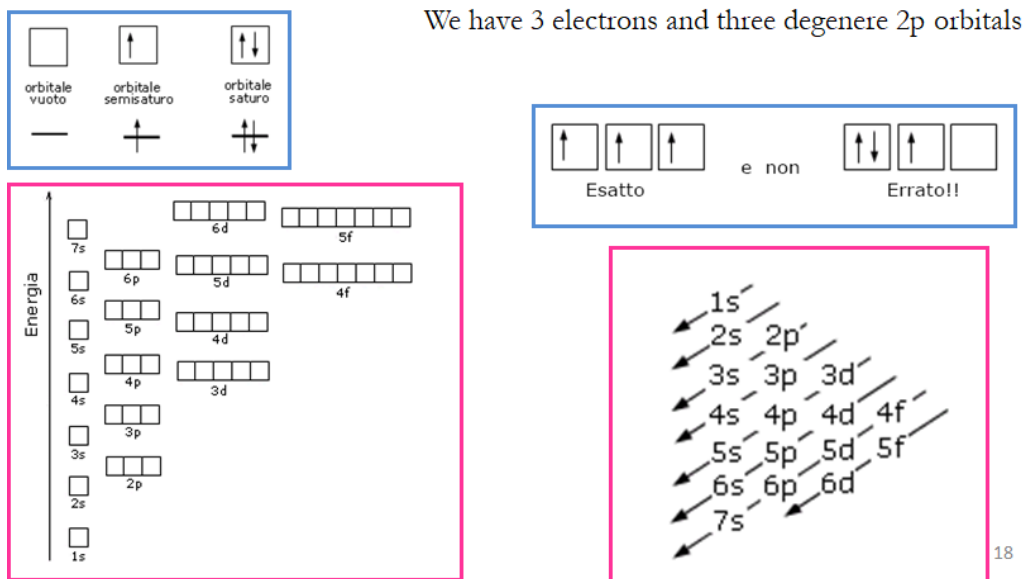
Each orbital can be occupied by only two electrons with antiparallel spin momentum

One electron can have only two different spin momenta

The spin momentum is represented by an arrow, facing upwards or downwards

3) Hund's principle of multiplicity

If there are more than one orbitals with the same energy (degenerate orbitals) the electrons will try to occupy them separately with parallel spin momentum until all the degenerate orbitals have been partially filled



1.2 ATOMIC ORBITALS

The s wave functions $\Psi(s)$ are spheric, meaning that the probability of finding one electron is equal in every direction, but gets smaller with the distance.

The s orbital, as every orbital is infinite, its squared modulus gives the probability to find an electron in the space.

$\Psi(s)^2$ maximum at the center

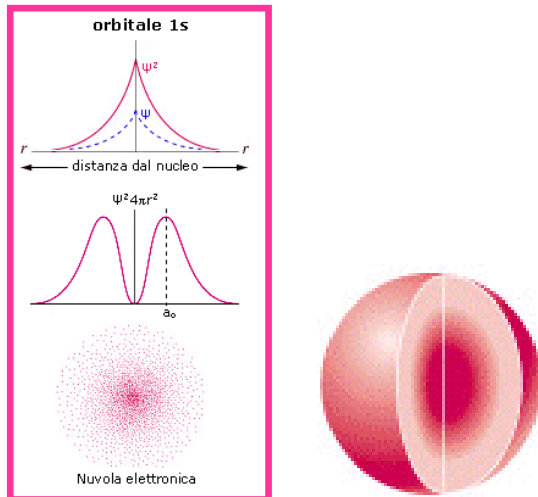


Figure 1.3: s orbitals

The p orbitals are cylindrical, there is a preferential direction.

There are three p orbitals for each energetic level and they are perpendicularly oriented into the three axes:

p_x , p_y , p_z

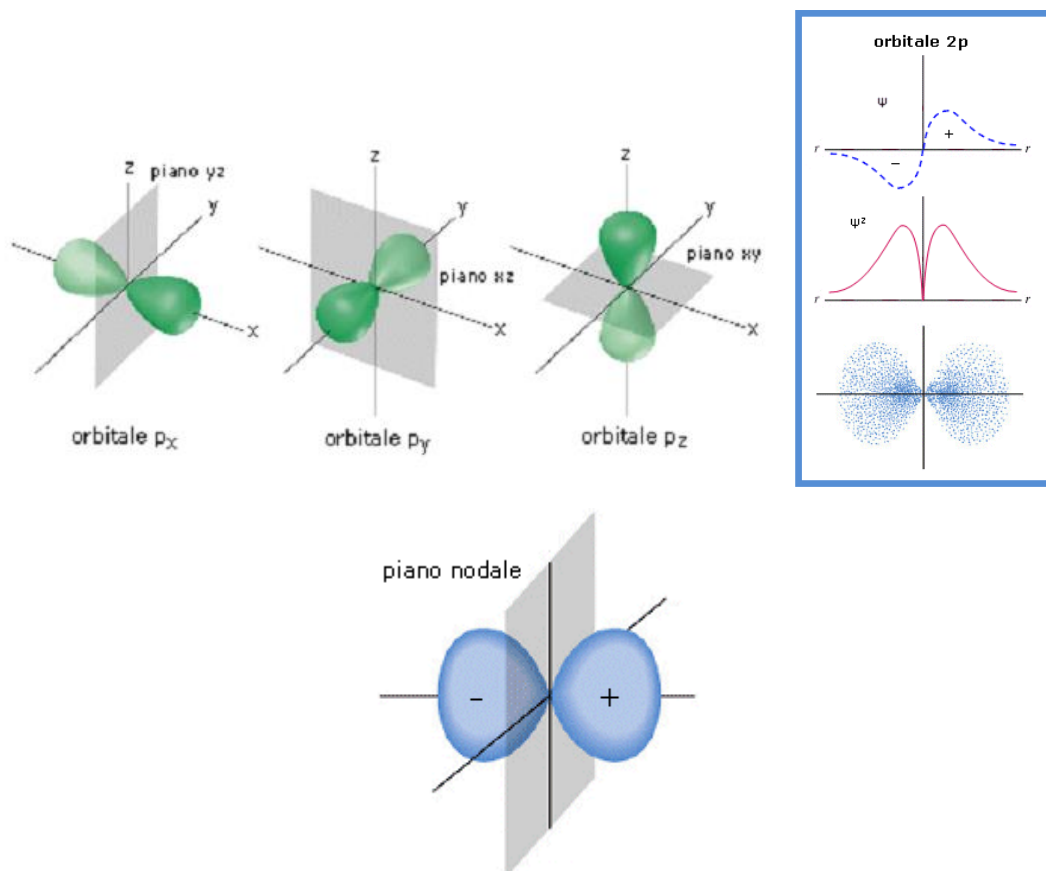


Figure 1.4: p orbitals

1.3 CHEMICAL BONDS

Valence Bond Theory (VB)

Overlapping of atomic orbitals. Each orbital has one electron, the two orbitals share their electron in order to have a pair. The two wave functions combines together in order to have a new wave function, a new orbital, where the two electron can move.

The new orbital is shared by the two atoms and hosts the two electrons with antiparallel spin momentum.

σ and π bonds

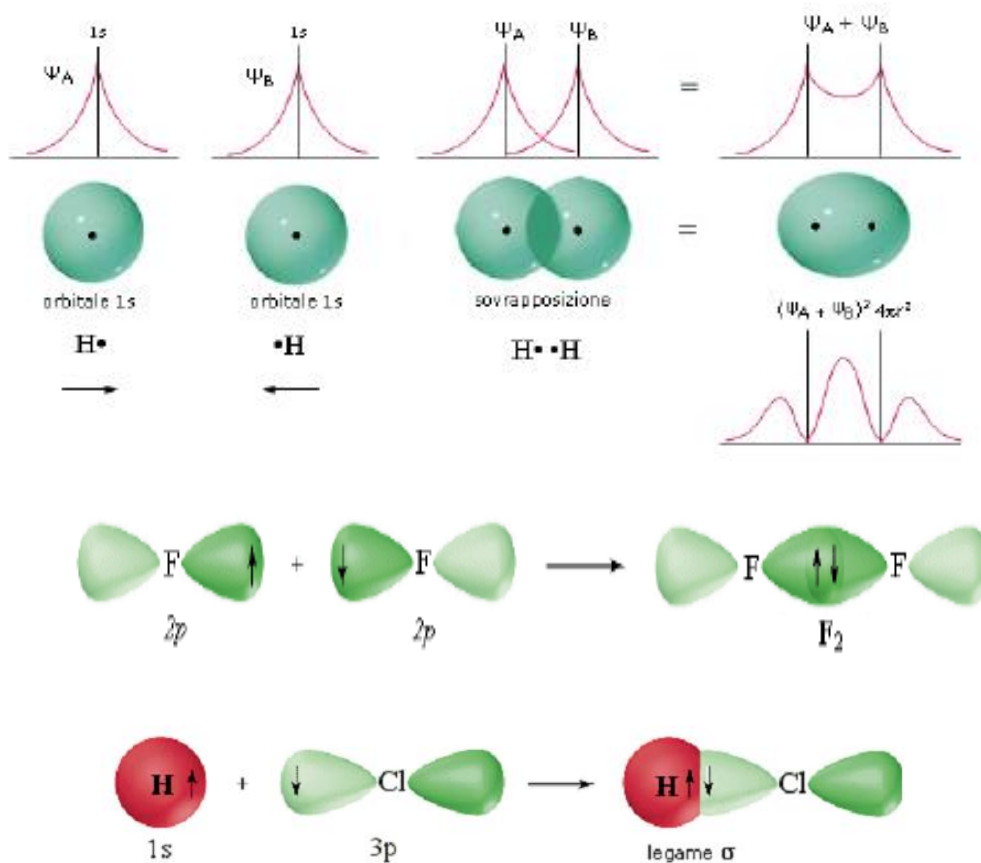


Figure 1.4: examples of sigma bonds

Sometimes double or triple bonds are required, therefore, it could happen that p orbitals which are perpendicularly oriented, with respect of the first two which have already formed a σ bond, can overlap laterally (along the smaller axes).

This bond is called π bond and its is energetically less stable, due to the lower overlapping between the two involved orbitals.

Internuclear axis $\rightarrow \sigma$ bond

Out of axis $\rightarrow \pi$ bond

When a covalent double bond takes place there will be a first σ bond in the direction between the two nuclei, and a second π bond that will take place above and below the previous one and will be much less stable.

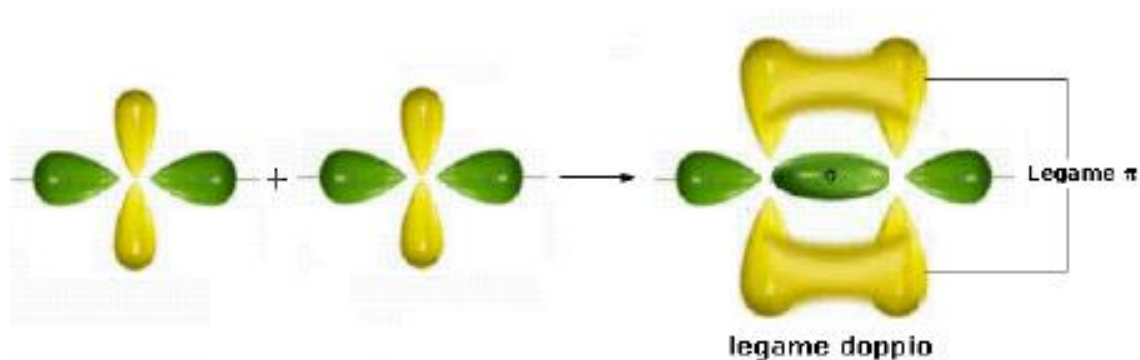


Figure 1.5: exemple of pi bonds

1.4 MOLECULAR ORBITALS

The molecular orbitals theory is quantum-mechanics theory that allows describing some effects that cannot be described with the Valence Band theory.

The combination of different atomic orbitals leads to the formation of new molecular orbitals (MO). The electrons placed in the MOs are delocalized in the whole molecule and not to the single atoms involved in the bond.

In other words the MOs theory is a polycentric theory that states that the electrons involved in the molecular orbitals are affected by the attraction forces of all the nuclei in the molecule.

L.C.A.O. Linear Combination of Atomic Orbitals

The wave functions of the molecular orbitals are obtained by a linear combination of the atomic orbitals wave functions, meaning that the two wave functions can give rise to constructive interference (sum) or destructive interference (difference)

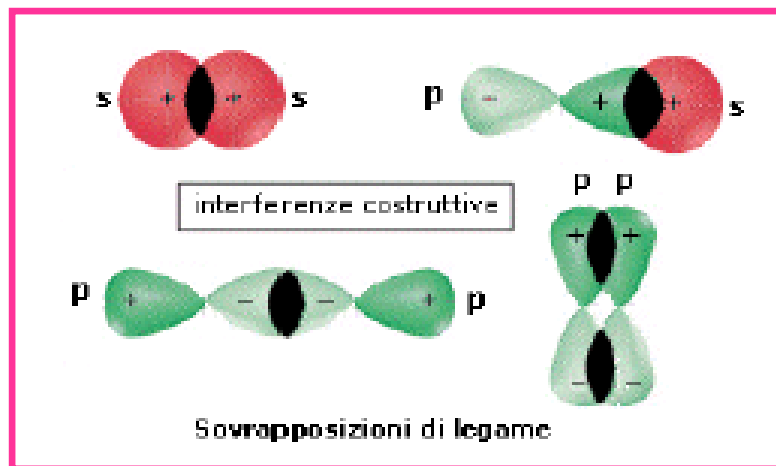
For each bond two molecular orbitals are therefore generated:

- Two wave functions
- Two energetic levels

Antibonding Molecular Orbital Ψ^*

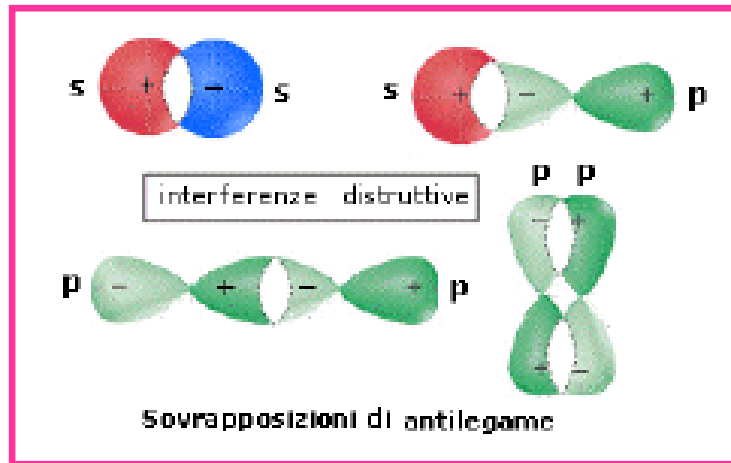
The molecular orbitals generated by the sum of two atomic orbitals has a smaller energy compared to the original ones, with a higher electronic density in between the two atoms nuclei \rightarrow Bonding Molecular Orbital Ψ_B

To obtain a bonding molecular orbital thw two atomic orbitals interact in phase (same sign of the wave funtion) giving place to constructive interference.



The molecular orbital generated by the difference between the two original atomic orbitals has a higher energy and the electronic density between the two nuclei axis is zero (node)

Opposite phase (opposite sign of the wave function) destructive interference



The bonding between atoms is stronger if the most of the electrons are allocated in the bonding molecular orbitals, lower energy, more stable.

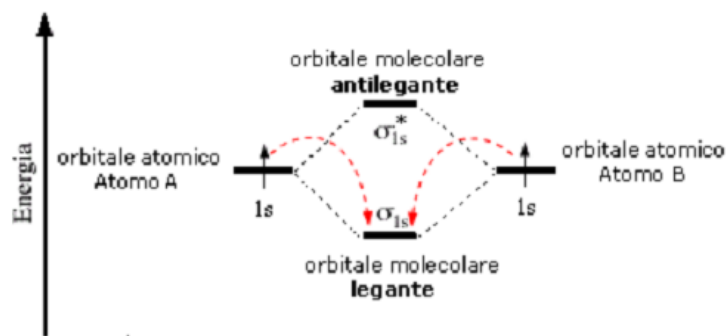


Figure 1.6: bonding ant antibonding orbitals

Let's make a very easy example and let's consider two hydrogen atoms which are forming an H₂ molecule. At first we sum the two 1s orbitals, obtaining the bonding molecular orbital $\Psi\sigma_{1s}$. In this case the Ψ (and also Ψ^2) value increases in the region between the two nuclei.

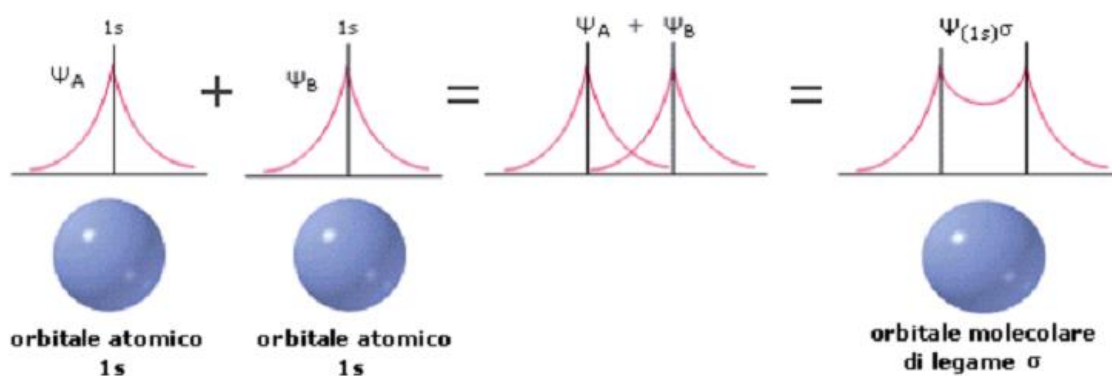


Figure 1.7: sigma bonding molecular orbitals

Afterwards, we consider the difference between the two wave functions $1s$, obtaining an antibonding molecular orbital Ψ_{σ^*1s} , it will have a nodal plane between the two nuclei. In this case Ψ (and also Ψ^2) value decreases down to zero in the region between the two nuclei.

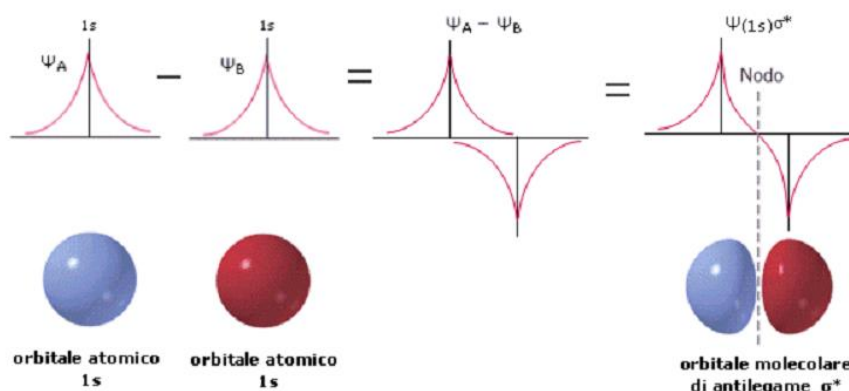


Figure 1.8: sigma antibonding molecular orbitals

p orbitals can interact in two different ways:

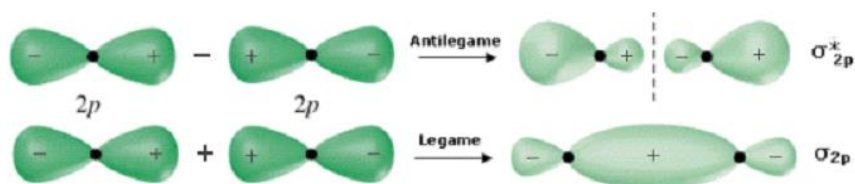


Figure 1.9: sigma bonding and antibonding molecular orbitals

Along the internuclear axis, forming σ e σ^* molecular orbitals

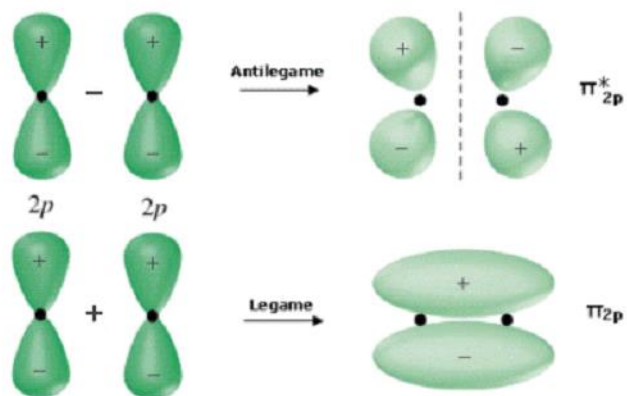


Figure 1.10: pi bonding and antibonding molecular orbitals

1.5 THE CARBON ATOM

The key element on organic compounds is the Carbon atom, generally bonded to other atoms such as Hydrogen, Nitrogen, Oxygen, Sulphur, Phosphor etc... The carbon atom is characterized by 6 electrons distributed as $1s^1 2s^2 2p^2$. It is very common that one of the two $2s^2$ electrons can jump into the free $2p_z$ orbital, thus leading to four valence electrons, $2s 2p_x 2p_y 2p_z$.

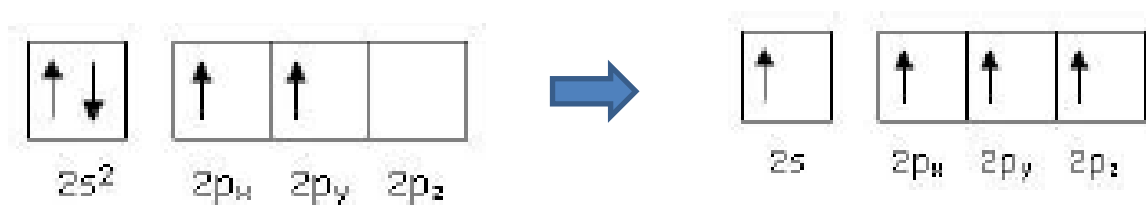


Figure 1.11: electronic configuration of the carbon atom

In order to give rise to more stable structures, forming bonds with other atoms, the atomic orbitals could change their wave function and recombine, giving rise to so called hybrid molecular orbitals.

Hybridization happens only among valence orbitals (outer shell) with very similar energy. Hybrid orbitals have the same energy and are differently oriented into the space in order to minimize their interaction.

The combination of one s orbital and one p orbital give rise to two hybrid sp orbitals. sp orbitals lay on the same plane and are shifted by 180°.

The other two p orbitals which are not hybridized will be oriented perpendicularly with respect to the two hybridized ones (y and z axis).

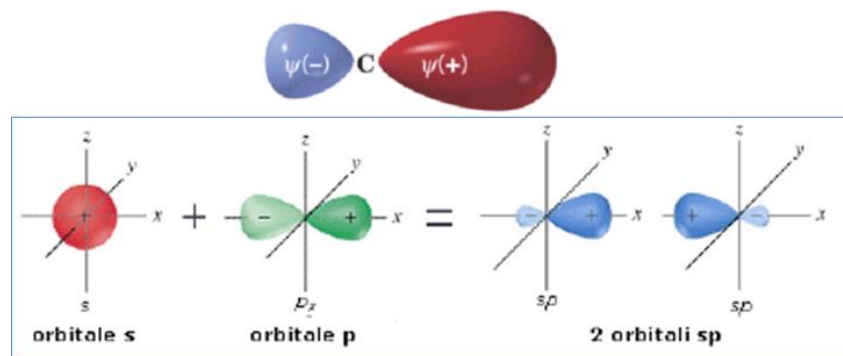


Figure 1.12: sp hybridization

The combination of one s orbital and two p orbitals gives rise to three sp^2 orbitals on the same plane but shifted by 120° and the remaining not hybridized p orbital will be perpendicularly oriented.

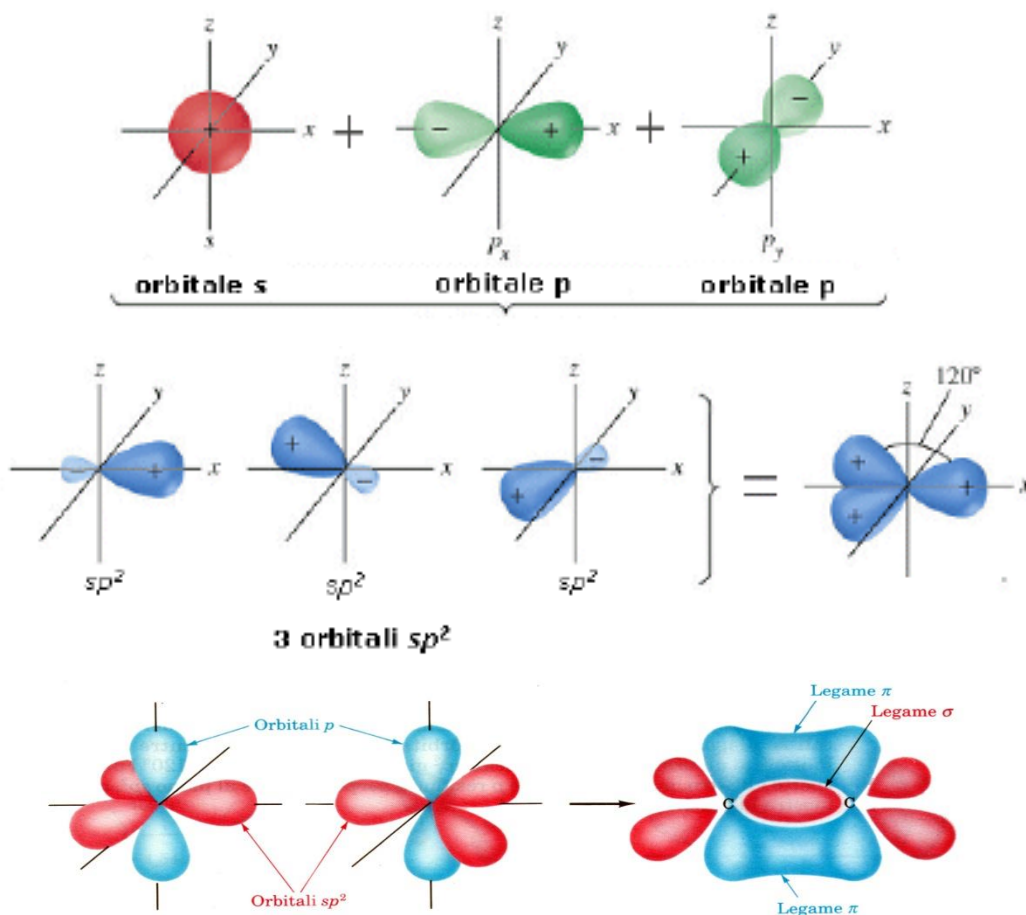


Figure 1.13: sp^2 hybridization

The combination between one s orbitals and all the three p orbitals, gives rise to four sp^3 orbitals \rightarrow tetrahedral structure, shifted by $109,5^\circ$

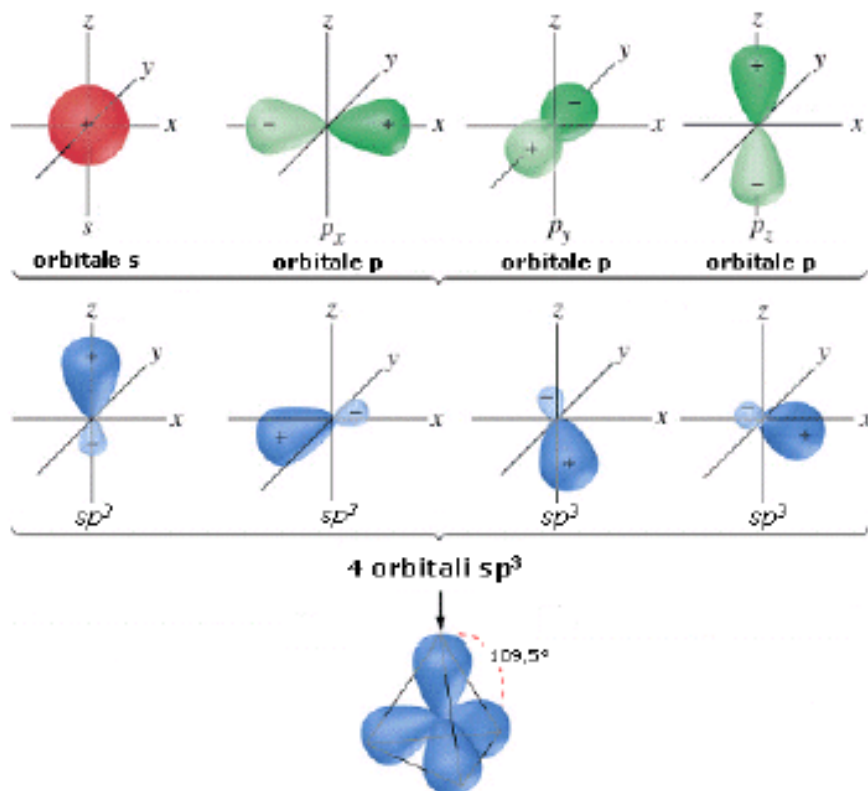
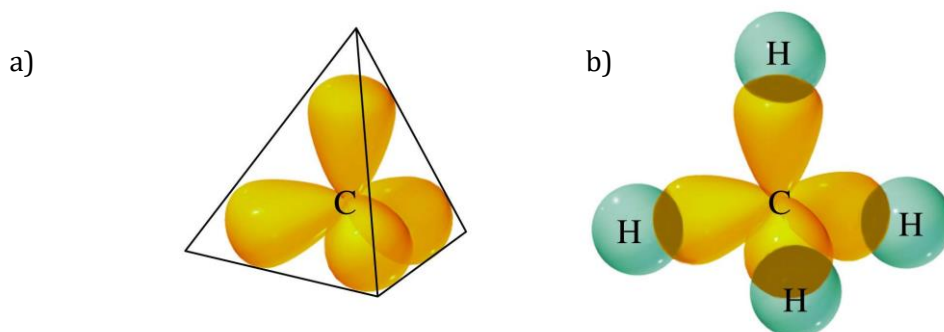


Figure 1.14: sp^3 hybridization

This case is not very interesting for us, just to give an example, Methane molecule has this kind of tetrahedral configuration (CH_4)



Four sp^3 orbitals are directed toward the corners of a tetrahedron (a); the orbital structure of methane, showing the overlap of the four sp^3 orbitals of carbon with the s

orbitals of four hydrogen atoms to form four σ (covalent) bonds between carbon and hydrogen (b).

When a carbon atom has four single bonds, the 2s-orbital and the three 2p-orbitals hybridise and form four equivalent sp^3 -orbitals, equally shaped and oriented towards the corners of a regular tetrahedron. All bonds between s-orbitals or hybrids of s-orbitals and p-orbitals are called σ -bonds, and the electrons involved are called σ -electrons. When one 2s-orbital combines with two of the three 2p-orbitals, three hybrid sp^2 -orbitals will be formed. As a result, there will be three sp^2 orbitals lying on the same plane and one unhybridized one ($2p_z$), that is standing perpendicular, as sketched in Figure.

If we consider sp^2 hybridization, this involves s, p_x e p_y orbitals, so that three equivalent bonds can be formed and they are located in the same plane, shifted by 120° . There will be a fourth not hybridized p_z orbital perpendicularly oriented and not hybridized.

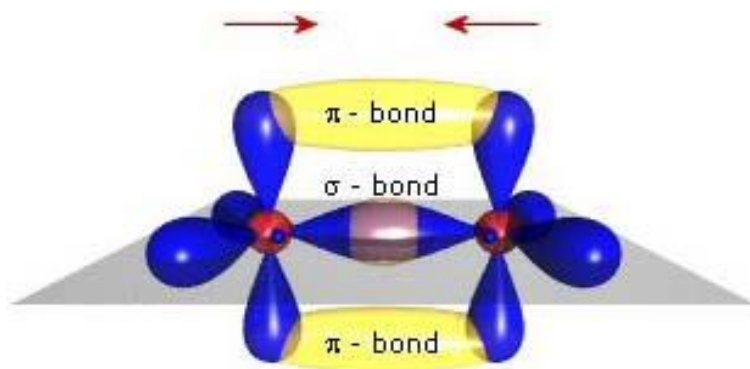


Figure 1.15: double bond in the carbon atom

If we try to form a bond between two carbon atoms we can at first form a σ bond, involving two hybrid orbitals, afterwards a π bond can be formed between the two not hybridized orbitals. In this way a double bond has been formed

Each carbon atom uses two single bonds to bond itself with a hydrogen atom and with a carbon atom, and a double bond to bond itself with one more carbon atom. There is no possibility to have two adjacent double bonds for carbon atoms, on the

contrary there could be an alternation between single and double bonds within the molecule. This alternation is called conjugation.

- *Single and double bonds alternation \rightarrow conjugation*
- *Conjugation length \rightarrow length of a molecular chain with a perfect alternation between single and double bonds*

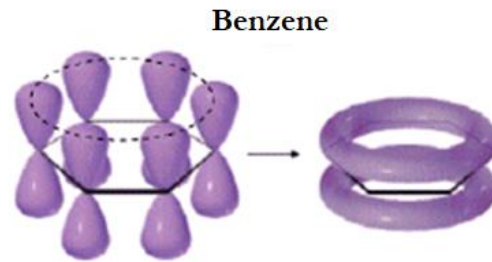


Figure 1.16: the benzene ring

It is noteworthy that σ -bonds are typically very strong bonds and the electrons involved are too localized to be free to move. As a result, σ -electrons are not involved in charge transport mechanism and σ -bonds form the skeleton of the structure, and are responsible for the geometrical properties of the resulting molecule. On the contrary, π -bonds are very weak and the electrons involved are much delocalized so that they can freely move across the molecule, in particular when an electric field is applied. In such kind of hybridized bonds, π -bonds occur alternatively every 2 molecules. The key structure in a conducting polymer is a linear chain of conjugated units, in which single and double bonds alternate.

1.6 RESONANCE AND DELOCALIZATION

When in a molecule there are π electrons (double or triple bonds) it can happen that such molecule can assume two different and equivalent (energetically) configurations. It cannot be stated, a priori, which one of the two is the most probable structure, the system resonates between the two states.

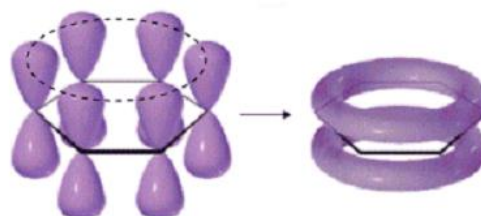
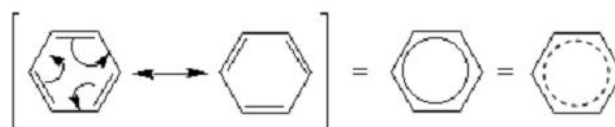


Figure 1.17: conjugation in the benzene ring

Where are the π electrons placed? It is impossible to answer, because the chance to get them is equal in all the molecule. This actually means that the π electrons have the same probability to sit in every area of the molecule, meaning that they are perfectly delocalized.

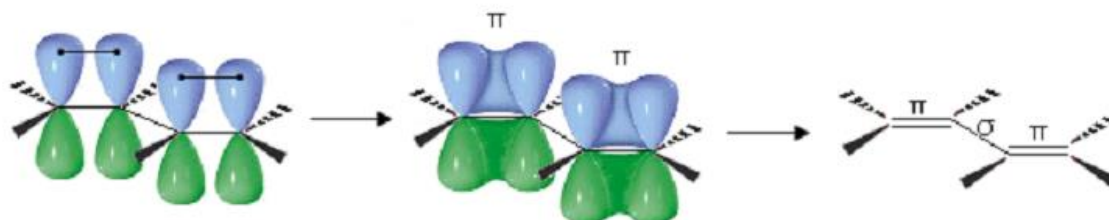
In other words, there will be an extended π orbital in all the entire molecule (conjugation length) and the electrons involved in those bonds are delocalized in this new extended molecular orbital. *Delocalization of π electrons.*

This means that those electrons are delocalized in extended states and therefore are free to move, within this region of space, conjugation length

Resonance is at the basis of electronic delocalization in conjugated systems.

Let's consider a system with a sequence of double $\sigma - p$ bonds, separated by a single σ bond. As long as conjugation is present we have resonance and delocalization.

There are several ways to represent a conjugated $\pi - \pi$ system.



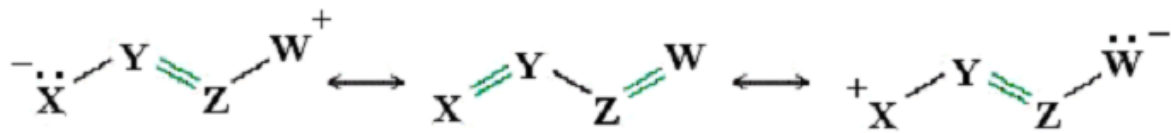


Figure 1.18: conjugation, resonance and delocalization

The nature of the chemical bonds, π or σ , determines the energetic gap between the two new created orbitals, bonding and anti-bonding. Therefore, this confers the electronic properties to the final.

σ Bonds are more stable, the electrons are highly localize

In fact, the energetic distance between bonding and anti-bonding MOs is relatively high, meaning that it will be very difficult for an electron placed in the bonding MO to jump into the higher antibonding level. In other words, these materials are generally insulators.

Being very strong, σ bonds typically are the one that determine the molecular backbone.

If we consider π bonds, the energetic gap between the two bonding and anti-bonding MOs is much smaller than in the previous case. Therefore, it is much easier for electrons placed in the bonding MOs to receive a sufficient energy to jump into the empty anti-bonding MOs. Such electrons are delocalized and much more free to move. Such energy can be given by an external field, exposure to light etc.

We have to consider that in a molecule, we have a lot of bonds, therefore the representation of these new energetic levels, MOs, is a little bit more complicated.

The amount of σ or π bond in one molecule determines the band gap amplitude, whereas, the number of atoms determines the energetic distance between these new states. Molecules with few atoms are characterized by discrete states, when the number of atoms is big enough such discrete states are so energetically close that can be considered as an energetic band.

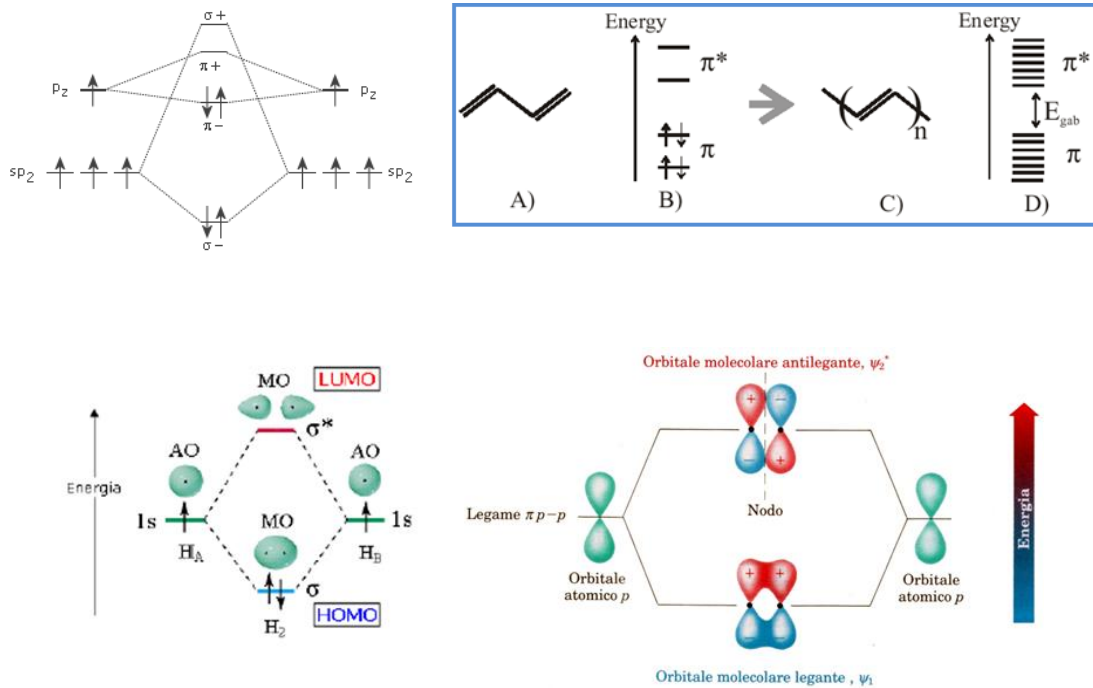


Figure 1.19: band formation in a conjugated material

- HOMO (Highest Occupied Molecular Orbital)
- LUMO (Lowest Unoccupied Molecular Orbital)

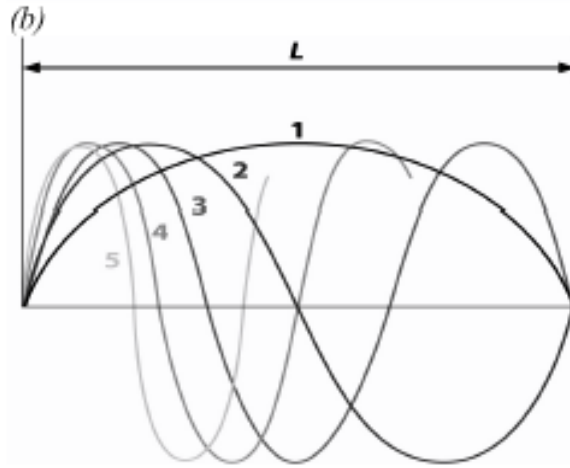
The energetic distance between HOMO and LUMO determines the band gap of the molecule.

1.7 THE BAND GAP IN CONJUGATED MOLECULES

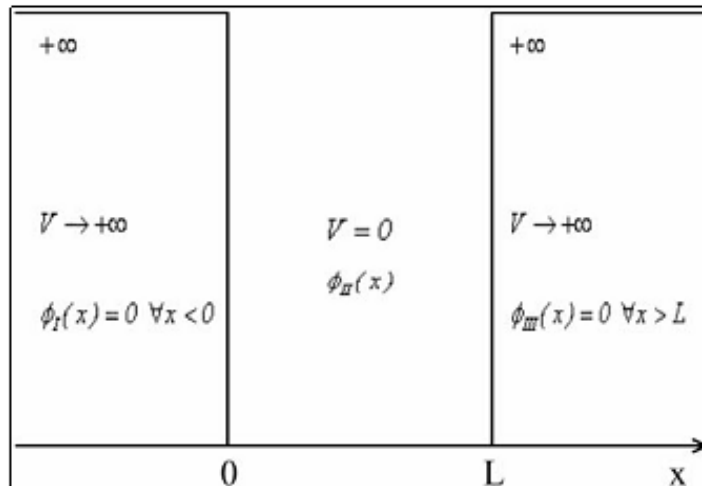
It is possible to estimate the band gap of one conjugated molecule by considering the π electron as an electron in a box with infinite walls and with a length L given by the conjugation length of the molecule. The conjugation length is the part of the molecule where a perfect alternation between double and single bond exists.

The π electron, being confined in such a well can be represented as a sinusoidal wave with a wavelength $\lambda_n = 2L/n$

Where n represents the n th state



Let's consider this example again. The electron inside the box can be represented as a free electron, but we have some border conditions.



Unidimensional case. The potential energy inside the box is 0

Which will be the eigenvalue equation?

$$E_T = E_{cin} = \frac{p^2}{2m} \Rightarrow H = -\frac{\hbar^2}{2m} \frac{d^2}{dx^2}$$

$$-\frac{\hbar^2}{2m} \frac{d^2\psi(x)}{dx^2} = E\psi(x) \Rightarrow \frac{\hbar^2}{2m} \frac{d^2\psi(x)}{dx^2} + E\psi(x) = 0$$

Which could be the solutions for this equation?

$$\psi_1(x) = A \cos(kx)$$

$$\psi_2(x) = B \sin(kx)$$

$$\psi_1(x) = A \cos(kx)$$

$$\frac{\hbar^2}{2m} \frac{d^2\psi(x)}{dx^2} + E\psi(x) = 0$$

$$-\frac{\hbar^2}{2m} Ak^2 \cos(kx) + EA \cos(kx) = 0$$

$$k = \sqrt{\frac{2mE}{\hbar^2}} = \frac{\sqrt{2mE}}{\hbar}$$

The most general solution is given by a linear combination of the previous two:

$$\psi(x) = A \cos(kx) + B \sin(kx)$$

$$\psi(x) = A \cos(kx) + B \sin(kx)$$

$$\psi(0) = 0 \Rightarrow A \cos(0) = 0 \Rightarrow A = 0$$

$$\psi(L) = 0 \Rightarrow B \sin(kL) = 0$$

$$kL = n\pi$$

B=0 is not acceptable

Therefore, we obtain

$$\frac{\sqrt{2mE_n}}{\hbar} L = n\pi$$

$$E_n = \frac{\pi^2 \hbar^2}{2mL^2} n^2 = \frac{h^2}{8mL^2} n^2$$

$$E_n = \frac{n^2 h^2}{8mL^2}$$

n = number of states; h Planck constant; m electron mass; L conjugation length.

Imagine we have N atoms within the conjugation length L, each one involves a π orbital with two electrons

If d is the distance between atoms L will be (N-1)d, for $N \gg 1$ it becomes Nd

n = number of states; h Planck constant; m electron mass; L conjugation length.

Imagine we have N atoms within the conjugation length L, each one involves a π orbital with two electrons

If d is the distance between atoms L will be (N-1)d, for $N \gg 1$ it becomes Nd

N atoms will form N/2 π bonds, i.e. there will be N π molecular orbitals (N/2 bonding and N/2 antibonding). Considering the Pauli exclusion principle, only two electrons can occupy the single orbital

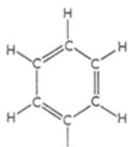
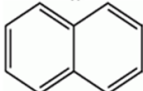
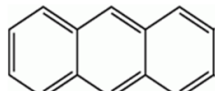
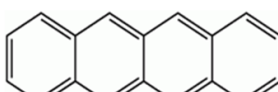
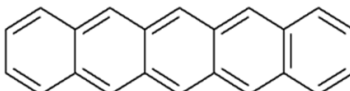
If the number of occupied states n will be $N/2$

$$E(\text{HOMO}) = \frac{\left(\frac{N}{2}\right)^2 h^2}{8m(Nd)^2}$$

$$E(\text{LUMO}) = \frac{\left(\frac{N}{2} + 1\right)^2 h^2}{8m(Nd)^2}$$

$$E_G = E(\text{LUMO}) - E(\text{HOMO}) = \frac{(N + 1)h^2}{8m(Nd)^2}$$

the band gap decreases when the molecule conjugation length (Nd) increases

		Band Gap
Benzene		6.0 eV
Naphthalene		4.3 eV
Anthracene		3.3 eV
Tetracene		2.6 eV
Pentacene		2.1 eV

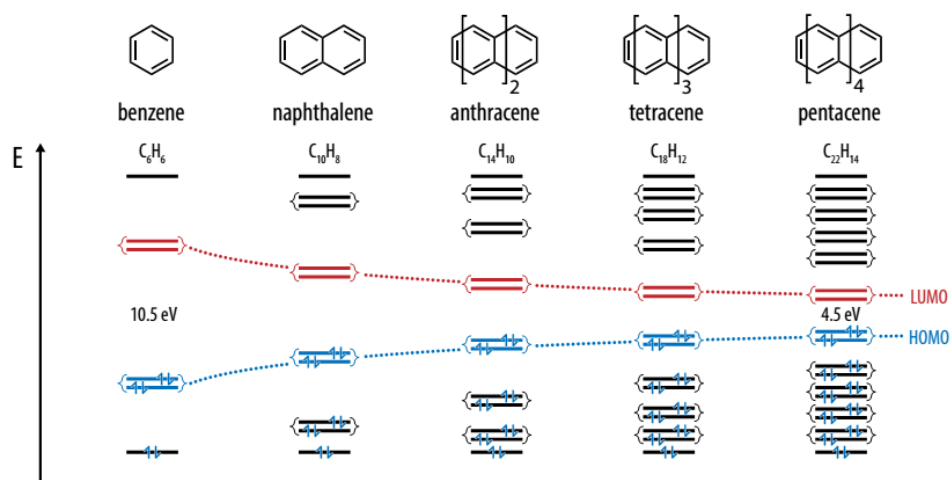


Figure 1.20: band gap in different conjugated materials

The band gap of the single molecule is larger than the one of the film, in which a multitude of molecules are present.

In fact, in the molecules in a film can interact, and the way these molecules assemble in the film determines the electronic properties of the film.

Molecular packing \rightarrow structural properties

pi-stacking

Domains dimensions \rightarrow morphological properties

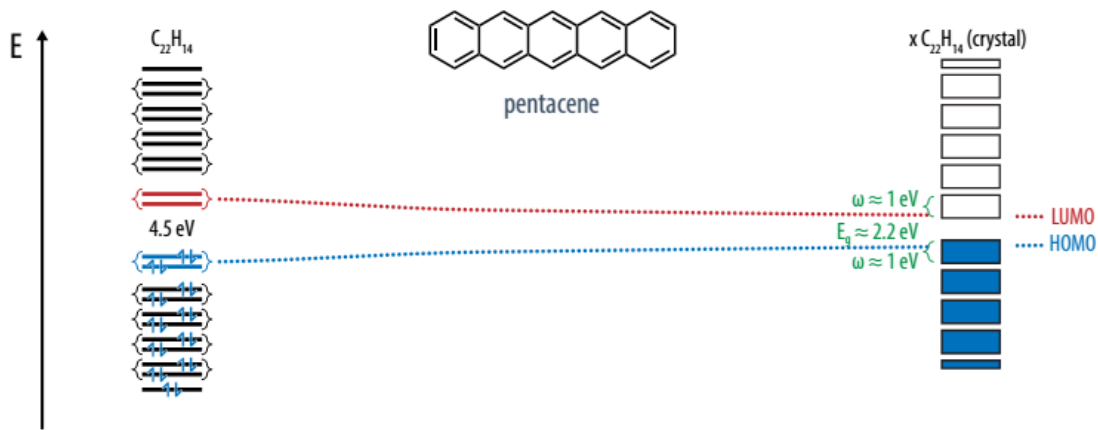


Figure 1.21: band gap difference between single molecule and thin film

In two close molecules it can happen that the extended p-clouds can overlap the extended p-clouds of the adjacent molecule. In this way the delocalized p-electrons of the first molecule are delocalized also in the second one. We call the overlapping of the p-clouds pi-stacking, and in order to have higher conductivity we need to have a good overlapping, i.e. a good pi-stacking.

If the pi-stacking is good, the pi-clouds can be extended in many adjacent molecules, meaning that such electrons are highly delocalized across the film, not only in the single molecule. Such extended pi-orbitals leads to the creation of additional energetic levels, bonding and antibonding, creation of small bands (ca. 1eV). Extended energetic bands where charge carriers can move, similarly to inorganic materials, which is the

reason for the reduction of the band gap in the film, compared to the single molecule ones.

Most organic materials employed for electronics applications can be classified into two families: i) aromatic compounds; ii) heterocyclic compounds. The core of the aromatic compound family is the benzene ring, reported in Figure 1.7 (a). The benzene ring (C_6H_6) consists of six carbon atoms bonded in a flat or planar hexagon ring. Each carbon atom in the hexagonal cycle has four electrons to share. One goes to the hydrogen atom, and one each to the two neighboring carbons, with an alternation of a single and a double bond. Aromatic compounds are basically formed by a concatenation of several benzene rings that leads to obtain a rodlike conjugated molecule. The core of the heterocyclic compounds is the thiophene ring. Thiophene (C_4H_4S) is a heterocyclic compound consisting of four carbon atoms and one sulfur atom in a five-membered ring. Also in this case carbon atoms are bonded to a hydrogen atom with a single bond and to the neighbour atoms of the ring by one single and one double bond.

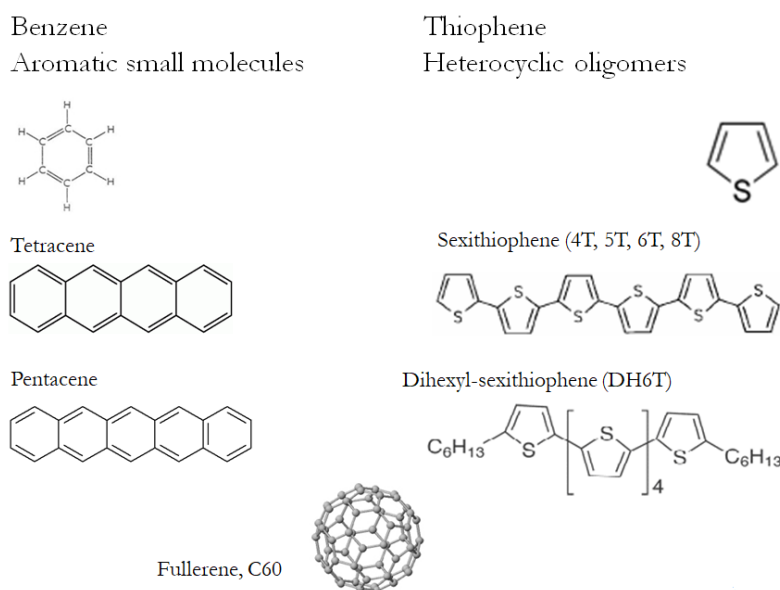


Figure 1.22: example of different organic molecules

2 MATERIALS

2.1 OLIGOMERS VS POLYMERS

- Oligomers are small molecules with a limited number (less than 10) of repeating units, called monomers. Generally, they are characterized by a small molecular weight, and are not soluble, therefore, they have to be deposited by the vapor phase.
- Polymers are bigger molecules, that can be divided in low molecular weight polymers and large molecular weight ones. They are characterized by a higher number (higher than 10) monomers and are generally soluble, so that, they can be deposited by the liquid phase

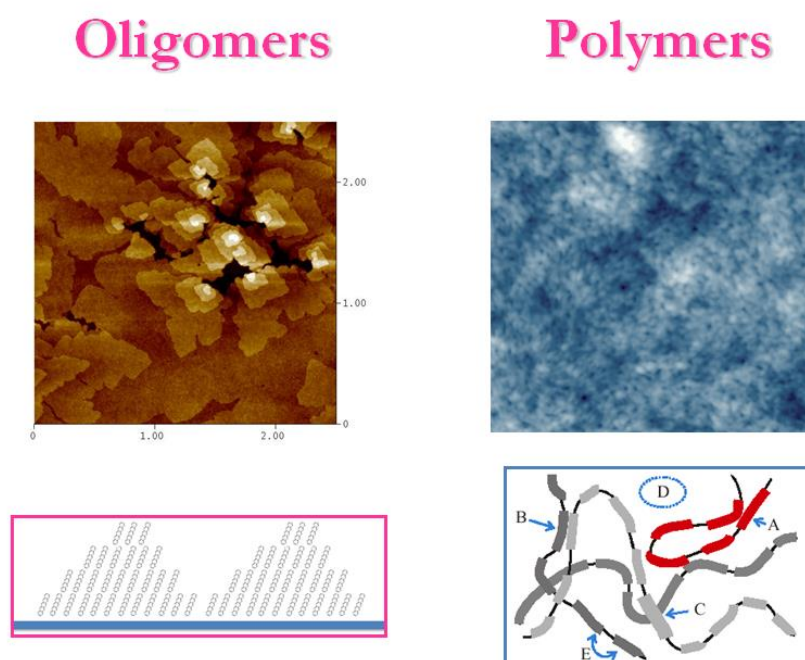


Figure 2.1: oligomers and polymers

2.2 PENTACENE

Pentacene is a polycyclic aromatic hydrocarbon molecule consisting of 5 linearly-fused benzene rings. Pentacene is one of the most used and the most promising organic semiconductors. This is the typical example of a rod-like molecule where one of the three axes is definitely longer than the other two. For a molecule like pentacene, charge

transport across the semiconductor film strongly depends not only on the overlapping of the π -orbitals in the direction of the longest axis of the molecule (intra-chain charge transport), but also on the interaction of the π -orbitals between two close molecules (inter-chain charge transport). Therefore, charge carrier transport properties, in particular mobility, are strongly influenced by structural morphological properties of the assembled film. At the state of the art, pentacene is the organic semiconductor that showed the highest performances in terms of stability and also in terms of the measured mobilities. Mobilities up to $1 \text{ cm}^2/\text{Vs}$ have been recorded for polycrystalline pentacene films, whereas even higher mobilities, up to $30 \text{ cm}^2/\text{Vs}$, were measured for pentacene single crystals. It is characterized by a wide band gap (as most organic semiconductors) around 2,2 eV. Pentacene has an Ionization Energy (which correspond to the HOMO energy level) around 5.2 eV and an Electron Affinity (LUMO level) around 3 eV. This means that it forms a very low hole injection barrier but a very high electron injection barrier when using Au as metal electrode. This is the reason why it is typically employed as p-type semiconductor in most organic electronics applications.

2.3 TETRACENE

Tetracene, also called naphthacene and 2,3-benzanthracene, is a polycyclic aromatic hydrocarbon. The molecule is very similar to pentacene, but it is characterized by four linearly fused benzene rings. If compared to pentacene, tetracene shows lower electronic performances. It is very unstable and quickly degrades upon exposure to light and oxygen. Moreover, the recorded mobilities for this material are in the range of 10^{-2} to $10^{-3} \text{ cm}^2/\text{Vs}$ up to $0.4 \text{ cm}^2/\text{Vs}$ for single crystal film, measured by Morpurgo et al. Nevertheless, this material has been extensively studied for its photoluminescence properties, and has been employed as active material for the realization of Organic Light Emitting Transistors (OLETs).

2.4 6,13-BIS(TRIISOPROPYLSILYLETHYNYL)PENTACENE TIPS PENTACENE

6,13-Bis(triisopropylsilylethynyl)pentacene (Pentacene TIPS) is a modified version of pentacene, in which two silyl ethers in 6 and 13 position. Such modification allows the molecule to be solution processable.

Its properties are very similar to the normal pentacene one, with an HOMO around 5.3 eV and a LUMO around 3 eV, for this reason when interfaced with high work function metals or conductive polymers electrodes, it generally work as a p-type material.

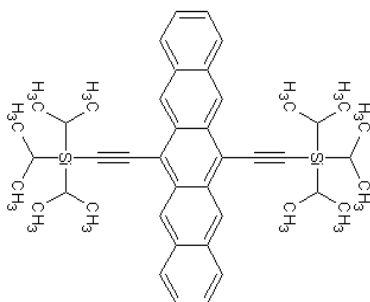


Figure 2.2: TIPS Pentacene molecule

Moreover, during the deposition process, the molecules tend to diffuse rapidly across the substrate giving rise to highly ordered thin film, with randomly oriented large crystals, as reported in the following figure.

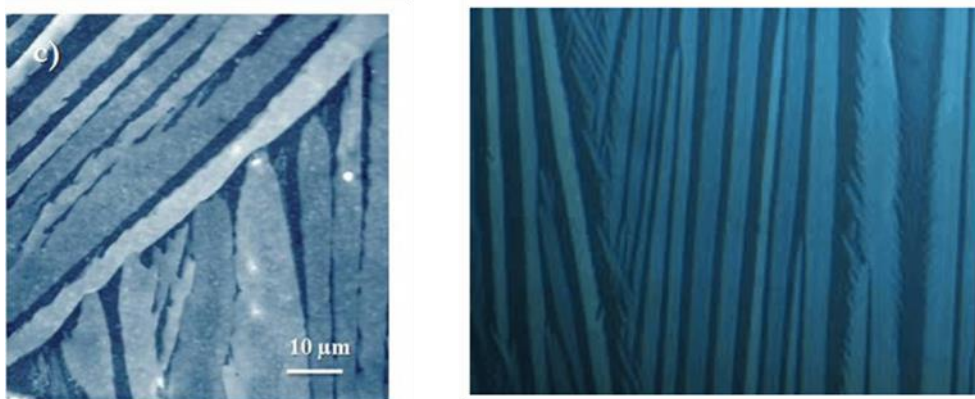


Figure 2.3: example of morphology of TIPS Pentacene thin films

2.5 A-SEXITHIOPHENE (A-6T)

Sexithiophene is a heterocyclic compound characterized by a concatenation of six thiophene rings. It is one of the most extensively studied oligothiophene compounds, mainly employed as active layer for the realization of OFETs. Several examples have

been reported so far in literature with mobilities up to $0.1\text{cm}^2/\text{Vs}$ and $1 \times 10^{-2}\text{cm}^2/\text{Vs}$ for single crystal and polycrystalline devices respectively. α -6T energy levels are very similar to pentacene ones, with a Ionization Energy close to 5 eV and a energy band gap around 2.3 eV. Therefore, also this material is generally employed as p-type semiconductor when using a high work function metal.

2.6 α,ω -DIHEXYLSEXITHIOPHENE (α,ω -DH6T)

One of the main advantages of organic electronics is the possibility to use molecular chemistry tailoring in order to tune and modulate the properties of the basic molecule itself. As can be clearly noticed from the following the α,ω -DH6T molecule is very similar to the 6T one. The only difference is the presence of two lateral alkyl-chain substituents located at both ends of the molecule, in α,ω position respectively. Mobilities in the range of $1\text{cm}^2/\text{Vs}$ and $0.1\text{cm}^2/\text{Vs}$ have been reported in literature for single crystal and polycrystalline devices respectively. As can be noticed from the energy levels diagram reported before, the presence of the alkyl chains substituents have a strong influence on the energetics of this system, leading to a reduction of its Electron Affinity (corresponding to the LUMO level) to 2 eV. Also in this case, due to the very high electron injection barrier that DH6T forms with the most common metals (even with low work function ones) it is seldom employed as n-type material. Unfortunately, having an ionization energy (which correspond to the energy associated to the HOMO level) smaller than the previous molecules, it is very reactive, in particular to moisture and oxygen, therefore it is less stable than the previous introduced molecules.

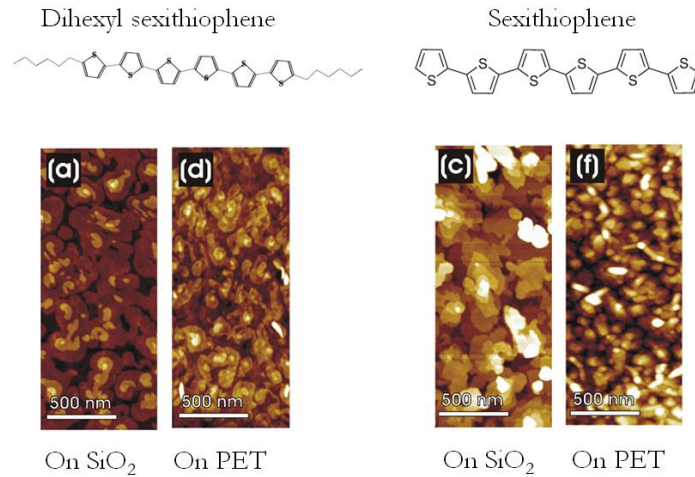


Figure 2.4: morphological differences between DH6T and 6T

2.7 FULLERENE - C₆₀

Due to their electronic band structure, nearly all organic semiconductors are able to transport only one kind of charge carrier, either hole or electrons. The reason for that, can be found in the fact that most metals employed for the realization of the electrodes are characterized by a high work function (typically around 4.5 to 5.5 eV), thus leading to have a very high electron injection barrier at the interface between metal electrode/organic semiconductor, since the typical values of the LUMO level for organic semiconductors is around 2.5 to 3eV. The materials introduced before, were mainly employed for the realization of OFETs working in p-type mode.

C₆₀ is one of the most interesting organic semiconductors. Due to its high photoluminescence and photoconductivity it has been extensively employed for optoelectronic applications, in particular for the realization of Organic Photovoltaic Solar Cells. Its relatively high LUMO level (3.7-4.1 eV) allows to minimize the electron injection barrier, therefore, it can be used for the realization of n-type OFETs even with high work function metal electrodes.

2.8 POLY (3-HEXYLTHIOPHENE) P3HT

Among the many polymer structure that can be synthesized polythiophene family is certainly one of the most employed on in flexible electronics.

Generally such molecule are functionalized by the employment of alkyl chains, with the aim of allowing them to be soluble and therefore solution processable, without affecting conjugation across the molecule.

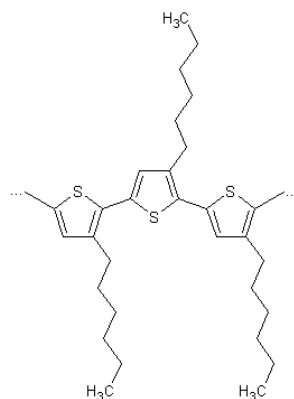


Figure 2.5: P3HT molecule

P3HT is certainly one of the most employed ones. It is characterized by a HOMO level around 4.8 eV, very close to gold work function, for instance, and therefore it is generally employed as p-type material. Unfortunately, having an ionization energy (which correspond to the energy associated to the HOMO level) smaller than the previous molecules, it is very reactive, in particular to moisture and oxygen, therefore it is less stable than the previous introduced molecules.

It is generally deposited by liquid phases, giving rise to highly disordered thin films, characterized by mobility values in the range of $10^{-2} - 10^{-3} \text{ cm}^2/\text{Vs}$.

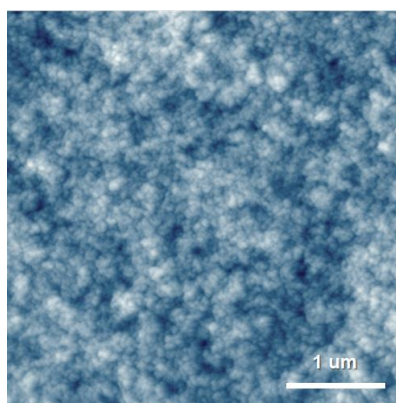
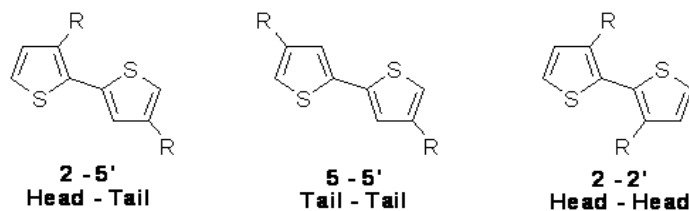


Figure 2.6: example of P3HT thin film morphology

P3HT is an asymmetric molecule, and three possible different molecular structures can be obtained.



When a mixture of the different configuration is present, the polymer is called regio-irregular. When only one is present, the polymer is called regio-regular. In order to achieve higher molecular order and also better transport properties regio-regularity must be the higher as possible.

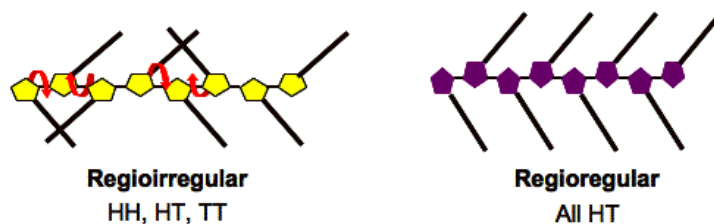


Figure 2.7: difference between regio regular and regio irregular molecules

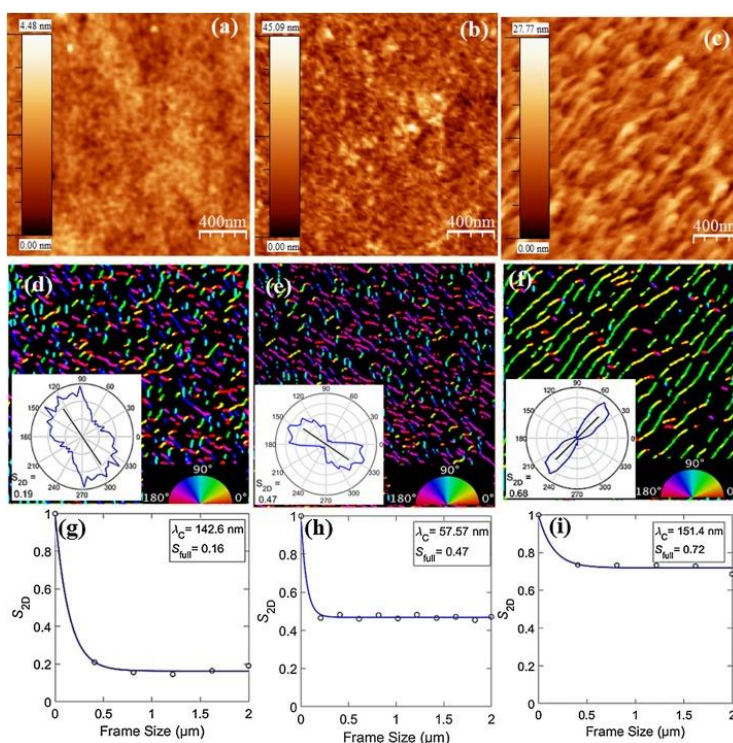


Figure 2.7 (Color online) AFM images (a, b, c), orientation maps (d, e, f), and (g, h, i) orientational order (S_{2D}) versus frame size of P3HT-CF(on), P3HT-DCM(on), and P3HT-DCM(off) films, respectively. In Fig. (a, b, c) the inset (right) is height scale. In Fig. (d, e, f) the inset (left bottom) is the orientation distribution and the inset (right bottom) is the color wheel.

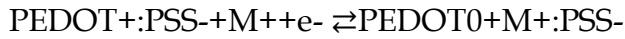
Recent studies have demonstrated that by properly treating the deposited thin film, for instance using a thermal annealing process, the structural and morphological properties of P3HT layers can be dramatically modified, and also in this case highly crystalline films can be obtained, boosting the carrier mobility up by orders of magnitude.

2.9 PEDOT:PSS

One of the most studied and characterised conjugated polymers is the p-doped poly(3,4-ethylenedioxythiophene) (PEDOT). The structure of PEDOT is shown in the following Figure (a). As the previously mentioned sexithiophene and dihexylsexithiophene, also PEDOT is a thiophene derivative.

In its pristine state PEDOT is a non-soluble semiconductor, characterized by a poor conductivity, however higher than the typical conjugated polymers. Conjugated polymers in general have conductivity in the range of $10^{-6} - 10^{-10} \text{ Scm}^{-1}$ in their neutral state, whereas PEDOT has a conductivity of 10^{-5} Scm^{-1} in the “neutral” state. When PSS is added to the molecule, the resulting co-polymer becomes soluble, therefore it can be deposited using most common deposition techniques from the liquid phase. Moreover, the PSS acts a dopant for the PEDOT molecule, removing one electron and leaving a free hole in the conjugated PEDOT backbone, that, therefore, is free to move across the molecular film.

The PEDOT:PSS film, in its pristine state, is a mixture of doped (oxidised) and undoped (neutral) PEDOT units. In an electrochemical cell, PEDOT:PSS can be switched reversibly between the conducting form (PEDOT⁺) and the semi-conducting state (PEDOT⁰), according to the reaction below:



Here M^+ represents the cation and e^- is an electron. The arrow to the right indicates the reduction of PEDOT while arrow to left indicates the oxidation process. PEDOT shows a relatively high conductivity. Since PEDOT has such a high conductivity in the neutral state it is possible to use it as its own electrode in electrochemical devices.

PEDOT is a low band gap polymer; it absorbs strongly in the red part of the visible spectrum, resulting in a deep blue colour. Upon doping PEDOT, the optical absorption shifts to longer wavelengths, which results in nearly transparent film.

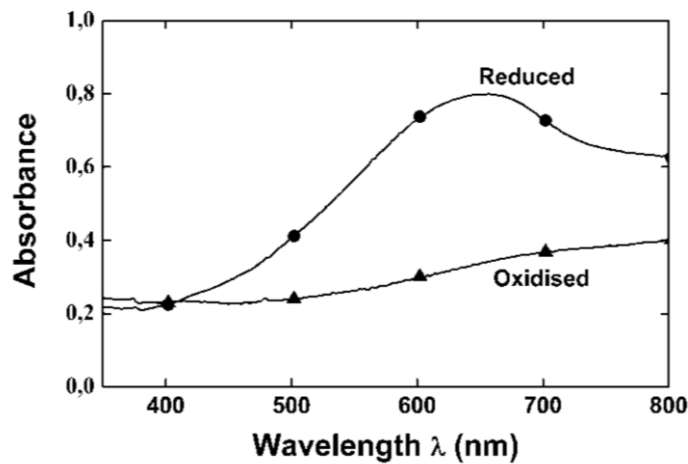


Figure 2.8: the optical absorption of PEDOT:PSS at the reduced and oxidised states

In other words, PEDOT is positively charged, whereas PSS is negatively charged



However PSS is an insulator! This means that depending on the way the PSS is finally deposited on the film dramatically influences the charge transport within the film. PSS for instance can create insulating islands surrounding the PEDOT molecules, thus not allowing the created charge carriers to move freely due to a bad percolation. This issue

can be significantly overcome by using post treatment processes, i.e. using some additives and thermal treatment to re-create the film morphology.

Among the many additives the following are the most employed ones:

- methyl sulfoxide (DMSO),
- N,Ndimethyl formamide (DMF)
- Glycerol
- Sorbitol
- Ethylene Glycole

In particular, Ethylene Glycole (EG) is widely used as his effect is twofold:

- Allows increasing conductivity
- Gives the film a better stability in water

The reason for that have been reported and discussed in many scientific papers and generally ascribed to a dramatic change in the thin film morphology. EG typically leads to a reduction of PSS island in the film thus dramatically increasing the percolation of the generated hole in the PEDOT molecule, and, also, allows the PEDOT molecule to get defold (less pronounced spaghetti configuration), thus reducing the selftrapping of charge carriers within the molecule.

Due to its high conductivity, it is generally employed, not only as active semiconductor material, but also for the realization of conductive electrodes in several applications such as OFETs and OLEDs. Some reasons for the popularity of PEDOT is its excellent chemical stability and its high conductivity. Depending on the counterion (which is the ion that accompanies the ionic species in order to maintain electric neutrality), PEDOT can exhibit conductivities higher than 1000 S/cm.

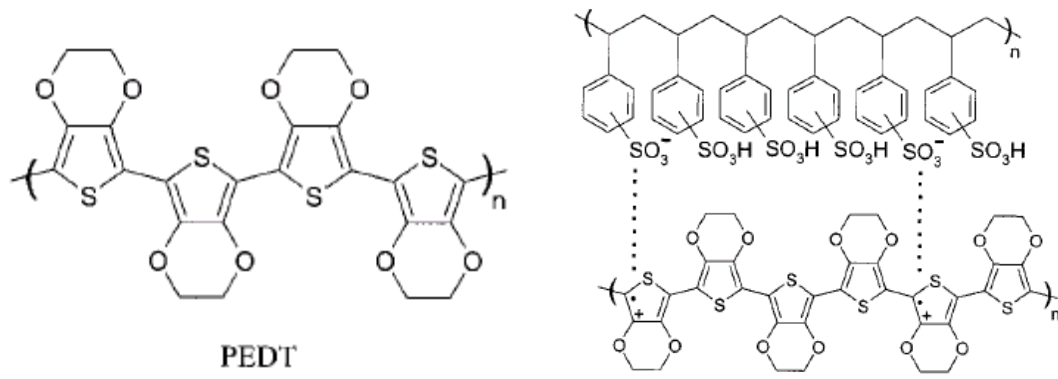


Figure 2.9: Chemical structure of PEDOT (a) and PEDOT:PSS (b)

3 DOPING IN ORGANIC MATERIALS

In their neutral state, conjugated polymers span a conductivity range from close to an insulator to semiconductors. Upon doping, their conductivity can be increased by several orders of magnitude. In crystalline semiconductors like silicon and germanium, only a very small percentage (ppm) of dopants, donors or acceptors, is needed to increase the conductivity several orders of magnitude. Here the dopant replaces an atom along the lattice structure and binds covalently to neighbor atoms in the matrix. For conducting polymers, doping occurs in a different manner. First the doping fraction required is much higher. If every monomer unit is considered to be a possible doping site, then several percent of the monomer units must be doped in order to achieve a highly conducting polymer.

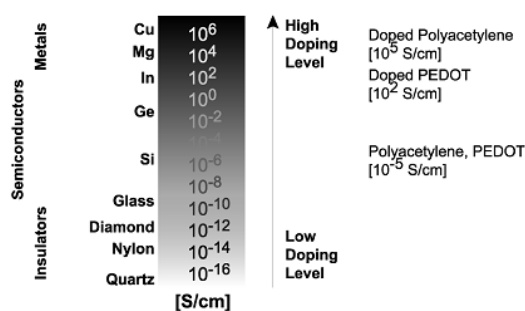


Figure 3.1 changes in the conductivity in doped polymers

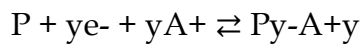
In the case of doping conjugated polymers, the dopant forms an ionic complex with the polymer chain.

Doping of polymers can be achieved by several methods; chemical doping, electrochemical doping, photo-doping and charge-injection doping.

The most commonly used methods are the chemical and the electrochemical doping approaches. Conjugated polymers can be both p-doped and n-doped. The process is based on a reversible redox process. The oxidation of the polymer chain is denoted to as p-doping. The process involved in p-doping is equivalent to withdrawing electrons from the π -system of the polymer backbone. This results in a positively charged unit in the conjugated system:



Where P denotes the polymer chain, A denotes the charge-compensating counterion, e⁻ the electron and y is the number of counter ions. If the chain is instead reduced compared to its neutral state it is n-doped. For n-doping, electrons are introduced into the π-system of the polymer backbone to form a negatively charged unit in the conjugated system.



So far, p-doped conjugated polymers are mainly used in devices and investigations since conjugated polymers that are easily n-doped are normally unstable in ambient atmosphere since they react quickly with oxygen in air. During electrochemical switching, electroneutrality must be maintained within the film. This is achieved by combining the solid polymer with an electrolyte. The electroneutrality is maintained by ions, counterions, which either enter or escape the conjugated polymer film. Fully doped conducting polymer can therefore be treated as a salt complex. In some cases, the counterion species can be immobile itself, an example is poly(styrene sulphonate) (PSS), see in the following section. For the case of PSS, cations move into and out of the polymer film in order to compensate for electronic charges during switching. An important point here is that conducting polymer conducts both electrons and ions. This is one of the key properties used in electrochemical devices.

In general, a conjugated polymer is neutral, therefore, to promote one electron from the valence band up to the conduction band an energy larger than the band gap has to be spent.

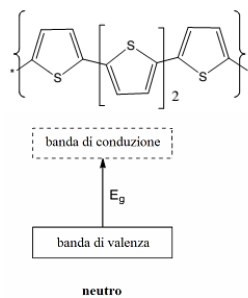


Figure 3.2: band gap in the neutral state

When a polymer gets oxidized, an electron is removed out of the molecule, as a consequence, a positive charge, hole, is created. Actually, a couple radical-cation is created.

3.1 FREE CHARGE CARRIERS IN CONJUGATED POLYMERS

In order to reach electrical conduction in a conjugated polymer, some form of electronic species must carry the charge. Charge carriers can be created through oxidative or reductive doping, as described above. These charge carriers are transported along the π -bonded polymer chain. The charge carriers can either be solitons, polarons or bipolarons, which are not real physical particles, but rather quasi-particles. When combining two chain segments of *trans*-polyacetylene, with different bond order, a defect in the form of an unpaired electron is created. The unpaired electron will end up at a new energy level inside the band gap. This defect is called a neutral soliton. The state of a soliton can carry from zero to two electrons. Thus, solitons can either be neutral, positive or negatively charged. Charged solitons have no spin, while the neutral soliton has spin but no charge.

For non-degenerate polymers with a preferred bond order, the charge carriers are called polarons or bipolarons. By oxidising the polymer, an electron is removed and the associated positive polaron occupies an energy level in the band gap. By withdrawing an electron from a polymer with a non-degenerate ground state, a cation-radical pair is formed. In between the cation and the radical, a change in the polymer structure is created. This confined change in bond order and the associated charge is called a **polaron**.

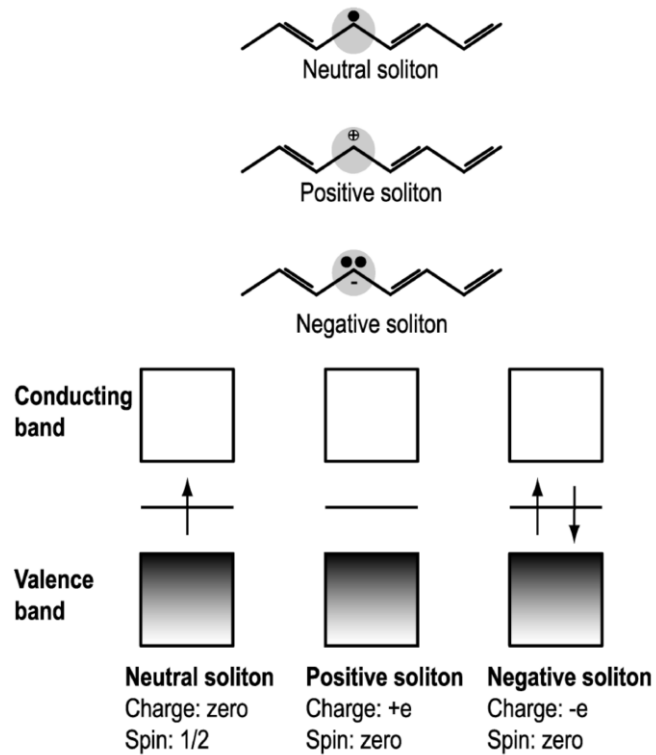


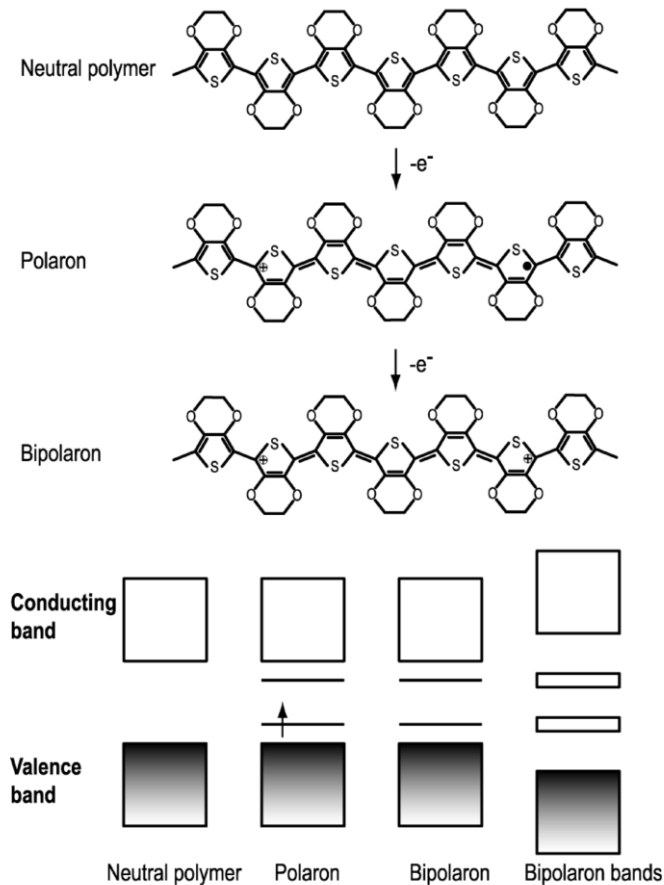
Figure 3.3: neutral, positive and negative solitons.

In the following figure is presented for PEDOT and the deformation from the aromatic form into the quinoid form upon creating a polaron is shown. The quinoid structure is a higher energy state compared to the aromatic form. In contrast to solitons, polarons must overcome an energy activation barrier related to the aromatic-quinoid transformation while moving. A polaron occupies up to approximately five monomer units along the polymer chain. If two electrons are withdrawn from the conjugated polymer, a positive bipolaron, with two positive charges, is created. If the polymer is then oxidised even further, bipolaron energy bands are generated in the band gap.

The conductivity in conjugated materials increases considerably upon doping. Doped conjugated polymers exhibit good conductivity for two reasons; the number of free charge carriers is increased and the charge carrier mobility is increased due the formation of new electronic bands. The conductivity σ is defined as

$$\sigma = ne\mu$$

where n is concentration of charge carriers, e the charge of an electron and μ is the charge carrier mobility. However, if the number of charge carriers is increased beyond a certain level, the conductivity starts to decrease due to interactions between the charge carriers. Highest conductivity is associated with “mixed valence” states of fractional charges per repeat unit of the polymer.

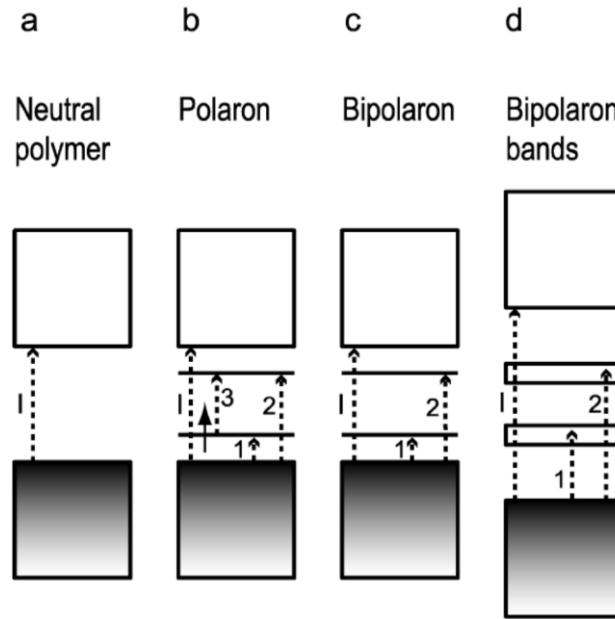


High conductivity should occur when the polymer contains both charged sites and non-charged sites to which the charged sites can move. Measurements on polythiophenes, polypyrroles and polyaniline suggest that a finite potential window of high conductivity is a general feature of conjugated polymers. A typical example of this is polyaniline, which starts to show a decrease in conductivity when the polymer chain is oxidised to a level of more than 0.5 electrons per repeat unit. Polyaniline shows the greatest conductivity when oxidised to a level of 0.5 electrons per repeat unit. Doping the polymer causes changes beyond the electronic conductivity. The optical

properties are also controlled since doping introduces new states in the energy band gap, causing the absorption to shift towards lower energies. Conjugated polymers have a band gap typically in the region of 1.7-3eV, i.e. they absorb visible wavelengths of light.

This strong absorption in the visible region in the neutral form is switched towards infrared absorption by doping. This phenomena is denoted as *electrochromism*. An undoped polymer absorbs at wavelengths matching electron transitions across the band gap. The band gap of the polymer is dependent on the structure of the polymer, which determines the conjugation length. A long conjugation length, i.e. large degree of electron delocalisation, yields a small band gap. By introducing different side groups along the polymer, the band gap can be tuned. Adding electron donating or withdrawing side groups allows the overall electron affinity of the polymer can be controlled. Adding more or less bulky side groups can control the conjugation length along the polymer. In addition to these factors, inter-polymer overlap of orbitals may contribute to the resulting electronic band. At low doping levels different low energy features become visible in the absorption spectra, caused by the polarons created. By further doping to bipolarons (causing bipolaron bands) the absorption at low energy is increased while the peaks widen. At high doping levels, the wide absorption at low energies is often called the free carrier tail since it originates from absorption by the free charge carriers.

Some conjugated polymers have a band gap greater than 3 eV. These materials are transparent in the non-doped state (absorption occurs in the ultravioletregion), while they have a deep colour in the doped state. The doping/dedoping behaviour of conjugated polymers can be studied and characterised by using various spectroscopy techniques and measuring the conductivity.



3.2 THE POLARON

We already said that conjugation is require in order to have charge transport in organic molecues. a charge moving in a conjugated molecule, interact with the molecule itself, creating a deformation of the molecule.

Such deformation is called POLARON

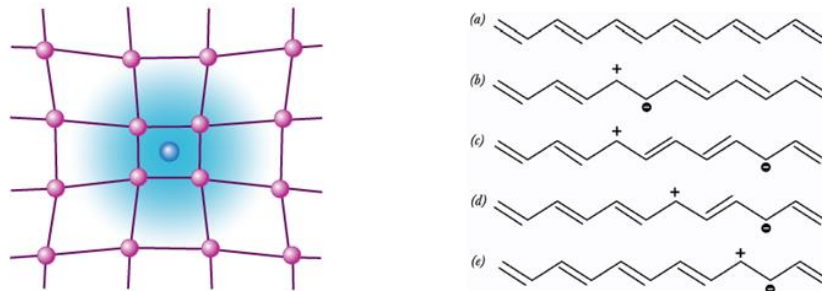


Figure 3.4: the polaron

In other words, in a conjugated molecule, a charge moving is self-trapped within the molecule due to the induced deformation of the surrounding. this process leads to a localized energetic state within the band gap of the material, i.e. between HOMO and LUMO.

The polaron can be seen as a new charge, a free charge moving in a conjugated system but with a high mass

- $m_{\text{eff}}(\text{polaron}) \gg m_{\text{eff}}(\text{free electron})$
- $\text{mobility}(\text{polaron}) \ll \text{mobility}(\text{free electron})$

Mobility, conductivity, in a conjugated molecule is generally small

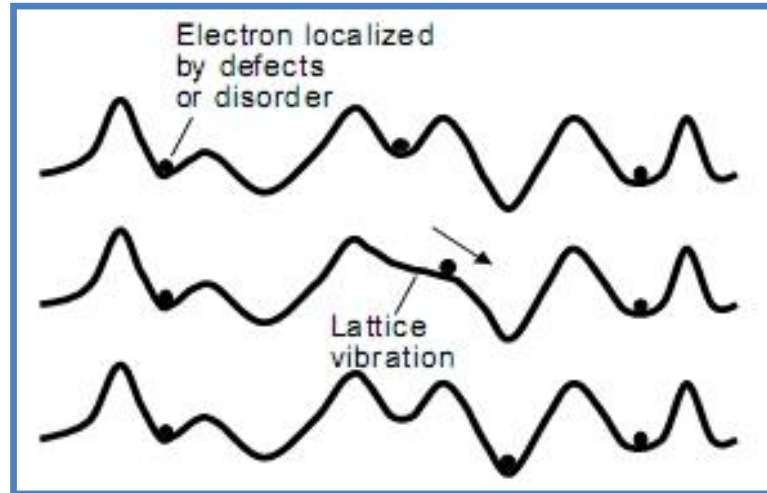
Actually, in all the systems where a charge is moving will exist a polaron, also if we consider a free electron moving in a period crystal structure. In inorganic crystal such effect is present but so small that can be not taken into account. On the contrary, in conjugated molecules, we have covalent bonds which are relatively weak, Van der Waals interactions, therefore, the electric field created by a moving charge can deform such bond, i.e. can deform the molecule, therefore, the polaronic effect is much more evident.

The molecule could be considered as the sheet and the ball as a charge carrier. The way the ball deforms the sheet could be different, depending on the mass of the ball, but also on the way this sheet is stretched.

- If the charge interaction radius is bigger than the atomic distance, we speak about **LARGE POLARONS** → band like transport.
- If the charge interaction radius is smaller than the atomic distance, we speak about **SMALL POLARONS** → thermally activated transport - hopping

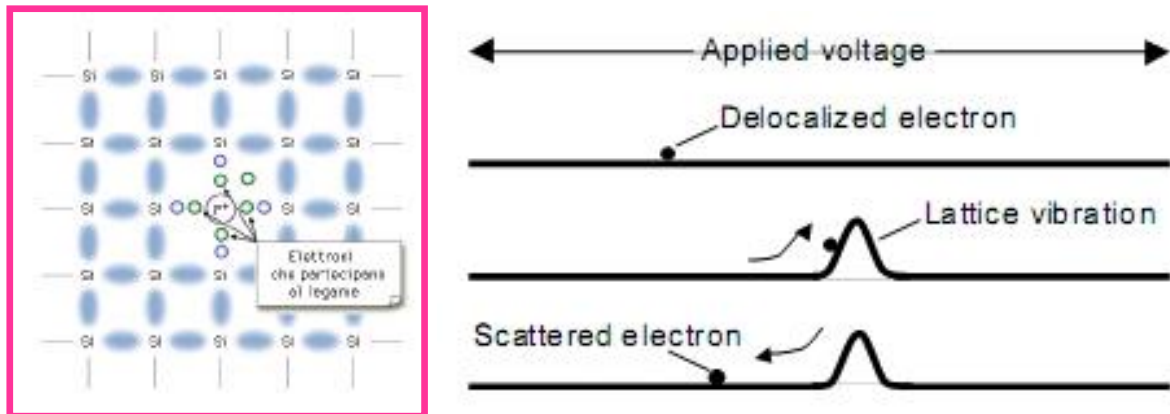
A charge carrier (polaron) moving in a molecule is self-trapped, there is a localized state. In order to move from one state to another, we have to spend some energy in order to allow it to make an energetic jump, i.e. hop from one state to another. This hops are allowed as long as in the molecule there is conjugation.

Note that in a film we have also to consider the charge transfer between different molecule



3.3 CHARGE TRANSPORT IN ORGANIC MATERIALS: INORGANIC VS ORGANIC

Inorganic semiconductors such as Si or Ge, atoms are held together by very strong covalent bonds and charge carriers move as highly delocalized plane waves in wide bands and usually have very high mobility. In these materials, charge transport is limited by scattering of the carriers, mainly on phonons, that is, thermally induced lattice deformations.



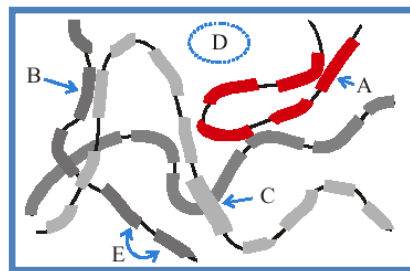
- Perfect crystal structure
- continuous bands
- Scattering limited:
 - Impurities*
 - Phonons*
- **Mobility decreases with Temperature**

This model is no longer valid for low conductivity materials as organic semiconductors. The weak intermolecular interaction forces in these materials, most usually Van der Waals interactions, lead the vibrational energy of the molecules to reach a magnitude close to the intermolecular bond energy at or above room temperature. In this case, the mean free path of charge carriers can be smaller than the mean atomic distance and transport occurs by hopping of charges between localized states. The main difference between the two cases is that in the former charge transport is limited by phonon scattering, whereas in the latter, it is phonon assisted. According to this, charge mobility increases with temperature and is generally thermal activated. One indubitable point is that charge transport in organics is directly connected to the structural characteristics of the organic film, either in the small scale, such as molecular packing, or in a large scale as grain nucleation within the film. Generally, it can be divided into three levels: i) charge transport within the same molecule (intra-chain); ii) charge transport between two close molecules (inter-chain); iii) charge transport between two close domains, usually called grains (inter-grain). There are several methodologies employed for estimating the electrical properties in organic films, i.e. charge carrier mobility. Many groups use to make Time of Flight (TOF) and Hall Effect measurements, which can give a clear indication of charge transport in the bulk of the material, but the most employed method, which is the one we will use during this thesis, is employing the deposited semiconductor film as active layer in a Field Effect Transistor and measure the channel mobility.

Unfortunately, compared to the tremendous progress that organic electronics has known during the past years, the theory of charge transport has scarcely evolved. However, several models have been developed, but a universal theory which can describe properly charge transport in organic materials does not exist and transport properties are still not fully explained. In the following sections a brief introduction to the most used models will be given.

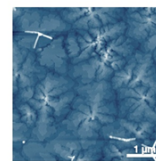
In organic materials, there is a very low molecular crystal degree: polycrystalline or amorphous films. Randomly oriented molecules that interacts with very small forces (*Van Der Waals*) this means that charge carriers, free mean path could be smaller than interatomic distance!

Worse delocalization, charge carriers moves through localized energetic states → Hopping charge transport.

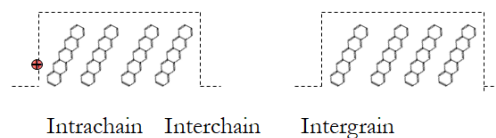


Morphological/structural properties of the organic semiconductor thin film:

- Low crystallinity
- Hopping transport
- Phonon assisted → thermal activation
- Transport through three different levels



Pentacene su SiO₂

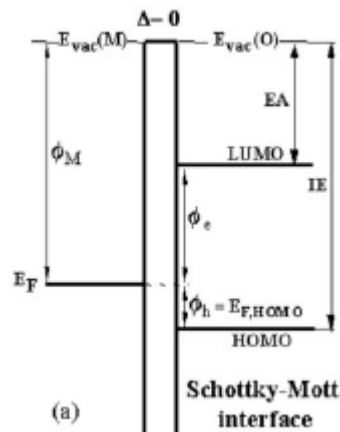


- 1) Molecular packing (pi-stacking)
- 2) Domains structure

3.4 A CONSIDERATION ON CHARGE CARRIERS IN ORGANIC SEMICONDUCTORS

Differently than the inorganic counterparts, organic semiconductors are typically ambipolar. It means that both kinds of charge carriers can be injected into such molecules and transported in along the molecular film.

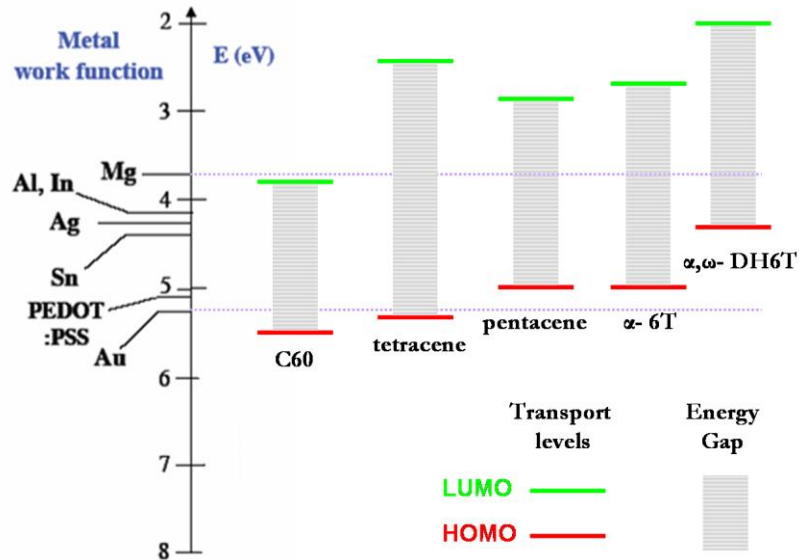
We have previously define the concept of HOMO and LUMO, which correspond to the upper limit of the valence band and the lower limit of the conduction band respectively. In order to have efficient charge transport, since such materials have and intrinsic very low concentration of carriers, the most of the carriers needs either to be generated by doping, as previously discussed, or injected by the electrodes the device is made with. Let's define the Hole Injection Barrier (HIB) as the energetic distance between the metal work function and the HOMO and as Electron Injection Barrier (EIB) as the energetic distance between the metal work function and the LUMO.



HIB and EIB can be very easily obtained by considering the Schottky-Mott model. However, as we will see in the following section dedicated to metal semiconductor interface, such model is rarely valid in metal/organic interfaces, as some chemical/physical phenomena generally take place changing completely this picture. In any case, once HIB and EIB are known (note that they can be measured very precisely using different experimental methods) it can be clearly understand if the specific system (metal/semiconductor) is more suitable for electron or hole injection and transport.

Very simply, the same organic semiconductor can transport holes if it is interface with a metal capable to form a small HIB, whereas, on the contrary, it will be able to transport electrons if it is interfaced with a metal capable to for a small EIB.

In any case, the Schottky-Mott model is usually taken as a reference model to start with in the initial engineering of organic electronic devices.



3.5 CHARGE TRANSPORT MODELS

3.5.1 The small polaron model

A slow moving electron in an organic semiconductor, interacting with lattice ions through long-range forces will permanently be surrounded by a region of lattice polarization and deformation caused by the moving electron. As introduced before, a polaron results from the deformation of a conjugated chain under the action of a charge. In other words, in a conjugated molecule, a charge is self-trapped by the deformation it induces in the chain and it is described by the formation of localized states in the gap between HOMO and LUMO. One model to describe charge transport in organic materials is the small polaron model introduced by Holstein. The problem generally consists in solving a (low-electron-density) Hamiltonian of the form:

$$H = H_e + H_{pol} + H_{e-pol}$$

where H_e describes the energy of the charge carriers in the unpolarized molecular material, H_{pol} represents the energy of the induced polarizations in the local environment and H_{e-pol} describes the interaction energy between the charge carriers and their surrounding polarizations. Besides the different methods that can be used to solve this Hamiltonian, the main differences between the various reported research works concern the simplifications that are made in the second and third term of the Hamiltonian. For simplicity, most authors choose to focus their calculations on only one of the three polarization processes, i.e. they study the electronic polaron (or Coulomb polaron), or the molecular polaron, or the lattice polaron. In Holstein model, the lattice energy is given by a sum of N harmonic oscillators that vibrate at a unique frequency ω_0 :

$$E_L = \sum_{n=1}^N \frac{1}{2M} \left(\frac{\hbar}{i} \frac{\partial}{\partial u_n} \right)^2 + \frac{1}{2} M \omega_0^2 u_n^2$$

where, u_n is the displacement of the n_{th} molecule from its equilibrium position, and M is the reduced mass of each molecular site. The electron-lattice coupling is given by:

$$E_k = E_0 - 2J \cos(ka)$$

$$\varepsilon_n = -A u_n$$

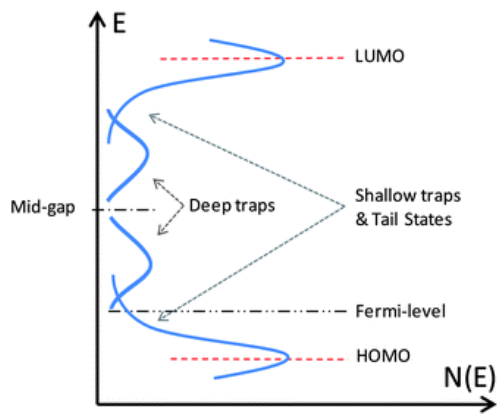
here J is the electron transfer energy, a is the lattice constant and A is a constant. An important parameter is the polaron binding energy E_b which is defined as the energy gain of an infinitely slow carrier due to the polarization and deformation of the lattice.

$$E_b = A^2 / (2M\omega_0^2)$$

The mobility of the small polaron is calculated by solving the time dependent Schrodinger equation. Its upper limit is given by the following equation, where it is worth to point out that the term ea^2 / \hbar has the dimension of a mobility and it is very close to $1\text{cm}^2/\text{Vs}$ in most molecular crystals.

3.5.2 Hopping Transport

The absence of an ideal 3D periodic lattice in disordered organic semiconductors does not allow to describe charge carrier transport in terms of band conduction. In this case, charge carriers move between localized states, and charge transfer is generally described in terms of hopping transport, which is a phonon-assisted tunnelling mechanism from site to site. This phonon-induced hopping mechanism was suggested by Conwell and Mott. Later, Miller and Abrahams proposed a hopping model based on a single-phonon jump rate description.

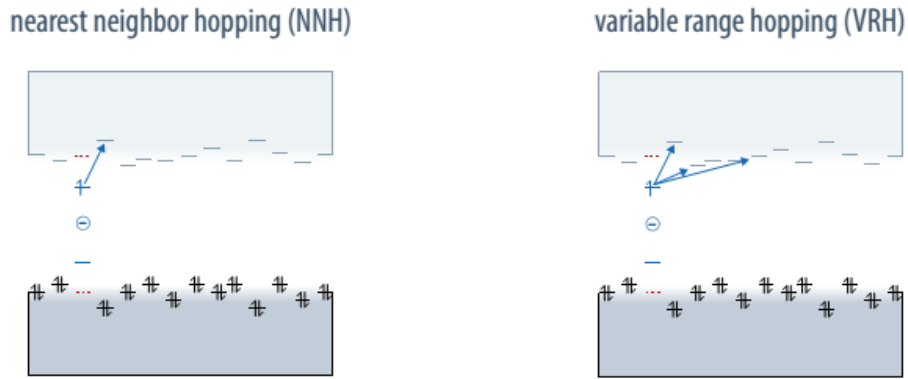


The localized states are shallow impurity levels. The energy of these levels stands in a very narrow range so the probability for a charge carrier on one site to find a phonon to jump to the closest site is high. The model predicts that the hopping rate between an occupied site i and an adjacent unoccupied site j , which are separated in energy by $E_i - E_j$ and in distance by R_{ij} is given by:

$$W_{i,j} = v_0 \cdot \exp(-2\Gamma R_{i,j}) \begin{cases} \exp(-\frac{\varepsilon_i - \varepsilon_j}{k_B T}) & \varepsilon_i > \varepsilon_j \\ 1 & \varepsilon_i < \varepsilon_j \end{cases}$$

where, Γ^{-1} quantifies the wavefunction overlap between the sites, v_0 is an empirical pre-factor, and k_B is the Boltzmann constant. Depending on the structural and

energetic disorder of the system, it can be possible that a charge carrier finds more favourable to hop over a larger distance with a lower activation energy than over a shorter distance with a high activation energy.



The starting point for the VRH model is a highly disordered energetic and spatial configuration of the semiconductor. No long range ordering (translation symmetry) such as in Si single crystals is present. As there is no repetition of unit cells, no periodic potential and so no Bloch states exist, which would lead to some band structure with conduction bands. Instead only localized states exist, described by two distributions:

- energy distribution describes the DOS that gives the probability for a certain binding energy of a charge in a trap site.
- spatial distribution accounts for the variable spacings of the traps sites with respect to the ideal repetitive points in a crystal

These two types of disorder are also called diagonal disorder in the case of energy variance, and off-diagonal disorder in the case of positional disorder. The names originate from the hopping matrix of neighboring sites. Note that not all hopping models take spatial distribution into account.

Conduction happens through hopping between the states. It is assumed that coupling of the charge to molecular modes is weak (molecular deformation energy as in the polaron model is not considered), thus the activation energy reflects the energetic disorder of the sites. Energy differences of the states result in absorption or emission of phonons. The probability for successful hopping is given by

$$\gamma_{ij} = \begin{cases} \gamma_0 e^{-\frac{2R}{R_0}} e^{-\frac{E_j - E_i}{k_b T}} & \text{for } E_j > E_i, \\ \gamma_0 e^{-\frac{2R}{R_0}} & \text{for } E_j \leq E_i, \end{cases}$$

where γ_0 is some weakly temperature dependent material constant. This equation is often referred to as Miller-Abrahams formula. The delocalization radius depends on the state energy:

$$R_0(E) = \sqrt{\frac{\hbar^2}{m(E - E_C)}}$$

where E_C is the conducting band edge energy (or some equivalent when no band conductivity exist). Note that tunneling conductivity between traps with the same energy is not temperature dependent. It could become the dominant charge transport mechanism at very low temperatures. The emission of phonons is necessary to remove excess energy, when hopping to a low energy trap site. The probability for emission is assumed to be equal to one, but if larger energy differences in the order of 2 eV are present, this approximation no longer holds. The mobility would then be more strongly temperature dependent.

Mott has calculated the conductivity for a constant DOS

$$\sigma(T) = \sigma_0 e^{-(T_0/T)^{1/\alpha}}$$

α between 1 and 4

An extension to the Miller-Abrahams model was introduced by Vissemberg and Matters, and describes the temperature and gate voltage dependence in OFETs introducing a percolation model based on VRH in an exponential density of states.

$$\sigma(\delta, T) = \sigma_0 \left[\frac{\pi N_t \delta (T_0/T)^3}{(2\alpha)^3 B_c \Gamma(1-T/T_0) \Gamma(1+T/T_0)} \right]^{T_0/T}$$
$$\delta(x) = \delta_0 \exp \left[\frac{qV(x)}{kT} \right]$$

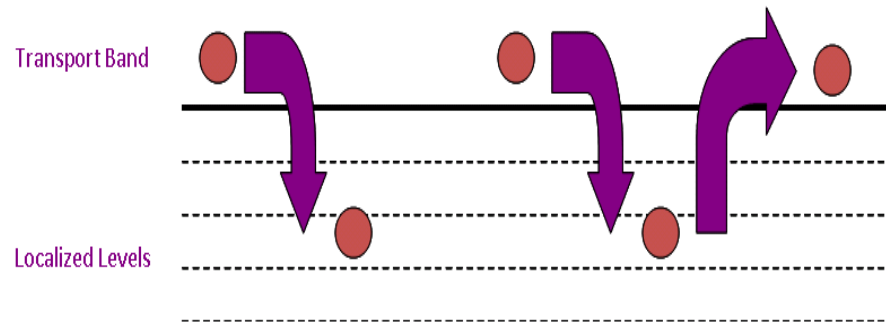
3.5.3 Multiple Trapping and Thermal Release (MTR)

Some studies have demonstrated that also in some organic systems band like transport can occur. In fact, it can happen when the molecular order is very high, as in molecular single crystals, the structure is almost defect free, with a much lower concentration of trap states. Therefore, a new model must be provided.

MTR model was developed by Shur and Hack to better describe charge transport in amorphous Afetrwards Horowitz extended such model also for organics.

They assumed that traps are not homogeneously distributed within the semiconductor film, but are mostly localized in the grain boundaries. In this model the organic semiconductor film consists of crystallites which are separated from each other by amorphous grain boundaries. In the crystallites charge carriers can move in delocalized bands, whereas in the grain boundaries they become trapped in localized states. The trapping and release of carriers at these localized states results in a thermal activated behaviour of the field effect mobility, which depends on the gate voltage. In other words, the model says that charge transport happens in extended states, but the most of the involved charge is trapped in localized states in the band gap. The MTR model takes into account that charge transport happens through three transport levels:

- Transport
- Trapping
- Charge release

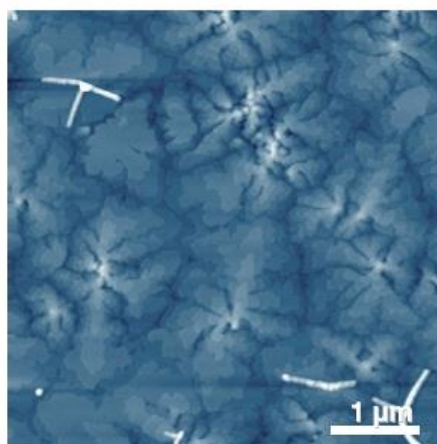


Charge transport is limited by the presence of localized states which are very close to the HOMO and LUMO. These states are due to defects, impurities etc.

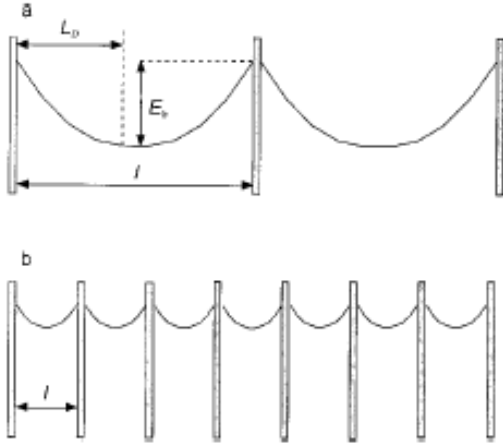
Charge carriers are trapped during their transition and are released afterwards thanks to thermal energy. Release dynamics depend on temperature, but also on the energy position of the state. As already said, temperature assists charges release from traps, also conferring carriers kinetic energy by means of phonons.

Horowitz describes an organic film as it is characterized by two different regions:

- grains - high molecular order
transport through delocalized bands → *high mobility*
- Grain boundaries - high defects concentration, charge *trapping in localized (back-to-back diode like structure)* → *low mobility*



Pentacene su SiO₂



Let's consider L_D as the Debye length for charge carriers

$$L_D = \sqrt{\epsilon_s kT / q^2 N}$$

A polycrystalline film can be seen in two different ways.

1. when $l < L_D$ Traps are uniformly distributed in the film
2. when $l > 2L_D$ Traps are mainly in the grain boundaries!

Because of defect-induced localized levels in the grain boundaries, back-to-back Schottky barriers are assumed to form at the intergrain regions. Note that L_D only depends on temperature and doping level, and has therefore the same magnitude.

Since the grains are, under the electrical point of view, connected as resistors in series, the total mobility can be given by:

$$\frac{1}{\mu} = \frac{1}{\mu_g} + \frac{1}{\mu_b}$$

where μ_g and μ_b are the mobility in the crystal grain and in the grain boundary respectively. If the defects are mostly located at the grain boundaries, then $\mu_g \gg \mu_b$ and the total mobility is almost equal to the mobility in the grain boundaries. A general assumption is that, due to the presence of defect states in the grain boundaries, a back-to-back Schottky barrier forms at the intergrain region.

According to the back-to-back Schottky barrier picture, the current flowing through a grain boundary at room temperature is limited by thermionic emission.

And mobility can be described as

$$\mu = \mu_0 \exp\left(-\frac{E_b}{kT}\right)$$

Where μ_0 is the defect free mobility value

For large grains ($l > 2L_D$) at low temperatures the transport mechanism is dominated by tunnelling and no thermal activation is required, therefore, the mobility changes in the following way:

$$\mu = \mu_0(T) \exp\left(-\frac{E_b}{E_0}\right)$$

Where E_0 is a constant depending on polaron mass and defects concentration.

At higher temperatures, the processes once again dominate by thermoionic emission and thermal activation of the mobility takes place. In this case, the mobility is given by the following equation where v represents the electron mean velocity.

$$\mu = \frac{q\langle v \rangle l}{8kT} \exp\left(-\frac{E_b}{kT}\right)$$

interestingly, the pre-exponential factor is not related to the mobility in the grain, that is, the mobility in a trap-free material. Such model suggests that the mobility would increase linearly with grain size, and the activation energy E_b can be easily estimated from the temperature dependence of the mobility.

4 CHARGE INJECTION INTO ORGANIC SEMICONDUCTOR

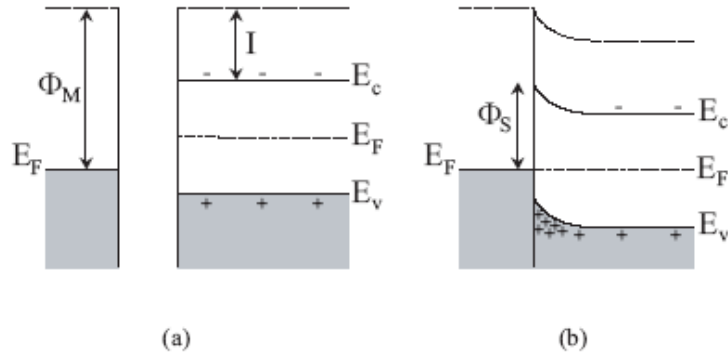
(Taken from Chapter 2 in Physics of Organic Semiconductors, W. Brutting and C. Adachi, Wiley VCH Verlag GmbH)

Charge transport along the active organic semiconductor film is not the only important subject for describing the physical properties of OFETs. Metal/organic semiconductor interfaces are very important and can strongly influence both the type and the amount of charge carrier injected into the channel. In principle, all organic semiconductors should be able to allow both kinds of charge carriers transport. Therefore, achieving n-type or p-type conduction should only depend on the metal employed for the electrodes that should be able to efficiently inject one type of charge carriers into the semiconductor layer. Indeed, charge injection strongly depends on the energy level matching between the Fermi level of the metal electrodes and organic semiconductors energy levels, namely, lowest unoccupied molecular orbital (LUMO) and highest occupied molecular orbital (HOMO).

4.1 MOTT-SCHOTTKY MODEL AND DEVIATIONS

One of the fundamental aspects of the metal/semiconductor interface is the Fermi level alignment, described by the Mott-Schottky model. When a neutral metal and a neutral semiconductor are brought in contact, the Mott-Schottky model predicts that their bulk Fermi levels will align, causing band bending in the semiconductor.

Due to the band bending, a non-Ohmic Schottky barrier can be formed at the interfaces between metal and semiconductor. As a consequence, charge transport can be limited by injection through the Schottky barrier and is characterized by thermal excitation of charge carriers over the barrier, resulting in thermally excited temperature dependence. Mott-Schottky model is generally used as a guideline for choosing the contact metal.



For organic semiconductors the picture is a little bit different.

The function and efficiency of most organic (opto)electronic devices, such as lightemitting diodes (OLEDs), thin-film transistors (OTFTs), and photovoltaic cells (OPVCs), are significantly depending on the electronic structure of the interfaces within the devices. For instance, in OLEDs and OTFTs, charges must be injected from electrodes into the organic semiconductor, which requires that energy barriers for charge injection must be minimized to achieve low operation voltages. Several layers of different organic semiconductors are used in OLEDs to separate charge injection/transport from the region of exciton formation and recombination, which necessitates proper adjustment of the energy levels at such organic heterojunctions to facilitate electron (hole) transport across the interface while holes (electrons) should be blocked simultaneously. The contact between an electron acceptor and an electron donor organic semiconductors represents the most important element of OPVCs because only at that very interface, the exciton dissociation can occur with high probability; once the electron and hole are separated, they can be transported to the respective electrodes. Consequently, the energy levels at these interfaces must be matched to allow optimal charge separation and thus energy conversion efficiency. The key electronic levels and energy parameters of such interfaces are summarized in next Figure. Most commonly, the relative energy positions of electrode Fermi level (E_F) and the highest occupied molecular orbital (HOMO) as well as the lowest unoccupied molecular orbital (LUMO) are used to characterize interface energetics, because these levels predominantly govern charge transport and optical excitations. HOMO and LUMO are the frontier orbitals of the conjugated molecules that comprise

organic semiconductors. In the case of long-chain polymers, these localized orbitals delocalize along the chains, which leads to the formation of one-dimensional bands (in full analogy to those known from inorganic semiconductors). Consequently, one can also use the terms valence band maximum and conduction band minimum when polymeric organic semiconductors are under consideration. The energy offset between EF and the HOMO defines the hole injection barrier (HIB), and that between EF and the LUMO corresponds to the electron injection barrier (EIB). Note that this frequently used terminology is a simplification that results from the way that HIB and EIB are measured by ultraviolet photoelectron spectroscopy (UPS) and inverse photoelectron spectroscopy (IPES), which are the most widely used methods to infer interface electronic properties. These methods do not yield the actual HOMO and LUMO energy positions of the organic semiconductor in the ground state, rather they provide the ionization and electron affinity (EA) levels, that is, the energies required to remove or add one electron to a conjugated molecule. The charged species of organic semiconductor molecules are the structurally and energetically relaxed (on the order of a few 100 meV compared to the neutral molecule energy levels) polarons, which represent the actual charge carriers. Therefore, UPS and IPES return the energy of the positive and negative polarons with respect to EF, that is, the HIB and EIB indeed. Because the polaron levels are directly derived from the respective HOMO and LUMO levels, literature has thus adopted the use of the terms for the ground state rather than the charged state.

As just discussed, the energy level alignment at interfaces in organic electronic devices is crucial to their function and efficiency. Consequently, device engineers long for rules that allow predicting the energy levels in devices based on parameters of the individual materials, such as work function, ionization energy (IE), and electron affinity. For instance, a common vacuum level upon interface formation is often assumed. However, the physics and chemistry of interfaces involving conjugated materials can be rather complex, which causes simple models to predict energy levels of two materials in contact often unreliably and can result in errors on the order of several 100 meV. Thorough fundamental investigations of organic/inorganic and

organic/organic interfaces over the past two decades have enabled, nonetheless, to derive a few general guidelines that – within limits – enable knowledge-based engineering of interface energy levels. In the following sections, some considerations regarding the intrinsic electronic properties of conjugated materials are discussed, followed by the most important physicochemical phenomena occurring upon interface formation, first of organic semiconductors with electrodes and then at organic semiconductor heterojunctions.

While an isolated individual molecule has only one ionization potential, multiple values are generally found for molecules in ordered assemblies. The existence of a surface dipole (SD) built into molecular layers was reported; its origin lies in details of the molecular electronic structure and its magnitude depends on the orientation of molecules relative to the surface of an ordered assembly. As prototypical planar conjugated molecule with an extended p-electron system, the simplest aromatic molecule benzene (C_6H_6) is now used to introduce the general concept of molecular electrostatics. The p-electrons reside in molecular orbitals (MOs) that have a node in the plane of the molecule and extend into space on either side. In contrast, the atomic nuclei and the charge distribution of all other electrons, that is, those residing in core- and s-orbitals, are centered in the molecular plane. This leads to the situation where negatively charged p-clouds on either side of the symmetry plane are compensated by a positive charge within the plane of the overall charge-neutral molecule. This particular arrangement of charges corresponds to a quadrupole, which can also be seen as two dipoles pointing toward each other. A 3D surface plot of the electron potential energy in a plane cutting through the molecule reveals regions of higher potential energy directly outside the negatively charged p-electron clouds, whereas regions of lower potential energy are next to the hydrogen atoms within the plane of the molecule. Importantly, the potential around the isolated benzene molecule converges rapidly (within a few angstroms) in all directions toward one common value, which corresponds to the vacuum level far away from any matter. A molecular solid can thus be represented as an assembly of many such quadrupolar charge distributions, which has profound consequences when the molecules within the solid

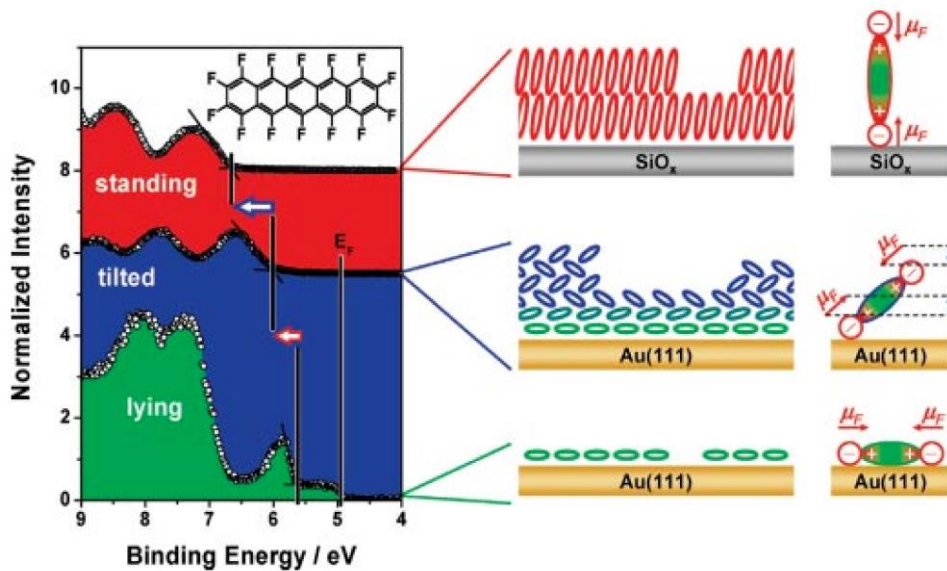
are not randomly oriented but preferentially ordered or even crystalline. The collective surface electrostatic potential created by all molecules will depend critically on the molecular orientation at the surface. For instance, if the benzene molecules are oriented on the surface such that the molecular plane is parallel to the surface (i.e., lying), the electron potential energy just outside the surface (U_{vac}) is raised by the surface-terminating dipolar layer m . Far away from the surface, the electrostatic potential will yet assume the common vacuum level, resulting in a potential well-being present at the surface of the organic solid. Recalling the definition of ionization energy (electron affinity) as the energy required to remove from (attach to) the sample an electron into (from) infinite distance, it transpires that the IE and EA values for this lying molecular surface orientation are increased by the amount of the potential well that electrons have to overcome, resulting in IE_0 and EA_0 .

On the other hand, U_{vac} is lower than the common vacuum level at infinity when the benzene molecules are upright standing at the surface of the solid. Consequently, the values IE_{00} and EA_{00} for such a molecular arrangement are lower than those found for the lying molecule case. The quadrupolar charge distribution of benzene can readily be extended to practically relevant molecules in organic electronics, such as pentacene (PEN) or α -sexithienylene. For ordered molecular layers of these, the differences in IE and EA for lying and standing surface orientation were found to be 0.4 eV.

Numerous molecules have, in addition to the electrostatic quadrupoles resulting from the p-electron distribution, strong intramolecular dipoles that also contribute to the surface electrostatic potential U_{vac} . In addition, molecular orientations different from just lying and standing result on yet other IE and EA values. For example, perfluoropentacene (PFP), which is the completely fluorinated analogue to pentacene, grows lying in the first monolayer on clean metal surfaces. The bottom UPS spectrum in Figure is that of a lying PFP monolayer on Au (111). The first clear peak is attributed to the molecular HOMO with an onset that yields $IE_0 \approx 5.80$ eV. For multilayer PFP, the molecules are still oriented with their long molecular axes parallel to the substrate, but with the molecular plane inclined relative to the surface, that is, the molecules

assume their typical “herringbone” arrangement as in the bulk crystal structure. As the entire molecular periphery is terminated with electronegative fluorine atoms, a surface dipole layer (negative on the outside) is thus formed, which raises U_{vac} above the sample. Consequently, the ionization energy increases to $IE_{tilted} \approx 6.00$ eV.

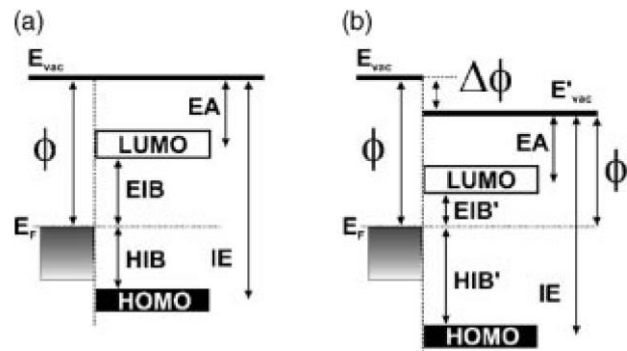
Layers of PFP can be grown with the long molecular axes standing (almost) upright on silicon oxide surfaces, yielding a UPS spectrum as shown in the topmost trace of Figure 2.3. As the projection of the polar F–C bonds onto the surface normal is higher in this case than for the “tilted” molecules, the ionization energy further increases to $IE_{00} \approx 6.65$ eV.



As expected, the situation is now reversed compared to pentacene. There, layers of standing molecules have a lower IE than layers of lying molecules due to the surface dipole caused by the p-electron clouds. In contrast, layers of standing PFP have a higher IE than layers of lying molecules, owing to the presence of intramolecular polar bonds that, collectively, form a surface dipole layer.

Barriers for charge injection at organic/electrode interfaces have commonly been estimated by assuming “vacuum level (E_{vac}) alignment” across the interface (i.e., the Schottky–Mott limit) using values for electrode work function (ϕ) and organic material ionization energy and electron affinity determined separately for individual samples. The neglect of physicochemical processes occurring at such interfaces often results in wrong barrier height (HIB and EIB) values (sometimes more than 1 eV) estimated from

vacuum level alignment, except for justified cases. Instead, significant work function changes Df after the deposition of organic molecules were found, predominantly for atomically clean metal surfaces under ultrahigh vacuum (UHV) conditions. Consequently, the change of f results in concomitantly different HIB0 and EIB0 values compared to vacuum level alignment. Df can have positive or negative sign, depending on the specific materials in contact. The origin of this phenomenon, often also termed “vacuum level shift” or “interface dipole” in literature, is – in general terms – a rearrangement of the electron density distribution at the metal surface and on the molecules due to the mutual interaction at the interface, and thus inducing changes in the electrostatic potential above the surface.

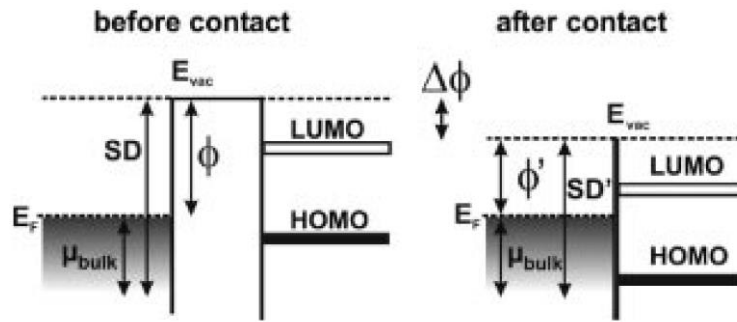


The individual processes that lead to Df can be manifold, and will be discussed in the following. Given that atomically clean metal electrodes in UHV have no practical relevance for fabrication of organic electronic devices, which typically occurs in high vacuum (HV) or inert gas, this section is rather brief, and emphasis will be given to application-relevant electrode materials, which may include a certain level of contamination from ambient.

The interaction between conjugated molecules and clean metal surfaces is a rather complex issue. Despite the huge number of material systems that have been investigated, no generally applicable rules to predict the energy level alignment have yet emerged. The possible types of interaction could be classified into physisorption (van der Waals) or chemisorption with certain degrees of charge transfer and covalent bond formation. A physisorbed molecule retains its chemical integrity and orbital structure upon adsorption. If chemisorption occurs, the ordering of orbitals of the adsorbed molecule differs from that of the free (gas phase) molecule, due to

hybridization with electron wave functions of the metal and a change in orbital population. Chemisorption can often be readily identified due to the appearance of a new density of states (DOS), for instance, in UPS and IPES experiments, different from those of the bulk molecular solid and the clean metal.

For the case of weak (physisorptive) organic-metal interaction (e.g., occurring at many interfaces between conjugated organic materials and clean Au), a qualitative picture of the interface energetics is shown in Figure. On the left-hand side, the clean metal surface and the molecule with its LUMO and HOMO levels are at large distance without interaction. The metal ϕ has two contributions: the bulk chemical potential of electrons relative to the mean electrostatic potential inside the metal. The height of the injection barrier will be given by the difference between the metal Fermi level and the HOMO or LUMO levels of the organic semiconductor for holes and electrons respectively. According to this, gold is generally used for the realization of p-type organic transistors, since its relatively high work function (5.1 eV) forms a low hole injection barrier with the most common organic semiconductors (i.e. pentacene, sexithiophene, dihexylsexithiophene). On the other hand, low work function metals, as calcium (i.e. 2.9 eV) are generally used as electron injectors. There are several aspects that can modify the Mott-Schottky-type of band bending. One of these is the formation of surface dipoles at the interface between the metal and the organic semiconductor. The large interface dipole was explained by the change of the surface dipole of the metal upon adsorption of the molecule. A metal surface is characterized by an electron density tailing from the free surface into vacuum. Adsorbed molecules tend to push back these electrons, thus reducing the surface dipole and decreasing the work function of the metal that can induce a vacuum level shift that can change the barrier height as carefully explained by Kahn et al.



μ_{bulk} and the surface dipole SD , which is due to electrons spilling out into the vacuum at the free surface; thus, $f = \mu_{\text{bulk}} + SD$. The HIB/EIB could easily be estimated from f and IE/EA assuming vacuum level alignment. However, it is observed that after contact (i.e., molecule adsorption), f is reduced by Df to f_0 , which leads to a higher HIB₀ and lower EIB₀ than expected. Effectively, the SD of the clean metal surface is reduced to SD_0 due to the “pushback effect”; the adsorption of the organic molecule “pushes back” the electron density of the metal surface that was spilling out into vacuum. The magnitude of the metal surface electron pushback depends on the details of how the molecules adsorb on the surface, for example, on the molecule conformation, bonding distance, and surface density. Typical values of Df for clean Au electrodes upon organic semiconductor deposition are in the range of 0.5–1.2 eV. Since f of clean Au in UHV is typically 5.4 eV, this means that the effective f of a gold electrode after molecule adsorption is only 4.2–4.9 eV, that is, much less favorable for hole injection than expected. On other metal surfaces, such as Ag and Cu, Df is typically on the order of 0.5 eV. Purely physisorptive interactions between conjugated materials and these metals, as well as those with even lower intrinsic work function are found only in rare cases because of the higher chemical reactivity of such metals. The exact change in total electron density distribution upon pushback at the organic–metal interface can be rather complex, and even more so when strong chemical interactions occur. In the following, a prototypical example for strong conjugated molecule–metal interaction is discussed. We consider the conjugated molecule tetrafluoro-tetracyanoquinodimethane (F4TCNQ) with an IE of 5.24 eV on a Cu(111) surface with a f of 5.0 eV. Assuming a common vacuum level at this interface would place the LUMO of F4TCNQ below the Fermi level (E_f) of Cu, that is, the lowest

unoccupied level of the molecule being below filled states of the metal. In the Schottky–Mott limit, this is thus a nonequilibrium situation, and charge transfer across the interface is needed to establish equilibrium. In the simplest possible model for interface charge transfer, one- or two-electron transfer from the metal into the LUMO of F4TCNQ may be assumed, resulting in the molecular negative polaron (anion) or bipolaron (dianion), with the now (partially) filled LUMO shifted below E_F . Photoemission spectroscopy in conjunction with theoretical modeling indeed showed that a new DOS just below E_F appeared upon F4TCNQ deposition on Cu(111), which can be derived from the filled molecular LUMO (Figure 2.6a). Since this DOS did not cross E_F , which is expected for a negative polaron state, it can be concluded that the LUMO is filled with two electrons, that is, bipolarons might be formed. The negatively charged molecule and the positive charge remaining in the metal result in a reaction-induced surface dipole, whose magnitude can be estimated by taking into account a typical binding distance of conjugated molecules on metal surfaces of 2.5 Å. Using the Helmholtz equation,

$$\Delta\phi = \frac{eN\mu}{\epsilon_0\epsilon}$$

which relates a dipole induced the surface work function change D_f to the area-density of dipoles (N) and the dipole moment (μ) (with elementary charge e , relative permittivity ϵ , and vacuum permittivity ϵ_0), D_f for a full monolayer of F4TCNQ on Cu(111) can be estimated to be about 5 eV. However, the experiment yielded a D_f of only 0.6 eV, evidencing that the simple model employing one- or two-electron transfer is not adequate. Two important phenomena occurring at this interface are missing: details of the adsorption-induced interfacial charge density rearrangement and the molecular conformation changes. The chemical interaction between F4TCNQ and Cu(111) is thus far more complex. Detailed theoretical modelling showed that a strong hybridization of (also deep lying) molecular orbitals and metal states occurred, involving bidirectional charge transfer across the interface. This is represented through the orbital occupation analysis in Figure 2.6b, where the calculated DOS of the interacting molecule/metal system was partitioned into contributions from the

molecular orbitals of the isolated molecule, and the degree of occupation of the individual orbitals was obtained via integration of the projections up to the calculated EF. This reveals that the original empty LUMO p-electron orbital of F4TCNQ becomes filled to 90% (1.8 electrons) through charge transfer from Cu, but at the same time deeper lying s-orbitals become depleted of electrons. Summing over all molecular orbitals, the net charge on F4TCNQ is only 0.6 electrons. Furthermore, the molecule does not remain planar upon adsorption on the metal surface, but it becomes significantly distorted, as schematically shown in Figure ©. The negatively charged cyano groups of the molecule are bent toward the metal, which induces a dipole that actually counteracts that of the net charge transfer. This conformation effectively decreases the work function. In conjunction with the dipole due to charge transfer (the bond dipole BD), the calculated D_f is 0.7 eV, in good agreement with the experimental value of 0.6 eV.

It is important to emphasize that many studies on organic/metal interfaces, similar to the ones mentioned, were conducted starting from atomically clean metal surfaces in UHV (residual pressure $<10^{-9}$ mbar), which is markedly different from the situations that prevail during the actual organic device fabrication. In high vacuum (typically 10^{-6} mbar) or inert gas atmospheres, and also in air, any surface is covered with about a monolayer of various molecular species (e.g., hydrocarbons, oxygen, and water) within seconds. As shown above, even physisorbed molecules induce significant changes of f . In addition, some adsorbed species may have permanent dipoles with some preferred orientation relative to the surface, leading to additional f changes (D_f) according to the Helmholtz equation. For instance, while an atomically clean Au surface has a f of 5.4 eV in UHV, it drops to 4.5–4.9 eV after exposure to HV or air, as a rule of thumb (the exact value will depend on the composition of the actual atmosphere). For more reactive metals, the formation of a surface oxide proceeds rapidly, forming a comparably inert interlayer, which electronically decouples molecules and metal. Molecules or polymers deposited on such “dirty” metal surfaces exhibit an energy level alignment that is markedly different from that obtained on clean surfaces in UHV. As a consequence, energy level alignment mechanisms differ

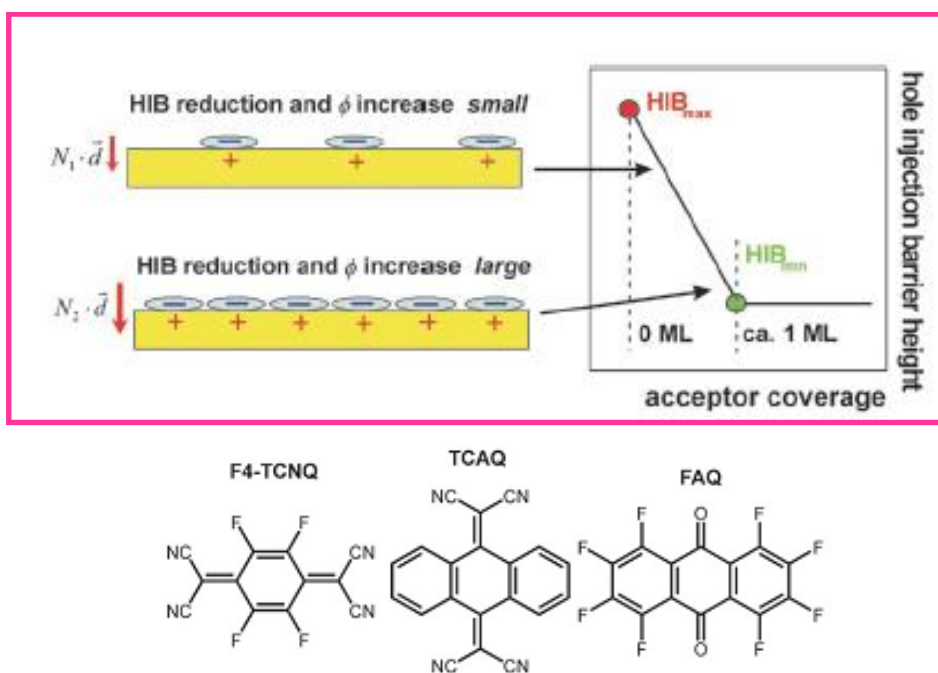
from those of atomically clean metals, and the chemically more inert character of contaminated metals even permits employing rather simple rules for energy level alignment at organic/electrode contacts. Another kind of “contamination,” however, introduced on purpose, can significantly lower the HIB at organic/Au interfaces: the exposure of Au surfaces to UV/ozone. Such treatment leads to the formation of a thin surface Au oxide layer that is accompanied by the adsorption of oxidized hydrocarbon species. This combination leads to an increase of ϕ to up to 5.5 eV, that is, even larger than ϕ of clean Au in UHV, which is stable in air for up to an hour. When depositing conjugated molecular materials or polymers onto UV/ozone-treated Au, the HIB can be reduced significantly (e.g., by 1.4 eV for the blue electroluminescent organic semiconductor p-sexiphenyl) compared to both atomically clean and air-exposed Au. Furthermore, the energy level alignment achieved after deposition of the organic semiconductor layer is remarkably stable even in air over many days. Contrary to that, an organic/metal interface that was fabricated under UHV conditions changes its energy levels upon exposure to air, mainly because oxygen and/or water can diffuse through a thin organic film toward the metal, and thus modifies its effective work function.

4.2 STRONG ELECTRON ACCEPTORS

A method that allows continuous adjustment of HIBs at organic/metal interfaces is the precoverage of the metal surface with strong electron-acceptor molecules. The chemisorption of such acceptors is accompanied by an electron transfer from the metal to the molecule, thus introducing local dipoles with their negative ends oriented away from the surface and increasing ϕ . The area-averaged work function of a metal surface can thus be adjusted by controlling the area density N of such dipoles. If depolarization effects are small, there exists a linear relationship between the effective ϕ and the molecular coverage from zero to about one monolayer. Subsequently deposited conjugated organic molecules feel this modified average surface potential, and the energy levels are shifted relative to E_F accordingly. For electron acceptors, the occupied levels of virtually any organic material deposited on top of this modified

metal surface shift rigidly towards EF, thus reducing the HIB. Any value for HIB between the two extreme values HIB_{max} (pristine metal surface) and HIB_{min} (ca. monolayer acceptor coverage) can be adjusted predictably by choosing the appropriate acceptor coverage. Specific cases that demonstrated the general applicability of this approach to reduce HIBs towards molecular semiconductors include tetrafluorotetracyanoquinodimethane (F4-TCNQ; on Au, Ag, Cu), tetracyanoanthraquinodimethane (TCAQ; on Ag), and octafluoroanthraquinone (FAQ; on Au and Ag). The largest reduction of the HIB achieved with this method so far was 1.2 eV for p-sexiphenyl on F4-TCNQ-precovered Au.

The shift can be tuned using different molecules or controlling the density of the molecules on the metal surface.



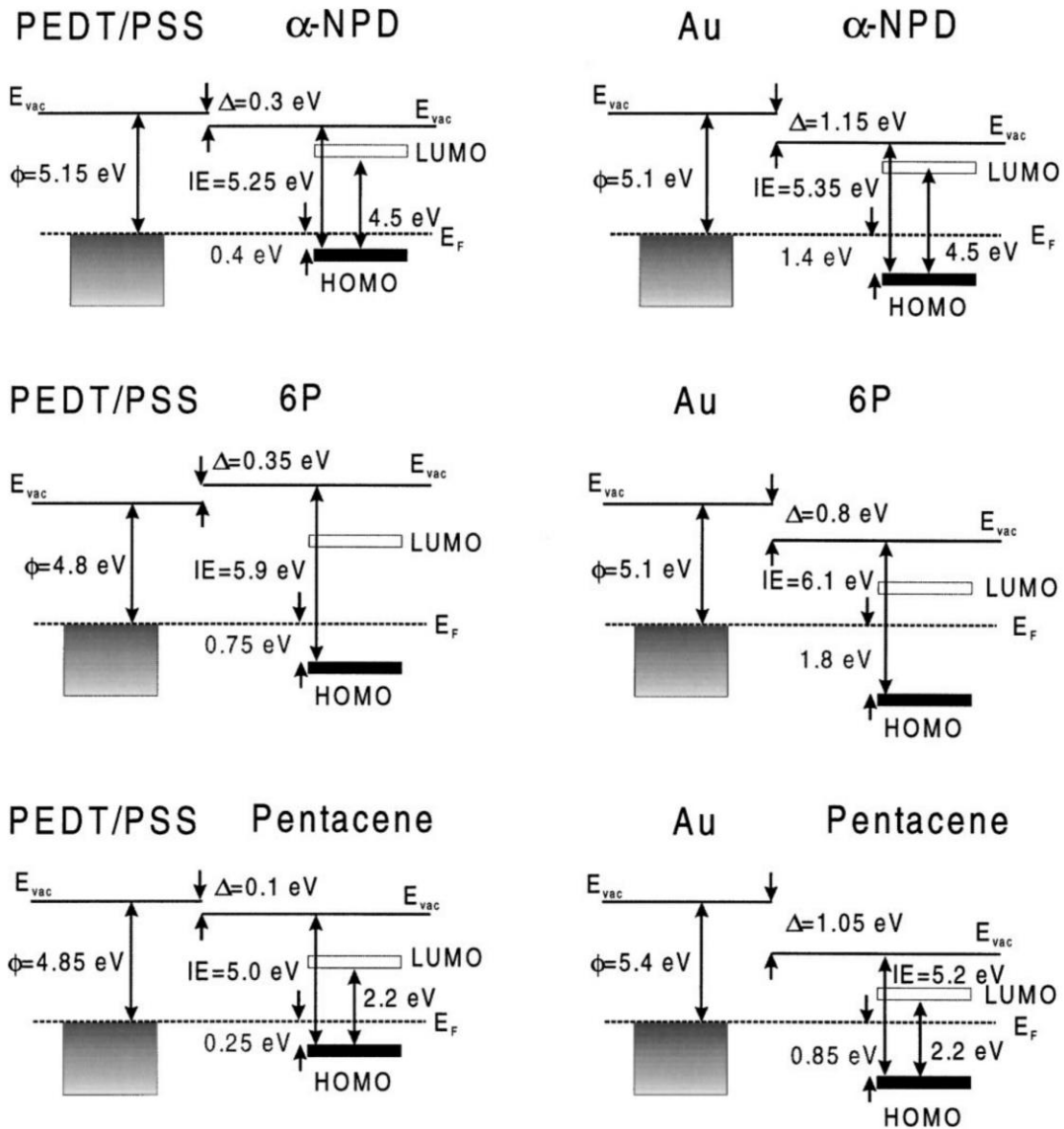
4.3 THE CASE OF CONDUCTIVE POLYMERS

We have already discussed about the fact that the electronic structure of most metal-organic molecular semiconductor interfaces departs from the simple Schottky–Mott limit and exhibits a substantial deviation of about 0.5–1.0 eV of the interface dipole barrier. Recent experimental and theoretical studies have suggested that a significant fraction of the interface dipole barrier at organic-on-metal interfaces corresponds to a

lowering of the metal ϕ by the adsorbed molecules. Indeed, the work function of a metal is comprised of both bulk and surface-dipole contributions the latter corresponding to the tail of electrons spilling out from the metal surface into the vacuum. This surface-dipole contribution is always substantially modified by the presence of an adsorbate. In the case of large adsorbates, such as conjugated organic molecules, the repulsion between the molecule electrons and the metal surface electrons leads to a compression of the electron tail leading to a lowering of the metal work function. This, in turn, causes an abrupt downward “shift of the vacuum level” from the metal to the organic film at the interface, i.e., a surface dipole barrier. The consequence of this systematic lowering of the metal ϕ is a downward shift of the molecular energy levels and an increase in the energy difference between the metal Fermi level (E_F) and the highest occupied molecular orbital (HOMO) of the organic film. The hole injection barrier is, therefore, systematically increased with respect to a vacuum level alignment situation, with the unfortunate consequence of a significant reduction in current injection performance. The reduction in metal work function being difficult to assess, a reliable prediction of the injection barrier is also difficult. On the other hand, a conducting organic polymer like PEDT/PSS is made of closed-shell molecules and has much fewer free electrons than a metal like Au. Its work function does not have a significant surface electron tail contribution and should not undergo the type of modification just described. This, in turn, should enable the formation of smaller hole injection barriers at a contact with a conjugated organic material (COM), as compared to a contact with a high work function metal.

A clear example is reported hereafter, where the hole injection barriers, measured directly with ultraviolet photoemission spectroscopy (UPS), at interfaces between three organic molecular materials and two high work function electrode materials, namely Au and PEDT/PSS, are reported. The three organic materials are N,N8-bis-~1-naphthyl!- N,N8-diphenyl1-1,1-biphenyl1-4,48-diamine (a-NPD), used as a hole transport layer in many organic light-emitting devices, pentacene, used as active material in field-effect thin-film transistors, and para-sexiphenyl (6P), which can be employed in both types of devices. The idea is to directly measure the HIB using two

different electrodes with very similar work functions. Meaning that, in principle, for all the three molecules employed in the study, a very similar HIB should be obtained. As it can be clearly seen, the fact that PEDOT:PSS is not a metal but a conductive molecular electrode, leads to a very different picture.



The explanation for the large interface dipole observed at the COM/Au interfaces is the change of the metal surface dipole contribution to the work function upon adsorption of the molecules. The electron density tailing from the free surface into vacuum is pushed back into the solid upon adsorption, thus reducing the surface dipole and effectively decreasing the work function of the covered surface. This leads to the relatively large interface dipole and fh values, in spite of the large

initial electrode ϕ . In contrast, the work function of PEDT/PSS is mainly controlled by the energy levels created by the charge transfer between the sulfonate and the ethylenedioxythiophene moieties. This charge transfer does lead to dipoles within the polymer, but they have random orientation and cancel each other macroscopically. The surface electron dipole layer contribution to the work function is minimal and the adsorption of molecules modifies only slightly the work function of the polymer. The resulting interface dipole barriers Δ and the hole injection barriers Φ_h are, therefore, systematically smaller (by 0.6– 1 eV) than those measured for the metallic electrode.

5 ORGANIC FIELD EFFECT TRANSISTORS (OFETs)

5.1 OFET MODEL

The interest for Organic Field Effect Transistors (OFETs) has drastically increased over the past few years, and they have been intensively studied for many applications such as displays, smart tags and sensors. The reason for focused research interest in the field of “plastic electronics” is the opportunity to produce low cost devices on plastic substrates on large areas, opening, indeed, an entire new market segment. So far, field effect mobilities up to $30 \text{ cm}^2/\text{Vs}$ have been reported for thin film and single crystal OFETs. However, this value is usually lowered by at least one order of magnitude for organic transistors made on plastic substrates. OFETs are close relatives of the classic Metal Oxide Semiconductor Field Effect Transistors (MOSFETs); typically, since the organic semiconductors are characterized by a low conductivity if compared to inorganic ones, Thin Film Transistor (TFT) architecture is preferred in this case. The core of an OFET is a Metal-Insulator-Semiconductor structure (MIS), which can in principle be considered as a parallel plate capacitor: the two capacitor plates are formed by a metal electrode, called gate electrode, and a semiconductor, which are separated by a thin insulating film, called gate dielectric. Two additional electrodes, called Source and Drain electrodes are patterned in order to contact the organic semiconductor allowing to probe the conduction across the organic film.

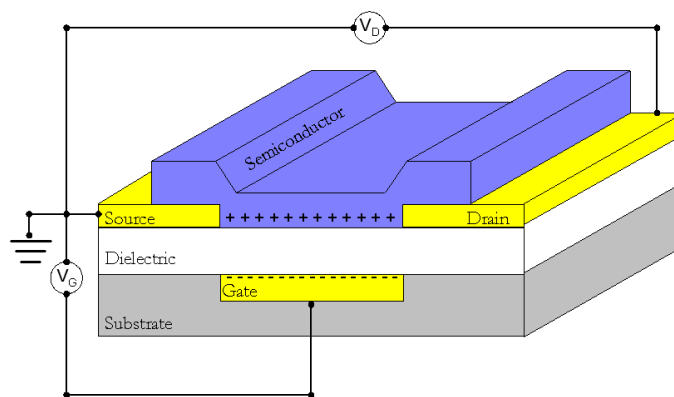


Figure 5.1: Schematic of the OFETs geometry.

One of the main differences between an OFET and the classic MOSFET is that while the latter typically works in inversion mode, OFETs usually work in accumulation mode. When a negative (positive) voltage is applied between the gate and the source electrodes, an electric field is induced in the semiconductor attracting positive (negative) charge carriers at the semiconductor/insulator interface between source and drain electrode and overlapping with the gate. Applying a negative (positive) voltage between source and drain electrodes, it is possible to drive the positive (negative) charge carriers across the channel area. Charge transport in OFETs is substantially two-dimensional. Charge carrier accumulation is highly localized at the interface between the organic semiconductor and the gate dielectric, and the bulk of the material is hardly or not affected by gate induced field, see following figure.

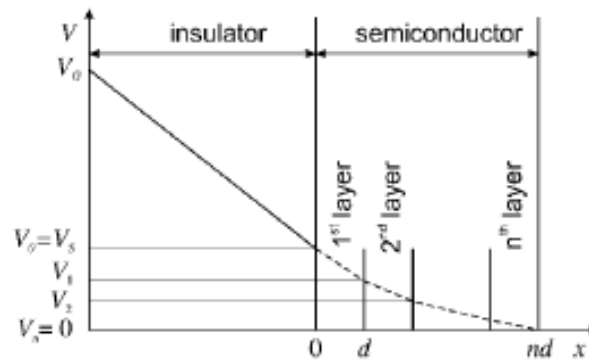
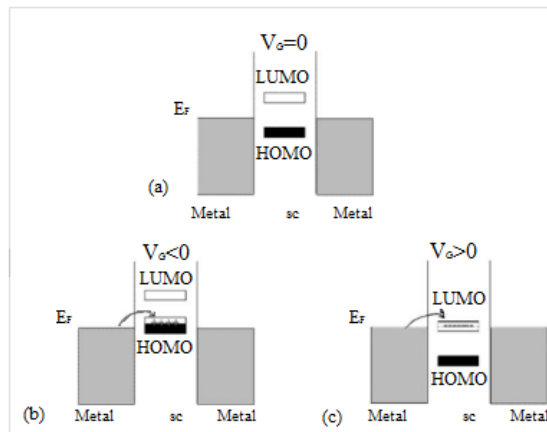


Figure 5.2: Potential distribution across the insulator/semiconductor structure in a multilayer structure

Upon increasing gate voltage to positive (negative) values, the number of charge carriers accumulated in the channel will reduce until the channel is fully depleted of free carriers. From this point on, negative (positive) charges are induced in the channel and the device should in principle work in inversion regime. In practice, when the gate voltage is lower than the threshold voltage of the transistor, channel conductivity is very poor and even by applying a Voltage between source and drain electrodes a very low current will be measured according to that. Since organic semiconductors are characterized by a very lo density of free carriers, the most of the charge carriers in the OFET channel have to be injected by the source electrode. Therefore, such interface

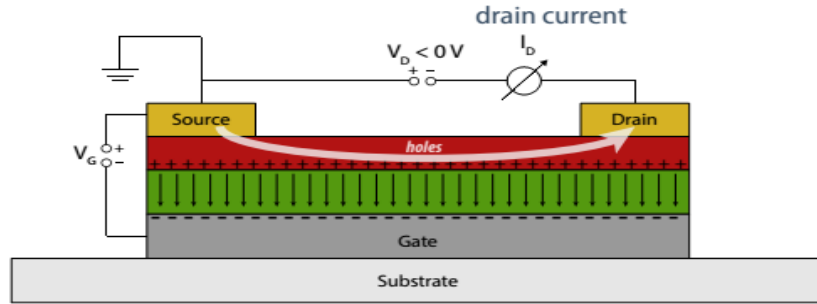
must be properly chosen in order to have an ohmic contact, i.e low HIB in a p-type transistor and a low EIB in a n-type one.

From a different point of view, the gate voltage allows to move upwards or downwards the HOMO-LUMO levels in the organic semiconductor as shown in the following figure.



If a low HIB configuration is chosen, by applying a negative gate voltage, the HOMO of the organic semiconductor is pushed much closer to the Metal WF, thus leading to dramatically increase the concentration of injected holes into the channels. When such concentration is high enough to create a channel (percolation path) at the interface the transistor is switched on and a significant current can flow between sourced and drain electrode.

As said before, the boundary between accumulation and inversion regime is called threshold voltage V_t of the device. Below the threshold voltage the device is in its off state, no free charge carriers are present in the channel and no current will flow across it. The equations that govern the OFET working principle are substantially the same of the classic MOSFET.



Let's imagine to consider a small piece of the device channel, Its resistance dR is given by:

$$dR = \frac{dx}{Z\mu|Q(x)|}$$

Where $Q(x)$ is the superficial charge along the x axes

In an OFET charge contributions are: the accumulation layer Q_s and the charge in the neutral region (bulk) Q_0

The latter has the following expression

$$Q_0 = \pm qn_0d_s$$

Where q is the electron charge, d_s is the organic semiconductor layer thickness and n_0 is the free charges density

$$Q_s(x) = -C_i[V_g - V_{fb} - V_s(x) - V(x)]$$

$V_s(x)$ is the ohmic drop in the semiconductor which can be neglected, and $V(x)$ is the voltage in the channel as function of position x . V_{fb} is the flat band voltage which takes into account the difference between the organic semiconductor and the gate electrode work functions and, also, possible charge trapped into the gate dielectric.

In the most of organic transistors the gradual channel approximation can be taken as valid, which states that, when the transversal field (E_y perpendicular with respect to current flow) in the channel is much larger than the longitudinal one (E_x across the

channel, parallel to current) $V(x)$ only depends on drain voltage and linearly increases from 0 to V_d moving from the source to the drain.

$$dR = \frac{dx}{Z\mu|Q(x)|}$$

$$dV = I_d dR = \frac{I_d dx}{Z\mu|Q_s(x) + Q_0|}$$

Considering the previous expressions and making the integral function across the channel, $x=0, V=0$ at the source, whereas at the drain $x=L, V=V_d$ we obtain

$$I_d \int_0^L dx = \int_0^{V_d} Z\mu[C_i(V_g - V_{fb} - V) \pm qn_0d_s] dV$$

Solving, considering the mobility constant

$$I_d = \frac{Z}{L}\mu C_i \left[(V_g - V_0)V_d - \frac{V_d^2}{2} \right]$$

where:

$$V_0 = \pm \frac{qn_0d_s}{C_i} + V_{FB}$$

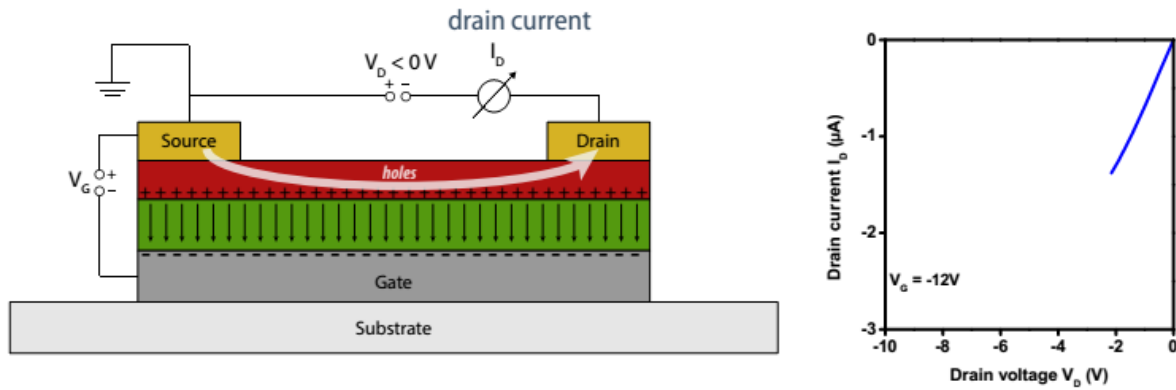
This actually takes into account that a not negligible current could also flow when $V_{gs}=0$ V.

When a gate voltage larger than the threshold one is applied, if the voltage applied between source and drain (V_{DS}) is small ($V_G < V_{DS} < (V_G - V_T)$), the induced electrical field is uniformly distributed in the whole channel where we have an extended accumulation layer.

$$I_d = \frac{Z}{L}\mu C_i \left[(V_g - V_t)V_d - \frac{V_d^2}{2} \right]$$

Where Z channel width, L channel length, C_i insulator capacitance μ is carrier mobility in the channel.

For small V_{DS} , ($V_{DS} \ll V_{GS} - V_T$) charges are uniformly distributed into the channel, and the channel behaves as a resistor, therefore the drain current will linearly increase upon increasing the drain voltage. This region is called Linear Region.

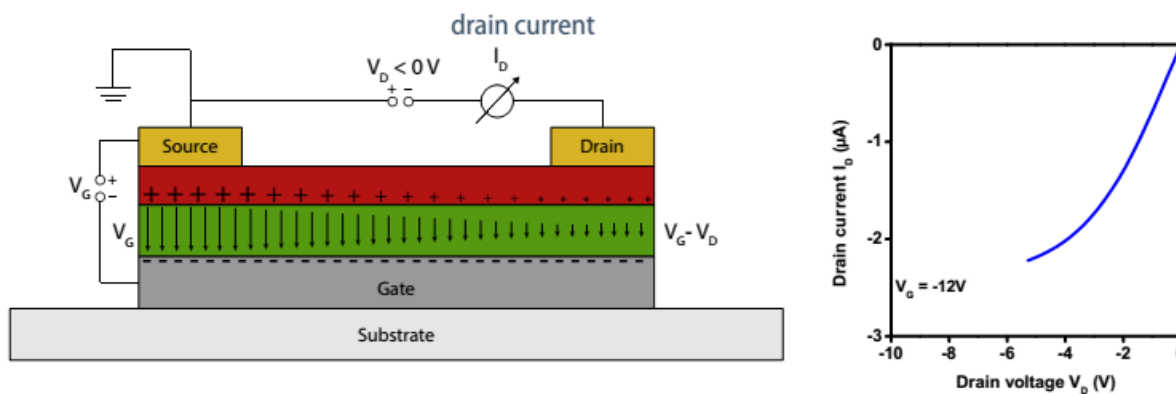


In this region, the last term $V_d^2/2$ can be neglected as much smaller than the previous one.

$$I_d = \frac{Z}{L} \mu C_i \left[(V_g - V_t) V_d - \frac{V_d^2}{2} \right]$$

$$I_d = \frac{Z}{L} \mu C_i \cdot (V_g - V_t) V_d$$

When V_{DS} increases ($V_{DS} \leq V_{GS} - V_T$) charge distribution is no longer uniform and current increases as a quadratic function.



$V_d^2/2$ cannot be neglected as it is no longer much smaller than the previous one, therefore the current expression remains:

$$I_d = \frac{Z}{L} \mu C_i \left[(V_g - V_t) V_d - \frac{V_d^2}{2} \right]$$

If V_{DS} keeps increasing the channel becomes asymmetric and thinner in the proximity of the drain. In this case we have to consider that $V_{GD}=V_{GS}-V_{DS}$, when V_{DS} increases, V_{GD} decreases, meaning that the vertical potential drops close to the drain ($V_{DS}>0$) and carrier concentration dramatically decreases in this region.

For a certain V_{DS} value, when $V_{GD}=V_T$, charge carrier concentration turns to 0, we have reached the pinch-off condition. Further increases in the drain voltage will not be able to induce a current increase in the channel that will stay constant (current saturation).

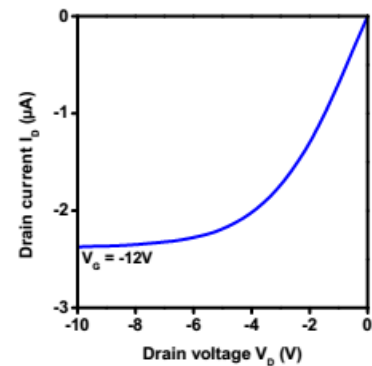
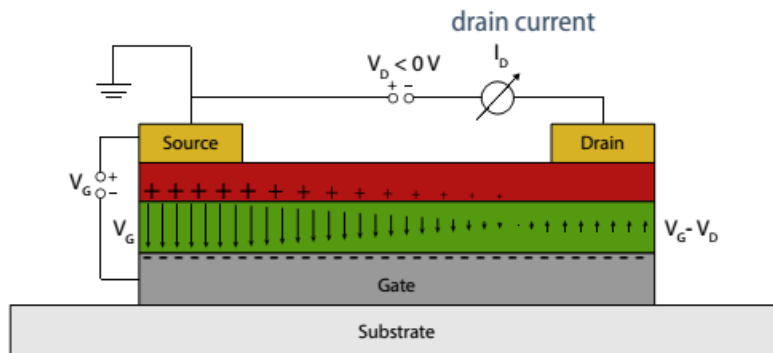
We have to remember that V_T is the voltage border under whom the channel is fully depleted. Let's call V_{Dsat} the V_{DS} value leading to $V_{GD}=V_T$

$$V_{GD}=V_T$$

$$V_{GS}-V_{DS}=V_T$$

$$V_{Dsat}=V_{GS}-V_T$$

Considering that, we obtain the following expression for the current flowing in the channel in these conditions.

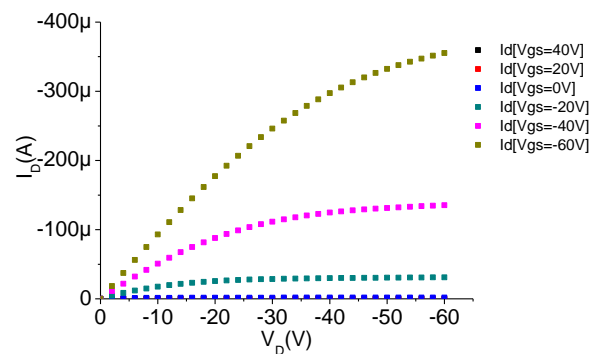


$$I_{dsat} = \frac{Z}{2L} \mu C_i (V_g - V_t)^2$$

5.2 OUTPUT AND TRANSFER CHARACTERISTICS

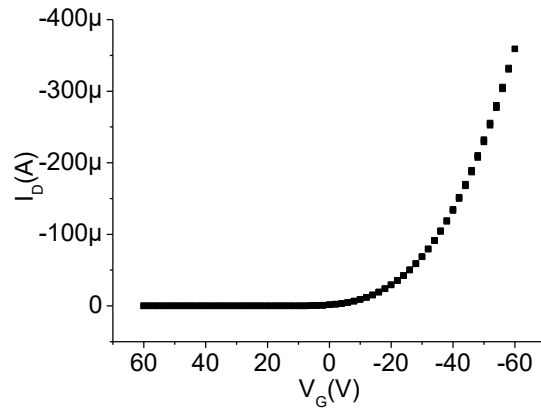
There are two different sets of measurements that are generally performed in order to establish the device performances and derive the most meaningful electrical parameters, i.e. output and transfer curves.

Output characteristics are a family of curves made by measuring the drain current while keeping the gate voltage constant and at the same time sweeping the drain voltage. After the completion of the first curve, the gate voltage can be changed and drain voltage can be swept within the same range used before. Generally a sufficient number of curves are acquired using this approach, changing the gate voltage from a value where we expect our transistor to be in the off state, to a value where it is in the on state, as reported below.



Transfer characteristics, also called transcharacteristics, are made measuring the drain current while by keeping the drain voltage constant and sweeping the gate voltage (generally from a value where the transistor is off up to a value where it is well above the threshold voltage).

Such transfer curves can be made by choosing a drain voltage small enough to be sure to have our transistor in the linear region for all the gate voltages used in the sweep. Alternatively, such curves can be acquired by keeping the drain voltage high enough in order to be sure that the transistor is in the saturation regime for all the gate voltages employed in the sweep.



From such curve some very important parameter can be derives, as channel conductance and transconductance. In the linear regime we will have:

$$g_d = \left. \frac{\partial I_D}{\partial V_D} \right|_{V_G = \text{const}} = \frac{Z}{L} \mu C_i (V_G - V_T)$$

whereas transconductance, is given by:

$$g_m = \left. \frac{\partial I_D}{\partial V_G} \right|_{V_D = \text{const}} = \frac{Z}{L} \mu C_i V_D$$

obviously, conductance in the saturation regime will be 0 for all the employed gate voltages, as current is independent on the drain voltage. Whereas the transconductance in the saturation regime will be:

$$g_m = \left. \frac{\partial I_D}{\partial V_G} \right|_{V_D = \text{const}} = \frac{Z}{L} \mu C_i (V_G - V_T)$$

Note that such parameters can be obtained from the ewcorde characteristics. The conductance is give by the inverse of the slope of the output characteristics in the linear regime (one conductance value for each employed gate voltage).

The transconductance in the linear regime can be obtained by the inverse of the slope of the transfer curve in the overthreshold region. In this case, the transconductance will be constant for all the employed gate voltages.

Differently, the transconductance in the saturation regime will be give by the inverse of the slope of the tangential line in each point of the curve, in the overthreshold

condition. Therefore, transconductance in the saturation regime varies with the gate voltage.

5.3 TYPICAL OFETS ELECTRICAL PARAMETERS

Mobility

Average values [10 - 10⁻² cm²/Vs]

Off current and I_{on}/I_{off}

Off current is the current obtained when the devices is off *typical I_{on}/I_{off} values 10⁵ - 10⁶*

Threshold voltage

Typical values [+10V ; -10V]

N.B. ideally $V_t=0V$

It is very important to remember at this stage that in thin film transistors charge conduction takes place in the first monolayer, therefore, the interface between the organic semiconductor and the gate dielectric plays a crucial role in device performances. In fact several effects can take place at this interface, affecting charge accumulation and transport mechanism:

- **Physical:**

Structural defects → charge carriers scattering semiconductor morphology → mobility and charge trapping

- **Chemicals:**

Charge trapping

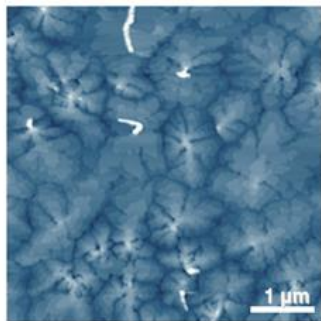
Threshold voltage Shift (surface potential induced by chemical groups at the interface)

In bottom gate structures the insulator is also the substrate where the organic film is grown, meaning that it determines the properties of the channel:

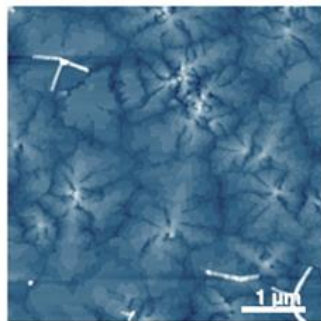
- Surface energy
- Idrophobic - Idrofilic

➤ Surface roughness

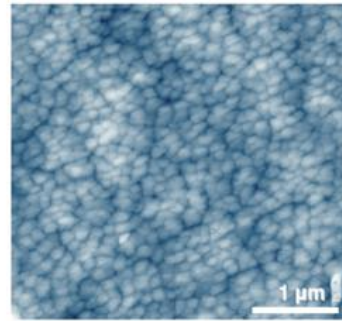
The same organic semiconductor can give rise to very different morphologies when deposited in thin films, according to the deposition parameters, but also depending on the substrates properties



Pentacene su Mica
RMSR=0.2 nm



Pentacene su SiO₂
RMSR=0.2 nm



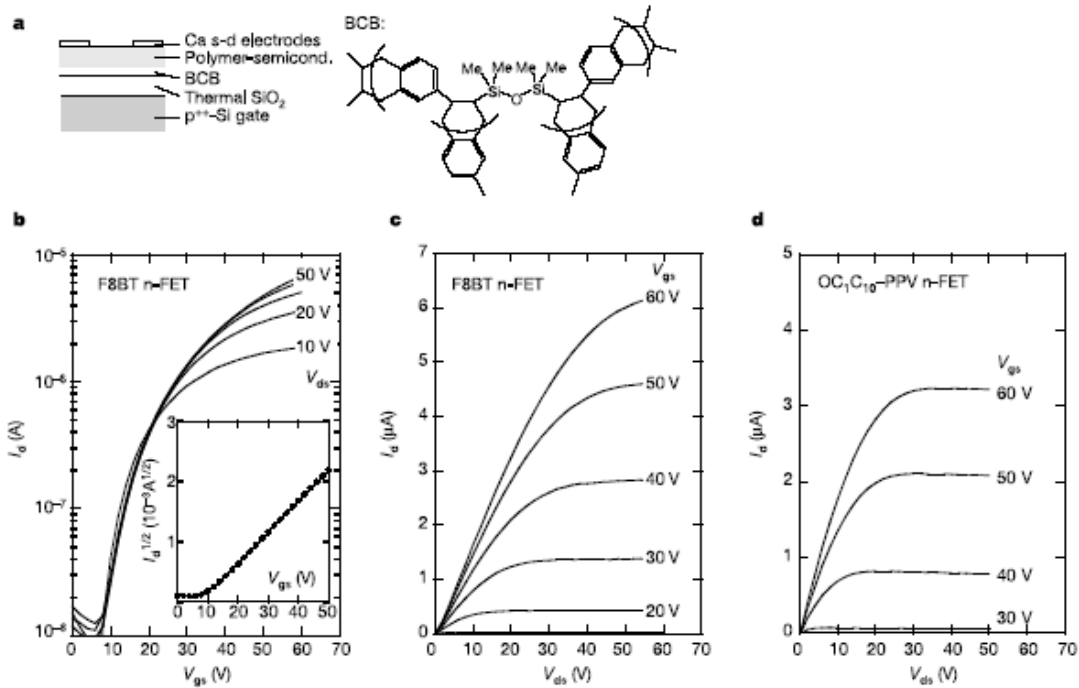
Pentacene su Mylar
RMSR=2 nm

Influence of surface roughness of the substrate on the organic semiconductor morphology

Also chemical groups at the interface with the gate dielectric could dramatically influence the electrical behaviour of such devices. For instance, having functional groups at the dielectric surface can create charge trapping or, also, induce some local field influencing the active channel formation.

5.4 THE ROLE OF OH GROUPS

In recent years it has been demonstrated that hydroxyl groups present at the gate dielectric surface are very active electron trapping sites, thus dramatically limiting electron transport in OFET made with polar dielectrics. On the contrary, non polar insulating materials have no OH groups, thus are preferable for the fabrication of n-type devices.



Examples of n-type OFET fabricated with different organic semiconductors using a OH free insulating material

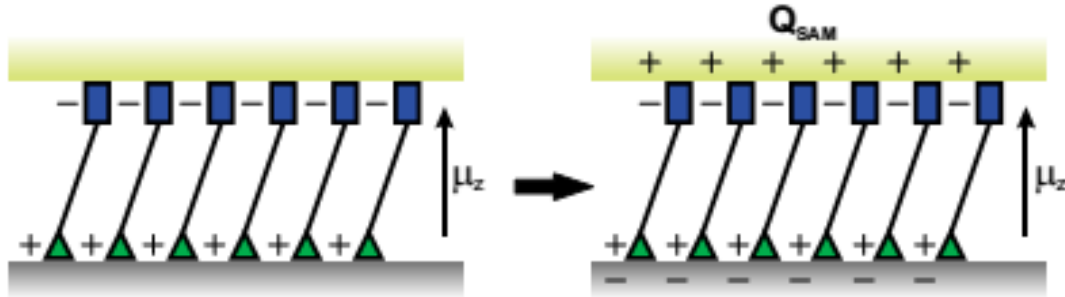
A possible way to minimize OH trapping effect is the employment of thin molecular layers that, deposited on the gate dielectric allows to passivate such trap sites, thus allowing achieving n-type conduction even when polar dielectrics are employed.

5.5 USING SAM FOR TUNING THE OFET'S THRESHOLD VOLTAGE

A very interesting approach that has been widely employed along the years for the modulation of transistors threshold voltages is the use of self assembled monolayers (SAMs). These molecules are characterized by a head that is functionalised with some chemical group that can create a covalent bond with the substrate, and a tail containing a functional group which can be use to modulate the electrical characteristics of the final devices.

Such molecules generally self assembled on the dielectric surface, forming a well packed and ordered layer. If such molecule have a permanent dipole moment, as indicated in the figure below, this molecular film will induce a local field superposing with the gate induced one,

thus, changing the intrinsic threshold voltage that the same device should have without the presence of such molecules.

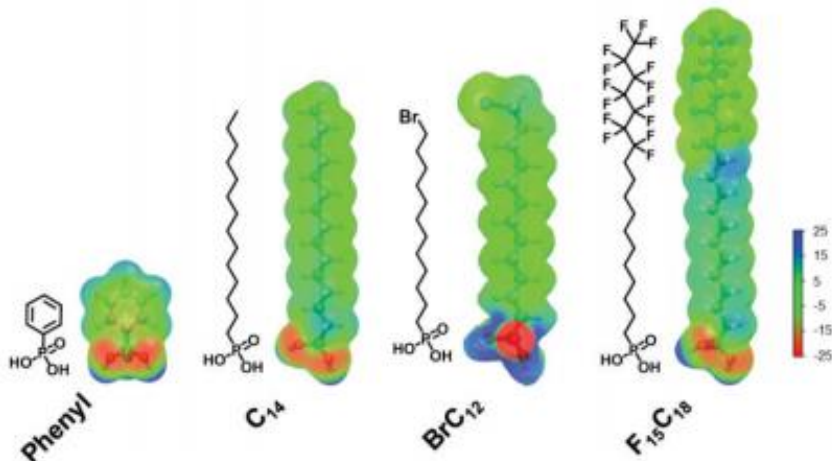


If the SAM layer is uniform and well ordered, the functional groups can induce a surface potential

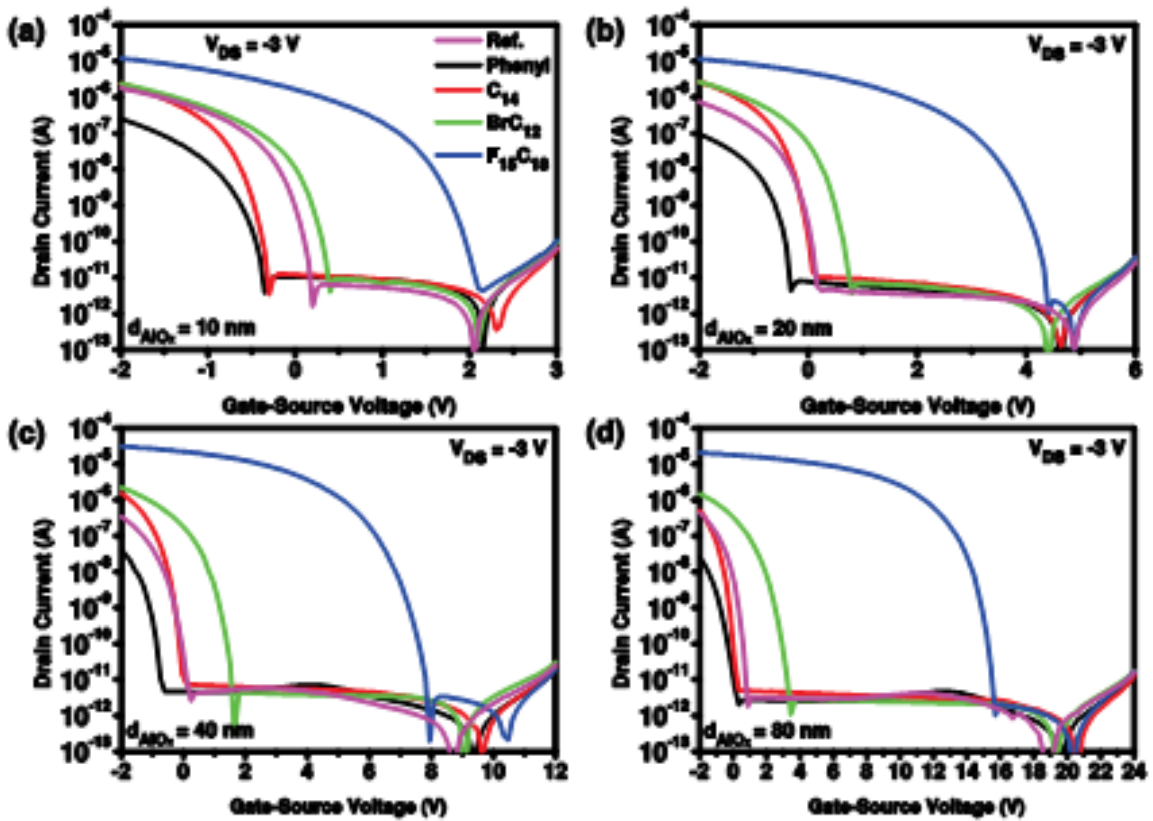
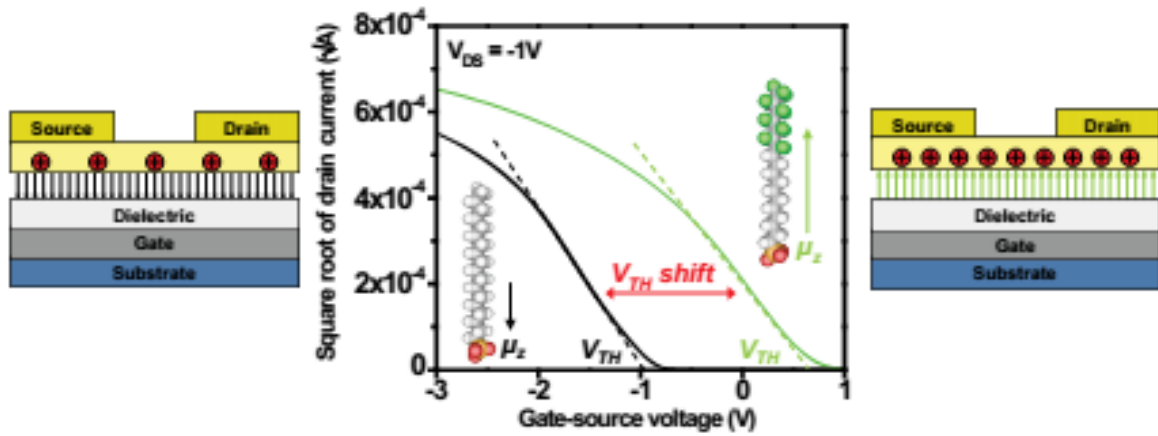
Helmholtz

$$V_{SAM} \propto \frac{N\mu_z \cos \theta}{\epsilon_{SAM}\epsilon_0}$$

For example, if the SAMs molecules are functionalized with electronegative elements, a very strong dipole moment can be induced, which attracts electron from the organic semiconductor, and leaves free holes into the channel. In other words, this means that the hole concentration in these devices will be higher than the one obtained in the same device without the presence of such molecules.



Having a higher intrinsic concentration of holes means that, considering a p-type transistor, the device threshold voltage will be shifted towards more positive values, as reported in the picture below.



5.6 NON IDEALITIES IN OFETs

5.6.1 Charge trapping

The first examples of OFETs were hybrid structures, where the only “organic” part in the device, was the semiconductor. Typically, the first OFETs were assembled on a highly doped silicon wafer, acting at the same time as substrate and as gate electrode.

A thin SiO₂ layer was employed as gate dielectric, whereas metals (i.e. Au, Al) were used for the fabrication of the source and drain electrodes. Nowadays, several examples have been reported concerning the realization of all organic FETs, where a flexible plastic foil is generally used as flexible substrate, a polymeric gate dielectric (PVA or PVP or PMMA) is used instead of SiO₂, and conductive polymers are employed as alternative to metals for the patterning of the electrodes.

Even though the MOSFET laws are taken as representative also for OFETs, it is well known that, in most cases, the typical behaviour strongly differs from the ideal case. The main reason for such discrepancy is generally ascribed to the intrinsic structural properties of the organic semiconductors. Usually, when we grow an organic semiconductor film, we do not obtain a crystal structure; a single organic crystal can be obtained only under strict deposition conditions. Therefore, when we talk about organic semiconductors, we suppose to discuss about polycrystalline thin film, with a very high concentration of structural defects which is the main reason for the non-linearity usually observed in such devices. Every defect acts as scattering site for charge carriers, causing the distortion in the, ideally, periodic lattice potential. Therefore, a band-like transport is usually impeded by such scattering process. The effect of defects is even stronger if the defects themselves act as trapping sites for charge carriers. Trapping is relevant when the defect induces one or more energy levels in the band gap of the organic "crystal". A charge carrier will prefer to occupy this lower energy level and the trap localizes the charge carrier in its site. Typically, traps can be divided into two categories, depending on the activation energy that is needed to free the charge carrier: i) shallow traps when the activation energy is in the order of $k_B T$; ii) deep traps, when the activation energy is outside the range of thermal excitation. Deep traps are often caused by chemical impurities, such as oxidized molecules or molecules that are side products of the main compound synthesis process. The presence of traps within the semiconductor layer can cause a decrease in the density of mobile charges, since trapped carriers are localized at the defect sites. In some cases, when the density of defects is high and they strongly localize charge carriers, their influence can completely dominate charge transport across the

semiconductor. This feature usually manifests a thermal activation dependence of the mobility, meaning that charge transport is dominated by defects that in the case of OFETs made of small molecules, are often grain boundaries, and defects at the organic/dielectric interface. Several experiments have been performed on OFETs and several models have been introduced to study charge transport of both polycrystalline and crystalline active layers and its dependence to charge trapping. However, a universal theory which can properly describe charge transport in organic materials does not exist and transport properties are still not fully explained. From a structural point of view we can consider different charge trapping mechanisms, which could be related to bulk defects in the organic semiconductors or, also to interfacial defects at the interface with the gate dielectric.

5.6.1.1 Charge trapping in the bulk

Usually charge trapping in the bulk of the material leads to space charge limited effects. In order to achieve transistor action these trap levels need to be filled by carriers induced by gate voltage. The field effect mobility is then determined by the ratio between free carriers n_f to the total number of charge carriers n_{tot} , $\theta = n_f / (n_t + n_f)$ and the intrinsic μ_0 mobility of the material is given by:

$$\mu_{FET} = \mu_0 \cdot \theta$$

$$V_{TFL} = \frac{2ed^2N_t}{3\varepsilon_r\varepsilon_0}$$

where, N_t is charge traps concentration, ε_r and ε_0 are the dielectric constant of the semiconductor and of the vacuum respectively and V_{TFL} is the trap filling voltage. In other words it is the voltage the system needs in order to fill all the bulk traps in the material. It is worth to mention that in this case we are considering a vertical electric field induced by the gate voltage.

5.6.1.2 Charge trapping at the dielectric/semiconductor interface

Device performance can be strongly influenced also by the insulator/semiconductor interface. The maximum number of interface traps can be estimated using the following equation, assuming that densities of deep bulk states and interface states are independent of energy:

$$N_{SS}^{max} = \left[\frac{S \cdot \log(e)}{kT/q} - 1 \right] \frac{C_i}{q}$$

$$S = \left[\frac{d \log(I_d)}{dV_g} \right]^{-1} = \frac{kT}{q} \cdot \ln 10 \cdot \left(1 + \frac{C_d + C_{it}}{C_i} \right)$$

where N_{SS}^{max} is the maximum number of interface traps states, k is the Boltzmann's constant, T the absolute temperature, q the electronic charge, C_d and C_{ox} are the capacitances of the depletion region in the semiconductor and the gate dielectric one respectively, whereas C_{it} is the capacitance associated to charges trapped at the interface. S is the inverse sub-threshold slope which can be directly estimated from the transfer characteristics of the device.

5.6.1.3 Trapping at the grain boundaries

In many cases, in particular for polycrystalline materials the currents instead of being controlled by traps, can be governed by grain boundaries. It is often very complicated to decide between a grain-boundary-barrier model and a trap model on the basis of the experimental results. As discussed by Street et al., the evidence for the barrier model can be found in the linearity of the so called Levinson plot of $\ln(I_D/V_G)$ vs $1/V_G$. This model is based on the predicted OFET drain current in the linear regime given by:

$$I_D = \mu_0 V_D C_G (W/L) V_G \exp(-E_B/kT)$$

$$\equiv \mu_0 V_D C_G (W/L) V_G \exp(-s/V_G)$$

where C_G is the gate dielectric capacitance, W/L the width to length ratio, E_B is the energy barrier, and the mobility is thermal activated as:

$$\mu = \mu_0 \exp(-E_B/kT) \equiv_0 \exp(-s/V_G)$$

$$s = \frac{q^3 N_t^2 t}{8\epsilon k T C_G}$$

where q is the electronic charge, N_t is the density of traps at the grain boundaries, t is the semiconductor thickness, and ϵ is the dielectric constant of the semiconductor (usually taken as 3 for most of the organic semiconductors). The parameter s is the slope of the Levinson plot, and provides an estimate of the grain boundary charge, and of the density of charge traps at the grain boundaries.

5.6.1.4 Poole-Frenkel

The influence of charge trapping can be neutralized by increasing the charge carrier density. When a trap state is filled by a charge carrier, it becomes no longer active for another charge carrier; therefore, it can freely flow. This phenomenon generally leads to obtain a field effect dependent mobility and was described by Pool-Frenkel model. Considering the longitudinal field caused by the source/drain voltage ($E_L = V_{DS}/L$) we obtain:

$$\mu(E) = \mu(0) \exp\left(\frac{-q(\Phi_B - \sqrt{qE_L/\pi\epsilon})}{kT}\right)$$

where, $\mu(0)$ is the mobility when the applied field zero, q is the elementary charge ($1.602 \times 10^{-19}\text{C}$), Φ_B is the trap depth, and ϵ is the semiconductor permittivity. This causes a non linear dependence of the current flowing from source to drain in the linear region. The ionization energy $q\Phi_B$ can be found by studying the activation energy $E_A = q[\Phi_B - (qE_L/\pi\epsilon)^{1/2}]$ as a function of temperature and voltage.

5.6.2 Contact Resistance

Measuring semiconductor mobility in a FET is a common way to derive conductivity properties of organics. Nevertheless, it should never be neglected that material properties strongly influence but do not coincide indeed with the device properties. In other words, the structural effect of the device itself, meant as e.g. parasitic effects that can be recorded on the electrical curves, should be carefully studied and possibly

eliminated. Recently a lot of efforts have been addressed towards the estimation and the reduction of the contact resistance for OFETs. Until some years ago this issue was underestimated since the OFETs performances were mostly limited by channel resistance effects. Nowadays, the performance of OFETs transistors has dramatically improved and the constant increase in the measured field effect mobilities led contact resistance effects to be a limiting factor for OFETs performances. Several methods have been developed for the extraction of the contact resistance in OFETs. In the following Figure some possible equivalent circuits are depicted. One is composed only by the device, in the second case, series resistances have been added at the source and drain electrodes.

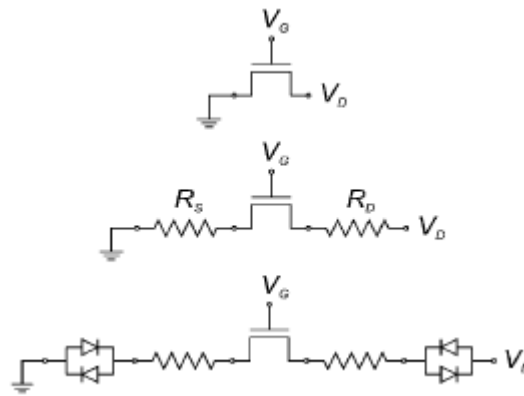


Figure 5.3: Equivalent circuit of the TFT without (top) and with (middle) contact resistances. The bottom circuit includes diode to account for non-linearity in the contact resistance.

A more complicated equivalent circuit was introduced by Necliudov et al., see the bottom circuit depicted in the previous figure, where also two diodes, which should take account of non linearities, are added. The model introduced by Necliudov et al. takes also account of charge trapping within the organic semiconductor film, which is modelled by considering gate voltage dependent field effect mobility:

$$\mu = \mu_0 (V_G - V_T)^\gamma$$

where, V_T is the threshold voltage and μ_0 and γ are two empirical parameters.

All resistive effects that do not scale down with channel length are call series resistance effects. The contact resistance is accounted by introducing a voltage drop $R_S I_D$, where R_S is the contact resistance; therefore, the drain voltage will be replaced by $(V_D - R_S I_D)$

$$I_D = Z/L\mu C_{ins}(V_G - V_{th})(V_D - R_S I_D)$$

$$g_D = \left(\frac{1}{\mu(W/L)C_{ins}(V_{GS}-V_T)} + R_S \right)^{-1}$$

$$R_{total} = R_S + \frac{L}{W\mu C_{ins} | (V_{GS}-V_T) |}$$

if we consider the model introduced by Necliudov we obtain a more complicated model given by:

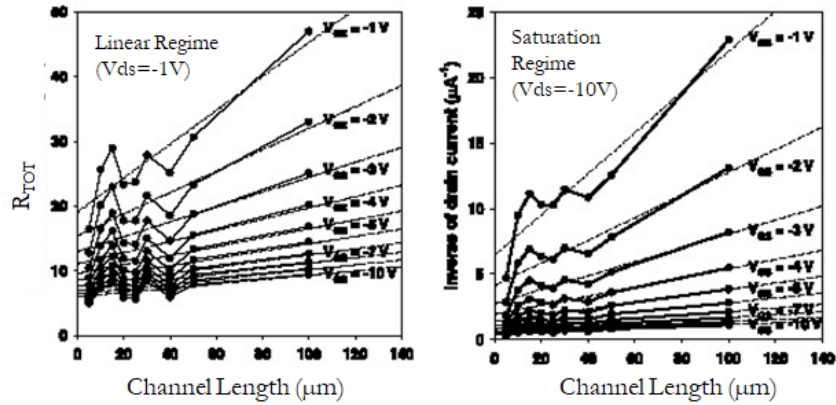
$$g_D = \left(\frac{1}{\mu(W/L)C_G(V_{GS} - V_T)^{1+\gamma}} + R_S \right)^{-1}$$

$$\frac{1}{g_D} = R_D = \frac{L}{W\mu_0 C_{ins} (V_{GS} - V_T)^{1+\gamma}} + R_S$$

More recently, several groups employed a different technique to estimate the Contact Resistance. One of the most used methods is called Transmission Line Method (TLM). This method, which was firstly developed for amorphous thin film transistors, consists in measuring the channel length dependence of the total resistance of the device. In fact, the total resistance of a FET (namely, R_T) is given by the sum of the contact resistance plus the channel resistance:

$$R_T = R_S + R_{Ch}$$

If several devices, with different channel length are realized on the same substrate and with the same active layer, it can be assumed that the contact resistance for all these devices is constant, since it is independent on the channel length of the device. As a result, if we plot the total device resistance as a function of the channel length, its extrapolation to zero channel length (where the channel resistance is equal to zero) should give the value of the Contact Resistance.



This method is highly diffused but it has also some problems. While measuring several devices we cannot be sure that the contact resistance or the channel resistance does not vary from sample to sample. Therefore, when plotting the total resistance as a function of the channel length, scattering can appear and data can be not strictly aligned. An alternative method, called four probe measurements, would avoid these problems. This method consists of introducing in the conducting channel two additional electrodes. Since the current through the channel is imposed by the source and drain voltage, the voltage drop between these two electrodes should not be affected by contact resistance and the real channel resistance can be then estimated by the ratio between the voltage drop, estimated between the two additional electrodes, and the current flowing from source to drain.

It is worth mentioning that contact resistance dramatically depends on metal/organic semiconductor interface issues. We have already discussed about possible charge injection barriers that can depend on energy levels alignment, surface dipoles and charge transfer happening at the interface. However, this is not the only situation that can give rise to contact resistance effects. In fact, such interface is generally characterized by a high concentration of defects in the organic semiconductor that are generally leading to a dramatic increase in the charge injection barriers.

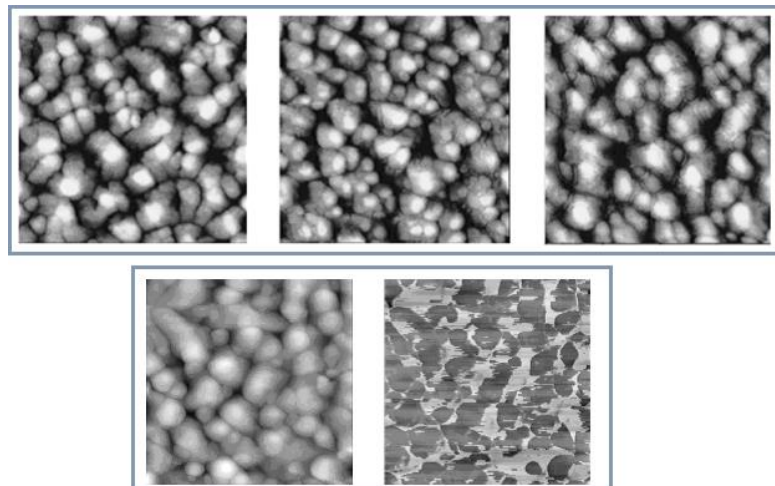
5.6.3 The effect of moisture on OFET performance

As already said many times, organic semiconductor thin films are generally polycrystalline, meaning that their morphology is characterized by the presence of multiple domains (grains) separated by so called grain boundaries. These crevices are

generally the weakest part of the film, in which external molecules, both in the vapor or liquid phase, can diffuse, interact with the semiconductor or even reach the gate dielectric/semiconductor interface, i.e. the place where the channel is formed, thus dramatically influencing charge carrier accumulation and also transport. One of the main issues for this kind of devices is that when exposed to ambient atmosphere, moisture can very rapidly condensate onto the active layer, create a thin film and also diffuse towards the channel.

When this happens, the device characteristics can be severely degraded. The interaction of water vapor with the organic semiconductor could be twofold:

- 1) water vapor, condensing on the semiconductor surface, forms a thin layer with an intrinsic conductivity higher than the one of the organic semiconductor. In other words it is like having a small resistance in parallel with the device channel. This means that, when the device is in the off state, i.e. no channel is formed. There could be a significant current flowing from source to drain, due to the low conductivity of this absorbed polar film present on the organic semiconductor.



Diffusion of water through a polycrystalline pentacene thin film

- 2) the polar molecules of water can interact with charge carriers in the channel creating scattering, and thus strongly limiting charge mobility. Therefore, in the on state, i.e. when the channel is already formed in the device, a significantly smaller current

can flow between source and drain due to this degradation of the mobility induced by the scattering process.

5.6.4 The effect of oxygen

Similarly, also oxygen can diffuse into the crevices of the organic semiconductor. Oxygen is relatively highly electronegative, thus it tends to attract and trap electrons from the organic semiconductor, leaving free holes into the bulk of the material. In other words, exposure to oxygen generally leads to a dramatic increase in the intrinsic hole concentration in the device channel, that can be seen as an oxygen doping effect. This point leads to a rigid shift of the transistor threshold voltage towards more positive values. In other words, a p-type transistor will be switched on much easily and could also pass from enhancement to depletion mode behaviour. On the contrary, considering a n-type transistor, oxygen interaction leads to dramatic loss of free electrons that will be trapped by the oxygen molecules. Therefore, it will be much more difficult to have a sufficient concentration of electrons, necessary to form the channel, and the devices will switch on for much higher voltages.

Such oxygen doping effect is very fast, and takes place immediately after exposure of the device to ambient atmosphere, fortunately, is reversible, in fact, by heating up the device in inert atmosphere, oxygen molecules can be desorbed from the film, thus leading to a cancelling of such doping behaviour.

On the other hand, oxygen can also chemically interact with the organic semiconductor molecules leading to an oxidation of the molecule. If this happens, the molecule will be transformed into a different one, and will locally lose conjugation because of oxidation. This process typically leads to a dramatic decrease in the device mobility, and it is not reversible. Moreover, it takes some time for the oxygen to chemically react with the molecules, therefore, such phenomenon is more visible in the long term, but leads to an irreversible degradation of the carrier mobility in the transistor.

The macroscopic effects of the interaction of oxygen with an organic transistor are therefore, on one hand an increase of the device output current due to a rigid shift of

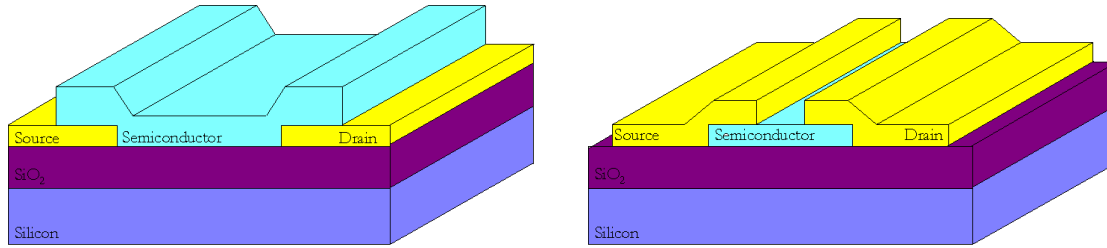
the threshold voltage and an increase of the intrinsic concentration of holes (for p-type devices! For n-type one is the opposite). On the other hand, as said before, a degradation of its performances due to a dramatic decrease of the channel mobility.

5.7 OFETs architectures

For more than a decade now, organic field effect transistors (OFETs) based on conjugated polymers, oligomers, or other molecules have been envisioned as a viable alternative to more traditional, mainstream thin-film transistors (TFTs) based on inorganic materials. Because of the relatively low mobility of the organic semiconductor layers, OFETs cannot rival the performance of field-effect transistors based on single-crystalline inorganic semiconductors, such as Si and Ge, which have charge carrier mobilities (μ) about three orders of magnitude higher. Consequently, OFETs are not suitable for use in applications requiring very high switching speeds. However, the processing characteristics and demonstrated performance of OFETs suggest that they can be competitive for existing or novel thin-film-transistor applications requiring large-area coverage, structural flexibility, low-temperature processing, and, especially, low cost. The first examples of OFETs were assembled on silicon. In fact, the only organic part of such devices was the active layer, which was realized employing an organic semiconductor instead of an inorganic one. The basic structures consist in the typical TFT configuration largely employed for the realization of field effect transistors with amorphous silicon. A highly doped silicon wafer was used both as mechanical substrate and as gate electrode. On the top of it a thin SiO₂ layer (typically from 50 to 500 nm. thick) is grown in order to obtain the gate dielectric. From this point we can then start for assembling the final device.

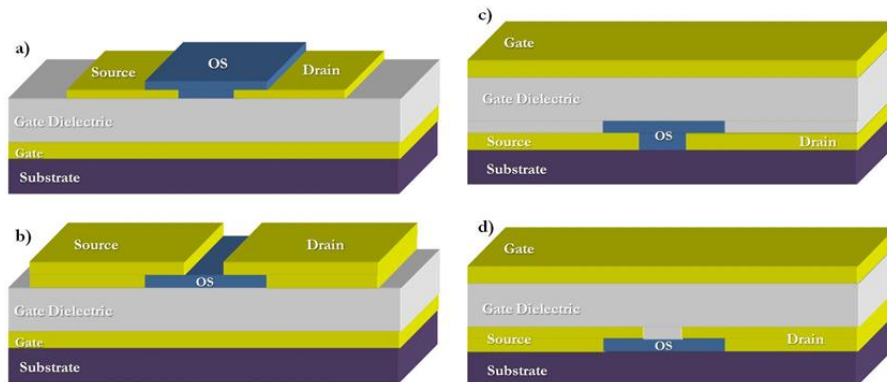
a)

b)



Schematic of OFETs in bottom contact (a) and top contact (b) configuration.

For this purpose, two electrodes and a semiconductor layer are needed. In the following Figure we show the two most common configurations: namely, bottom contact (BC) and top contact (TC). The difference between these two architectures is that in the BC transistors the organic semiconductor layer is deposited after the patterning of the source and drain electrodes. In the TC configuration the active layer is deposited in advance on the bare silicon dioxide surface and the source and drain electrodes are patterned afterwards onto the organic semiconductor film.



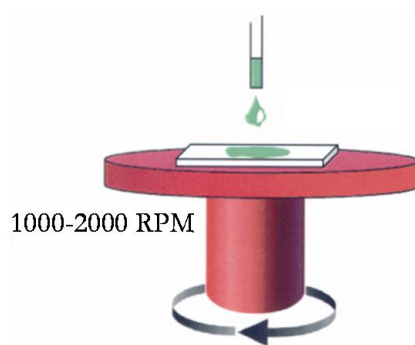
- a) Bottom gate, Bottom Contact
- b) Bottom gate, Top Contact
- c) Top Gate, Bottom Contact
- d) Top Gate, Top Contact

5.8 DEPOSITION TECHNIQUES IN ORGANIC ELECTRONICS

The technique employed for depositing the organic active layer usually depends on the solubility of the material we are using. If the material is soluble, it is generally deposited in thin films by a spin coating process, otherwise, it is deposited by means of thermal evaporation.

5.8.1 Spin Coating

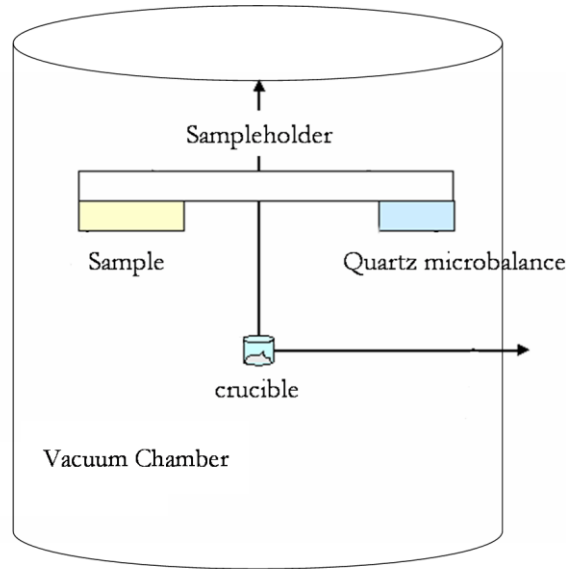
Spin coating is a procedure used to apply uniform thin films to flat substrates. A certain amount of the material in solution is placed on the substrate, which is then rotated at high speed in order to spread the fluid by centrifugal force. A machine used for spin coating is called spin coater, or simply spinner. Rotation is continued while the fluid spins off the edges of the substrate, until the desired thickness of the film is achieved. The applied solvent is usually volatile, and simultaneously evaporates. So, the higher the angular speed of spinning, the thinner the film. The thickness of the film also depends on the concentration of the solution and the employed solvent.



Schematic representation of the spin coating process.

5.8.2 Thermal Evaporation

This technique is generally used when the employed organic material is not soluble. In this thesis, we used small molecules that are characterized by a very low degree of solubility, therefore, in all our experiments the organic active layers were deposited by means of thermal evaporation. This deposition takes place inside a High Vacuum Chamber, with a nominal pressure ranging from 5×10^{-5} to 1×10^{-12} mbar.



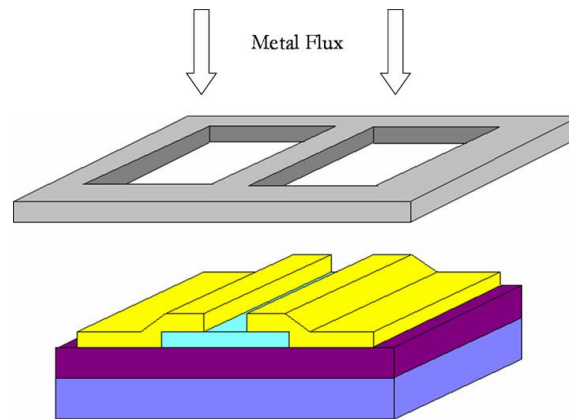
Schematic representation of the thermal evaporation system.

The organic material is located inside a crucible wrapped by a high resistive wire, usually made out of tungsten, connected to two electrodes. The crucible can be resistively heated up by applying a bias to the two electrodes until the temperature needed to let the organic material start evaporating. The evaporator system is usually provided with a Crystal Quartz Microbalance used to measure the nominal thickness of the deposited film. In this way it is possible to control in a very efficient way the deposition rate and the final thickness, two parameters which are very important for the optimization of the electrical behaviour of the final assembled devices.

5.8.3 Patterning of the electrodes

In most cases, the source and drain electrodes are realized with metals (i.e. Au, Al, Ag etc...), and are usually patterned by means of a photolithographic process followed by an etching procedure, which will be described in details in the next section. These procedural steps are not suitable for the realization of top contact devices, since the organic materials are very sensible to external agents and the solvents and the etchant can pollute it. For the patterning of the source and drain electrodes a shadow mask is generally used. The procedure consists in interposing a shadow mask between the sample and the source of the metal flux. As a consequence, the regions where the metal is deposited are selected by the shadow realized by the mask. The limit of such

technique consists in the poor highest reachable resolution. It is not possible to realize high resolution shadow masks and the typical features are in the range of 100 μm , therefore, this technique is not suitable for the realization of devices with channel length in the order of the micrometer.

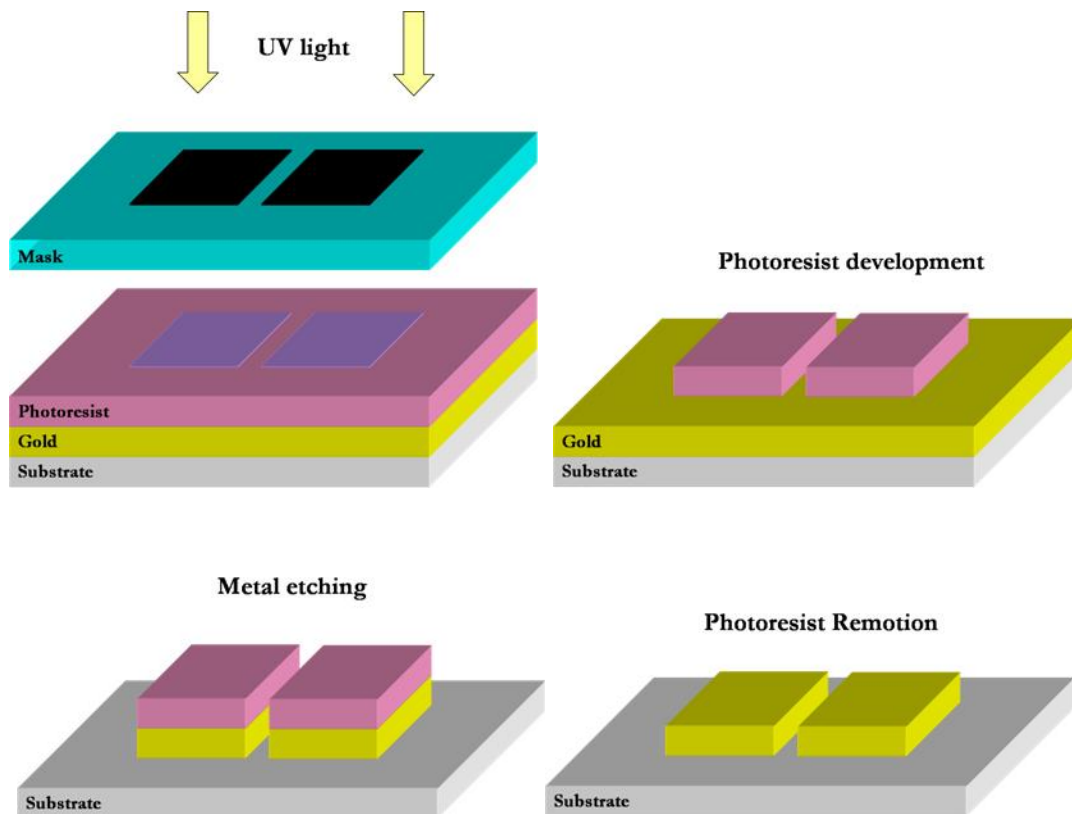


Schematic illustration of the procedure for the realization of top contact electrodes by means of a shadow mask.

5.8.4 Photolithography

Photolithography is a very common technique widely used in the Semiconductor industry for the patterning of the devices. The goal of this technique is to transfer a certain pattern on a substrate. For this purpose, two elements are required: i) a mask which reproduces the image to transfer on the substrate and it must be opaque to ultraviolet light; ii) a photosensitive material, called photoresist, which is exposed to ultraviolet light during the process by interposing the mask between the UV source and the surface. There are two types of resists, namely, positive and negative photoresist. Positive resist is 'softened' by exposure to the Ultra-Violet (UV) light and the exposed areas are subsequently removed in the development process, the resist image will be identical to the opaque image on the mask. Negative resist is 'hardened' by exposure to ultra-violet light and therefore it is the unexposed areas that are removed by the development process, the resist image will be a negative image of the mask. Photoresists are sensitive to a wide range of wavelengths of light, typically 200

- 500 nm, this range of wavelengths includes the visible blue and violet contained in normal white light. For this reason, photolithography fabrication areas use a special filtered light to remove all of the wavelengths to which the resist is sensitive.



Schematic representation of the main steps required in a photolithographic process.

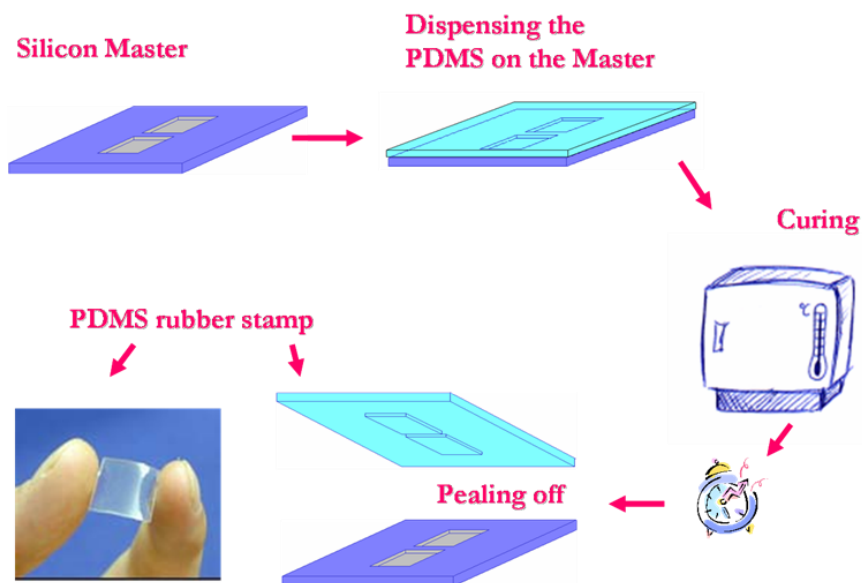
In the previous Figure we show the main steps required in a photolithographic process. In particular, we show the steps required for the patterning of the OFET structures we employed during this thesis. First of all, a thin metal film is deposited over the surface. In our case, we deposited a thin gold film, deposited by thermal evaporation, over the Mylar® surface. Afterwards, a thin positive photoresist film is deposited onto the sample surface; generally this process is made by spin coating. Before the exposure process, a soft baking process of the sample is usually required in order to dry the deposited photoresist film. During the exposure process, the photoresist layer is exposed to UV light through the opaque mask; in this way it is possible to define the pattern on the resist film. After exposure, the sample is developed in order to remove the unwanted resist, thus leaving only the define pattern on the substrate. Usually, a post baking step is made to increase resist adherence with the substrate and in particular to increase its resistance to etch process. Taking

advantage of the presence of the patterned resist film, it is then possible to etch the metal in the undesired areas. Once the etching process is performed we can remove the photoresist by using an organic solvent, generally acetone, and the basic structure for the realization of the final device is assembled.

5.8.5 Soft Lithography: Overview

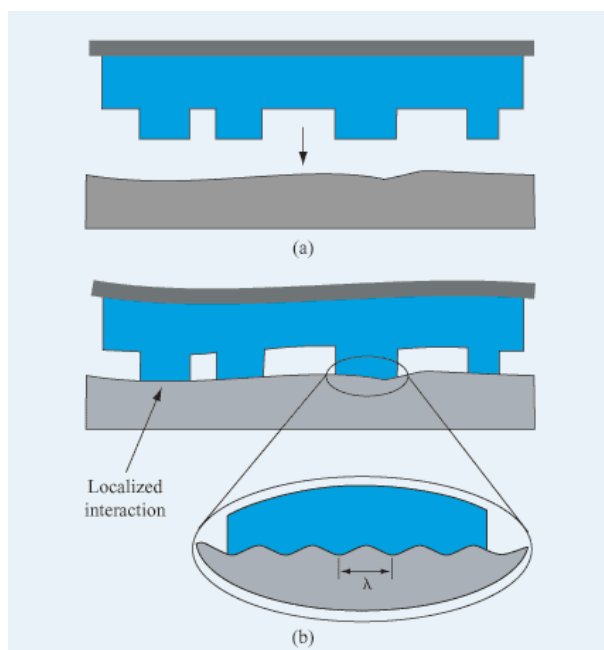
"Soft lithography represents a non-photolithographic strategy based on self-assembly and replica molding for carrying out micro- and nanofabrication. It provides a convenient, effective, and low-cost method for the formation and manufacturing of micro- and nanostructures. In soft lithography, an elastomeric stamp with patterned relief structures on its surface is used to generate patterns and structures with feature sizes ranging from 30 nm to 100 μm."

"Soft lithography" is a new high resolution patterning technique developed at Harvard by Prof. George Whitesides. The key element in Soft Lithography is an elastomeric stamp with patterned relief structures on its surface. Usually the stamp is made out of elastomeric polymers, as polyurethane, polyimide, and cross linked Novolac™ resin, but the most used material is poly(dimethylsiloxane) (PDMS). This material has very low glass transition temperature and it is liquid at room temperature, moreover, it can be easily and quickly converted into solid upon a cross-linking process. In this thesis Sylgard™ 184 obtained from Dow Corning was used. The provided kit consists in two part: a liquid silicon rubber base (i.e. a vinyl-terminated PDMS) and a catalyst or curing agent i.e. a mixture of a platinum complex and copolymers of methylhydrosiloxane and dimethylsiloxane). Once mixed, poured over a certain master, and heated to elevated temperatures, the liquid mixture becomes a solid, cross-linked elastomer in a few hours via the hydrosilylation reaction between vinyl (SiCH=CH₂) groups and hydrosilane (SiH) groups. In the following Figure the main steps for the realization of PDMS rubber stamp are shown. The starting point is the realization of a master, typically made on silicon. The master is fabricated using microlithographic techniques such as photolithography, micromachining, e-beam writing, and should reproduce the negative of the pattern desired to be transferred.



Main steps required for the realization of a PDMS rubber stamp. The final stamp reproduces the features of the electrodes to be transferred onto the substrate.

The procedural steps for the realization of an elastomeric stamp are very easy; once the PDMS is mixed with its curing agent, the mixture is dispensed over the master. The following step is a thermal curing procedure that will lead the blend film to become a solid, cross-linked elastomer via the hydrosilylation reaction between vinyl ($\text{SiCH}=\text{CH}_2$) groups and hydrosilane (SiH) groups.



Conformal contact between a hybrid stamp and a hard substrate. (a) Stamp composed of a patterned elastomer and a flexible backplane adapts its protruding zones to (b) the macroscopically uneven substrate and (b, inset) its microscopic roughness, whereas recessed zones do not touch the substrate.

After thermal processing, the PDMS stamp can be peeled off and will consist of a fully flexible and transparent elastic stamp reproducing the negative of the master pattern. The possibility to realize micro and nano-structures by means of this technique relies in the intrinsic property of PDMS elastomer to form a conformal contact with the surface which it has been brought into contact to.

“Conformal contact comprises 1) the macroscopic adaptation to the overall shape of the substrate and 2) the microscopic adaptation of a soft polymer layer to a rough surface, leading to an intimate contact without voids. Adhesion forces mediate this elastic adaptation, and even without the application of external pressure, an elastomer can spontaneously compensate for some degree of substrate roughness, depending on the materials properties”.

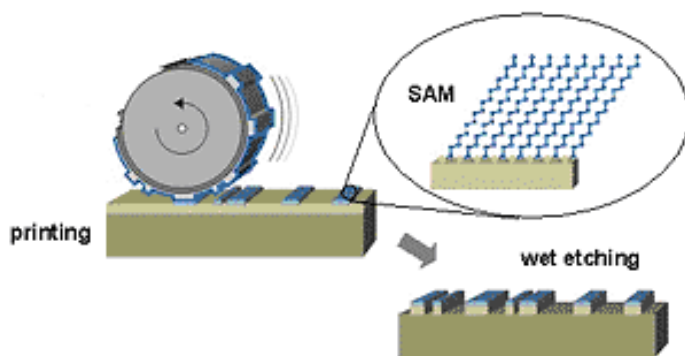
Several different techniques are known collectively as soft lithography. We report below the most important:

- *Near-Field Phase Shift Lithography.* A transparent PDMS phase mask with relief on its surface is placed in conformal contact with a layer of photoresist. Light passing through the stamp is modulated in the near-field. If the relief on the surface of the stamp shifts the phase of light by an odd multiple of λ , a node in the intensity is produced. Features with dimensions between 40 and 100 nm are produced in photoresist at each phase edge.
- *Replica Molding.* A PDMS stamp is cast against a conventionally patterned master. Polyurethane is then molded against the secondary PDMS master. In this way, multiple copies can be made without damaging the original master. The technique can replicate features as small as 30 nm.
- *Micromolding in Capillaries (MIMIC).* Continuous channels are formed when a PDMS stamp is brought into conformal contact with a solid substrate. Capillary action fills the channels with a polymer precursor. The polymer is cured and the stamp is removed. MIMIC is able to generate features down to 1 μm in size.

- *Microtransfer Molding*. A PDMS stamp is filled with a prepolymer or ceramic precursor and placed on a substrate. The material is cured and the stamp is removed. The technique generates features as small as 250 nm and is able to generate multilayer systems.
- *Solvent-assisted Microcontact Molding (SAMIM)*. A small amount of solvent is spread on a patterned PDMS stamp and the stamp is placed on a polymer, such as photoresist. The solvent swells the polymer and causes it to expand to fill the surface relief of the stamp. Features as small as 60 nm have been produced.

MicroContact Printing (μ CP)

It is probably the most known and used soft lithographic technique. In this section we describe it more in details, since it has been widely employed during this thesis for the patterning of all organic FETs. The basic application or at least the most used one, of μ CP concerns using as “ink” Self Assembled Monolayers (SAMs) to be transferred onto the surface of a substrate by contact. In details, an “ink” of alkanethiols is spread on a patterned PDMS stamp. The stamp is then brought into contact with the substrate, which can range from coinage metals to oxide layers. The thiol ink is transferred to the substrate where it forms a self-assembled monolayer that can act as a resist against etching.



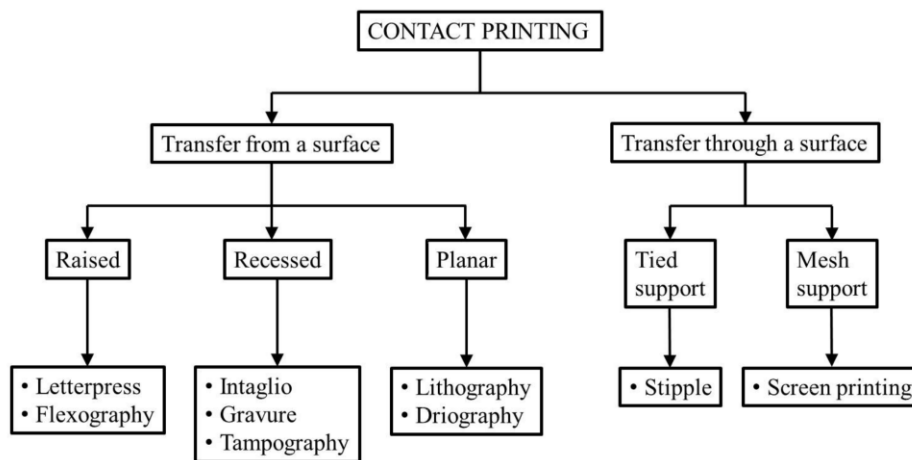
μ C printing of alkanethiols employed as protective mask during the wet etching procedure for the patterning of the metal electrodes.

Features as small as 300 nm have been made in this way. Although these monolayers do only have a thickness corresponding to the length of just one ink molecule, which typically has a longer axis of about 2-3 nm, they are very stable and resistant against

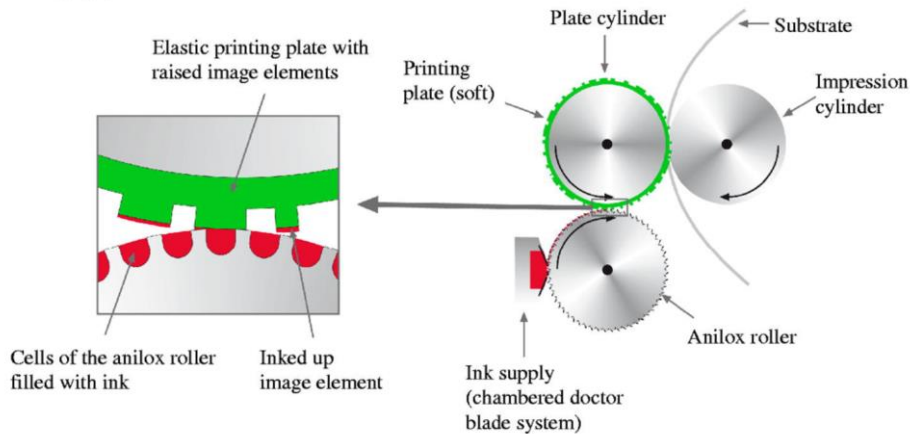
chemical and physical stresses during processing. This makes them ideal as etch resists in a photo-mask-free process. In the same way it is possible to use also other molecular “inks” instead of alkanethiols. As will be describe in details in Chapter 4, we used μ CP to pattern Source and Drain electrodes by employing the conducting polymer PEDOT:PSS as “ink” to be transferred onto the gate dielectric surface. With this technique it was possible to realized all organic FETs either in Bottom Contact and Top Contact configurations with very good performances.

5.9 CONTACT PRINTING TECHNIQUES

A schematic classification of contact printing techniques is shown in the following figure. Contact printing techniques can be divided into two major groups: in the first one the ink is located on the printing plate, in raised, recessed or planar position, and is directly transferred from the plate to the substrate by direct contact; in the second group the ink passes through a perforated surface in contact with the substrate. Four important examples are analyzed in the following: flexography, gravure printing, lithography and screen printing.



Flexography



Flexography, schematized in the previous figure, is a roll-to-roll contact printing technique which employs a set of cylinders. The first cylinder, called anilox, is characterized by engravings, i. e. small cavities separated by small walls, where the ink is deposited by an ink supplier. From the anilox, the ink is transferred to a second

cylinder, the printing cylinder, surrounded by a soft mold, the printing plate, that reproduces the positive image of the final pattern.

The ink is transferred in a precise controlled way to the molded printing plane, in a raised position. The printing substrate is pressured between the rolling plate cylinder and a third hard cylinder, called impression cylinder: the ink is impressed from the raised position of the soft mold to the sliding substrate and the final pattern is the exact positive reproduction of the patterned soft mold. A wide range of inks can be printed with such technology, and no strict physical requirements are necessary for the ink formulation. On the contrary, the major drawback is the halo effect, i. e. the spreading of the ink outside the image areas due to the compression applied, which limits the resolution of this process.

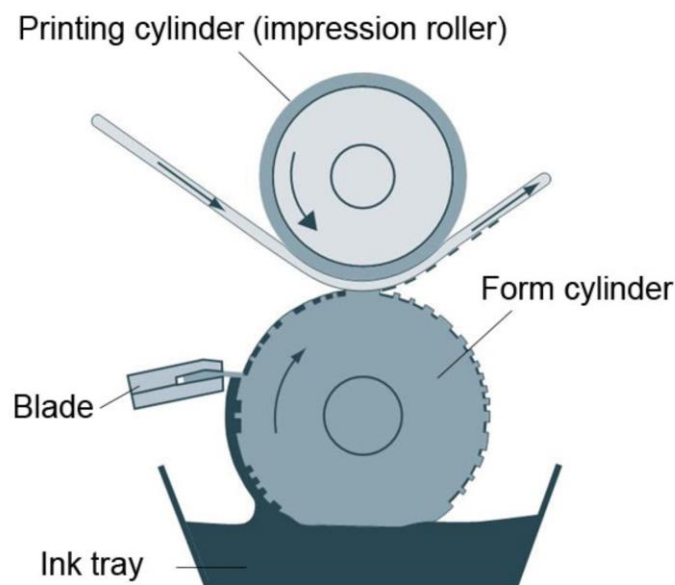
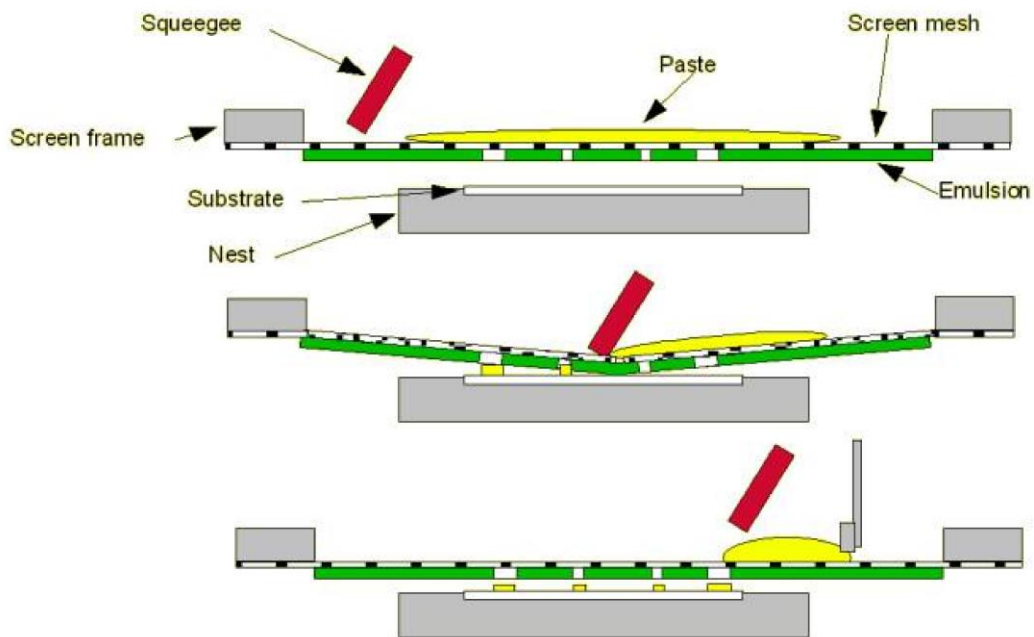


Figure 1.27: Schematic of the gravure printing technique.

Gravure printing is another roll-to-roll printing technique based on the opposite principle with respect to flexography. It is schematized in the previous figure. An ink tray covers a molded form cylinder with inks, while a blade removes the surplus. Therefore the ink is kept only in the cavities of the mold in a recessed position and, when the printing cylinder and the printing cylinder press the sliding plastic substrate,

the printed pattern is the negative pattern of the molded form. This technique is generally characterized by the same advantages (versatility, speed) and disadvantages (non-high resolution) as flexography. Standard molds are made of small separated points which allow the fabrication of electronic device components. Where continuous conductive elements are required, such as RFID tags, the mold is engraved with linear structures: in this case the technique is called intaglio.

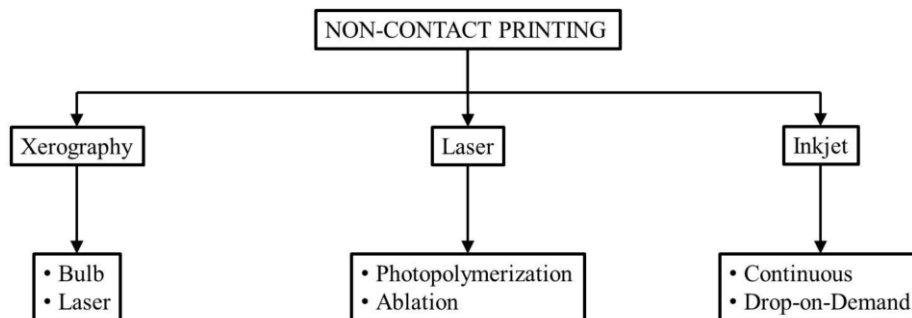


Screen printing is a contact printing technology where ink is transferred through, and not from, a patterned surface. This deposition technique is well schematized in figure. It is composed of a screen mesh stretched over a screen frame. In a pre-printing process, an emulsion, whose properties depend on the chemical and physical properties of the ink to be printed, is poured onto the back side of the mesh. An exposure unit removes the unnecessary emulsion, leaving a pattern which represents the negative image of the desired final pattern. Then the screen is placed atop the plastic substrate and the ink is poured on the front side of then mesh; a flood bar is used to push the ink through the mesh holes. The actual printing process starts when a rubber blade, called squeegee, is slid along the screen, moving the mesh down in contact with the substrate. The ink which fills the mesh holes is therefore pumped

through the openings, i. e. the emulsion vacancies, directly to the substrate: by an opportune tuning of the printing parameters, such as the ink's properties, the thickness of the mesh and the pressure applied to the squeegee, only the desired amount of ink in the desired position creates the final pattern. This technique is most employed for the fabrication of organic photovoltaic cells.

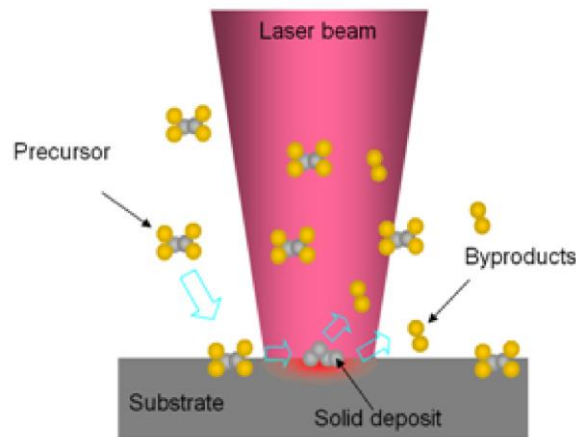
5.10 NON-CONTACT PRINTING TECHNIQUES

The following Figure shows a schematic classification of the main non-contact printing techniques. This class includes a wide range of printing technologies, therefore it is not possible to describe them all. Roughly, they can be divided into three main sub-classes, depending on the physical principle they work by: Xerography, Laser-based techniques and Inkjet printing. In the following, an example is given of the laser group, namely the Laser Direct Writing, and then all the attention is focused on the inkjet printing technology, which has been developed during this thesis and which actually is one of the most promising processes for the deposition of organic electronics materials.



Laser Direct Writing is a set of non-contact printing techniques used both for the deposition of inorganic and organic materials. A detailed overview of the process is given by Hon et al., while an example of specific application in the organic field is reported by Ribierre et al. A wide range of materials can be printed by means of this technologies, from metals to polymers to ceramics, and they also can be deposited

from a vapour, liquid or solid precursors. Three examples, one for each phase, are given.



Laser Chemical Vapour Deposition (LCVD) uses an argon ion laser that can focus on spots as small as 2 μm by means of optical microscope lenses. In this case the precursor is in gaseous phase and contains the material to be deposited. When the laser beam scans over the substrates, the increased temperature causes the material to dissociate from the gas and to be deposited on the substrate, forming a uniform layer. The repetition of this process over the same spot leads to the deposition of multiple layers. Next Figure shows a simplified schematic of the LCVD working principle. The main limits of this technique are the relatively high processing costs, due to the sophisticated equipment employed, such as the vacuum pump, and the employment only of volatile materials. A detailed review was presented by Duty et al.

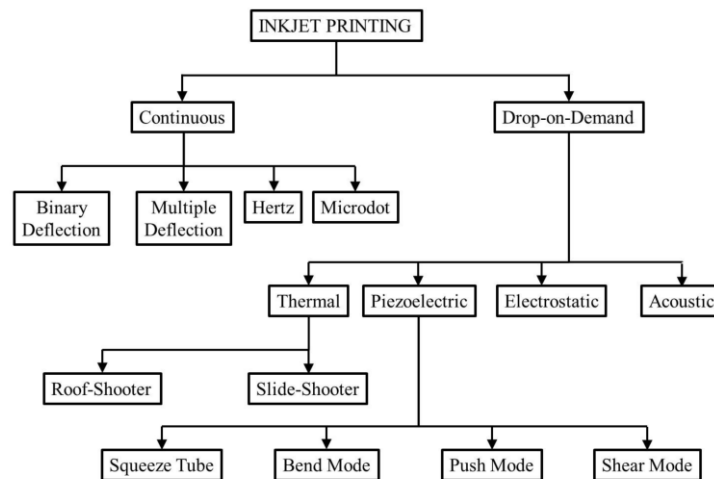
Laser-Enhanced Electrodes Plating (LEEP) employs a liquid precursor forming a solution in which the substrate is immersed. As for LCVD, the laser beam, focused on a spot, causes a rapid heating that leads to the liquid decomposition and to the printing of a metallic plate on the substrate. This technique, described in many reviews, does not allow a precise control of the layer thickness.

Laser-induced forward transfer (LIFT), finally, is based on a solid transparent support containing the material to be deposited. The target substrate is placed in parallel at a distance of about 100 μm below or above. In this case, the laser beam vaporizes the

solid precursor which rapidly condenses on the substrate. The versatility of this technique allows the deposition of a wide range of materials, since it does not have strict physical requirements, while the main limitation is that target surfaces must be very flat due to the proximity with the solid support containing the material precursor.

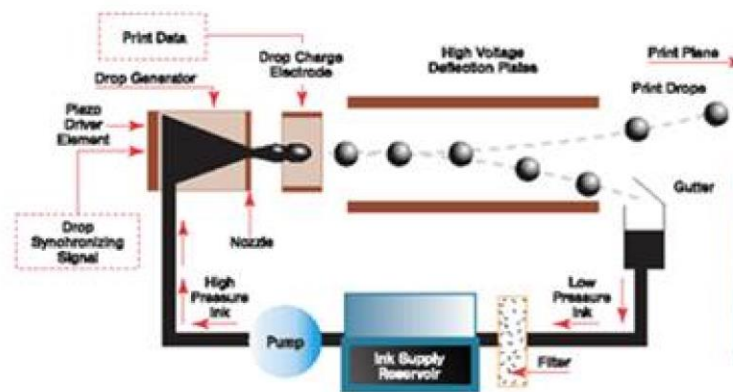
5.11 INKJET PRINTING TECHNIQUE

Inkjet Printing is the main material deposition technique employed in this thesis. It mainly consists of the ejection of fixed quantities of ink from a chamber through a hole, called nozzle. The ink droplets, under the gravity force, fall on the target substrate and form a patterned layer. An annealing process is then necessary to make the ink solvents evaporate leaving a solid layer on the substrate. The drop ejection can be caused by various transducers and in different ways: the most common, described in the followings, include continuous Inkjet Printing and Drop-on-Demand Inkjet printing. Moreover, the latter can be actuated most commonly by means of a thermoelectric or a piezoelectric transducer. The following Figure gives a summary of all the possible Inkjet printing technologies.



Several interesting articles describe them and offer an overview on their versatility and on the different possible applications. Next Figure shows a schematic of Continuous Inkjet Printing mode. The ink is continuously pumped from a "drop generator"

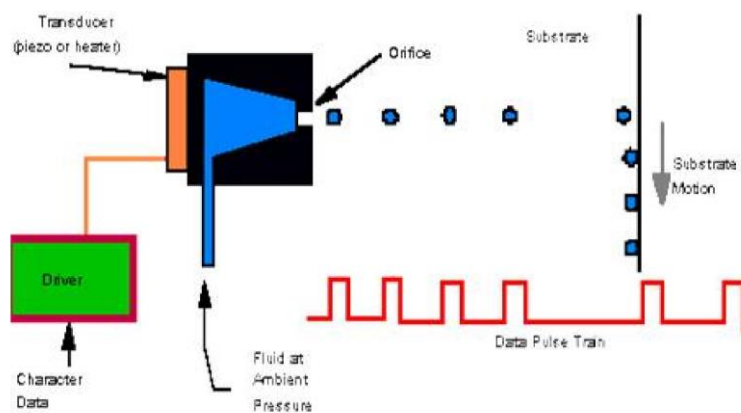
module through a nozzle, by means of a transducer, usually piezoelectric. The ejected ink flow breaks down into drops, due to the Rayleigh instability. These drops pass through a system of charging plates and, under the effect of an electrostatic field, they get electrically charged. Then they pass through a system of highvoltage deflection plates which generate a variable electromagnetic field: the charged drops are deflected to the desired direction onto the substrate and, together, form the patterned layer. The more the droplets are charged, the more they are deflected: thus the charging plates actually receive the digital input and control the printing process. When a drop is not required to be printed, the charging plates turn off, the drop does not get neither charged nor deflected, but it is collected in a recirculation system. Thus, they are conveyed into the main ink reservoir and then pumped again to the drop generator. With the continuous approach high printing frequencies (up to 80 kHz) and jet velocity (20 m/s) can be reached, but a resolution not better than 100 μm can be achieved. Moreover, due to the recirculation process, a high contamination probability can degrade the ink. This technique finds its best application in high-speed textile printing.



A different approach is used with Drop-on-Demand Inkjet Printing (DoD), schematized in the following figure. Here the drop ejection is not continuous, but occurs only when the transducer, that can be based on the thermoelectric or piezoelectric effect, is biased with a voltage pulse. Therefore, all the droplets ejected are directly deposited to the target substrate and form the patterned layer, without passing across charging plates or deflection plates. Moreover, no recirculation system is needed, leading to a reduced contamination risk. The working principle of a Thermal DoD inkjet printer is based on the Joule effect. The transducer of the drop

chamber is a simple heating resistor. When it is subjected to a considerable current flow, its temperature increases rapidly (Joule effect) as well as that of the surrounding ink. If the ink solvent is volatile, it starts to vaporize and a vapor bubble is generated, causing an abrupt pressure increase. Thus, the ink is forced through the nozzle. As the current is suddenly cut off, the resistor temperature decreases and the vapor bubble vanishes: the ink previously forced outside is then detached from the nozzle and a droplet is formed.

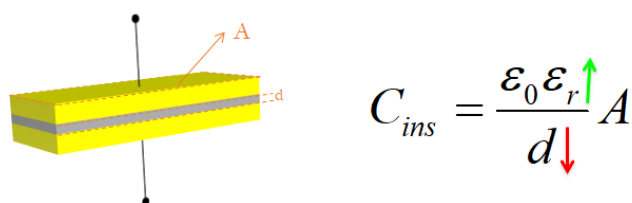
The other most commonly used inkjet printer is based on the piezoelectric DoD mode. It is based on the piezoelectric effect: a piezoelectric crystal is deformed when a high voltage is applied on it. In this case the transducer is a piezoelectric crystal biased with a desired voltage waveform. In its stand-by position, the crystal is slightly depressed in order to prevent the ink to flow out of the nozzle. Then, in rapid sequence, the crystal is set to its neutral position and then to its maximum deflection: due to the initial depression the ink is first drawn from the ink reservoir and then, after a rapid pressure increase, suddenly ejected from the nozzle. This multi-phase working principle is explained more in detail afterwards, where the piezoelectric DoD inkjet printer used in this work is shown. In conclusion, it is worth remarking that piezoelectric DoD does not have any specific limitation about the ink volatility, as for thermal DoD, thus the former is theoretically more versatile. Specific ink requirements regard their chemical and physical properties, in order to obtain a good and controlled jet, and depend on the printer characteristics.



6 LOW VOLTAGE ORGANIC TRANSISTORS

One of the main issues that actually dramatically slowed down the employment of OFETs in practical application is related to the relatively high voltages they have to be operated with. Fortunately, in recent years, many different strategies have been developed in order to lower down the operative voltages in OFETs.

The main point in this case is trying to increase as much as possible the gate dielectric capacitance, allowing achieving a much higher capacitive coupling with the device channel.



Increasing gate capacitance is the key factor for realizing low-voltage OFETs

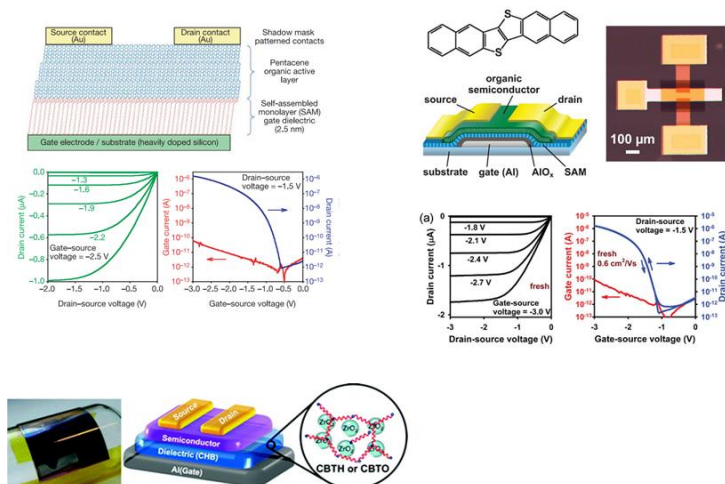
There are two possible way to increase the gate insulator capacitance: i) using high dielectric constant materials; ii) using ultrathin insulating films.

The first approach unfortunately has a strong limit for plastic electronics. In fact, the most of high dielectric constant materials need to be processed at very high temperatures which are not compatible with the most of the normally employed plastic substrates, therefore, are not really suitable for the development of organic electronics.

The latter approach is much more promising, however, not trivial. In fact, in order to obtain a sufficiently high gate dielectric capacitance, using typical insulators having a dielectric constant around 3, thicknesses around tens of nanometers should be reached. Considering that the average surface roughness of plastic substrates is generally ranging around 5-10 nm and that they are also characterized by high concentration of surface defects, a highly reproducible coating is required in order to maximize the yield of the process.

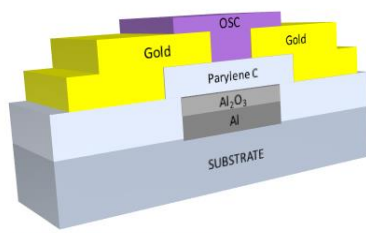
In recent years, many different approaches have been reported for the fabrication of low voltages thin film transistors. A brilliant solution to this problem was proposed in 2000 by J. Collet et al. who first introduced the use of Self Assembled Monolayers (SAMs) for realizing the gate dielectric of the transistor. Halik et al. in 2004 further improved these first results, demonstrating that by realizing a high quality SAM on silicon dioxide, also the gate leakage through the SAM may be lowered by several orders of magnitude. Finally, Klauk et al. in 2007, were able to obtain a good insulating layer from Self Assembled Monolayers (SAMs) deposited on a metal oxide that can be obtained at low temperature on flexible (plastic) substrates, i.e. they demonstrated that the packing density of SAMs on metal oxides may be high enough to obtain a dielectric layer with a very low leakage current and the desired surface properties for optimizing the dielectric/semiconductor interface. However large scale extension of this approach does not appear very easy.

Other interesting solutions for lowering bias voltages of OTFTs have been proposed by several authors: for instance Chen et al., employed dielectric layers based on TiO₂ nanoparticles embedded in a PVP matrix to obtain devices with moderately low voltages, while V. Shin et al. employed a high- κ HfLaO (20 nm) in combination with PVP, to obtain a very low voltage device. In this case, the gate dielectric capacitance was increased by increasing its dielectric constant, thus allowing a thicker layer to be employed. However, this fabrication procedure is not suited for application on the majority of plastic substrates as the processing temperature (300° C) is close to the melting limits for such materials. More recently, the use of cross-linked polymer blends was proposed for the optimization of dielectric performance in OTFTs. Results look promising, but the small thickness required for achieving large capacitances implies that spin-coating is the only deposition technique available for such materials. Scalability to very large areas is therefore not obvious.



A different approach has been developed by Cosseddu et al. In this case, the fabrication process starts from a flexible plastic substrate on which an aluminum thin film can be deposited. Such film will act as bottom gate electrode, therefore its geometry has to be shaped, typically through a photolithographic process. Aluminum has a relatively low ionization energy, meaning that it gets oxidized very rapidly when exposed to air. Such oxidation process can be intentionally increased by exposing such thin film to oxygen plasma, or to UV-Ozone, or also, by thermal treating the film in ambient atmosphere for a sufficient amount of time (generally 12 hours are enough). In this way, a very thin, 6 to 10 nm thick aluminum oxide layer is formed. Unfortunately, such film is not too homogeneous and generally characterized by a high concentration of interfacial defects. Therefore, cannot be used alone for the fabrication of transistors. One way to improve the performances is to use a second insulating materials that can be deposited over large area, at relatively low costs, and that is able to form uniform thin films. Parylene C, introduced in the previous sections is a very promising material in this sense, as it is widely used also at an industrial scale and is able to form pinhole-free films of thicknesses from 10 nm up to several micrometers.

Considering this, at the top of the aluminum oxide layer, an ultrathin Parylene C film can be deposited. Afterwards the device can be completed by the deposition and patterning of source and drain electrodes, and the deposition of the organic semiconductor.



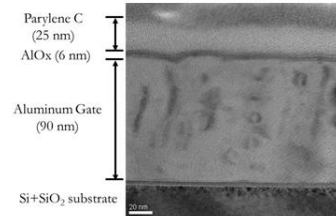
- Gate: Aluminum

- Gate Dielectric:

AIOx [UV-Ozone treatment at room temperature]

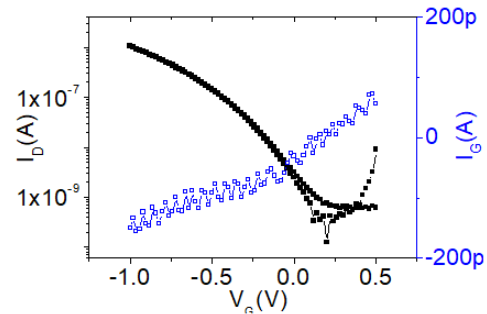
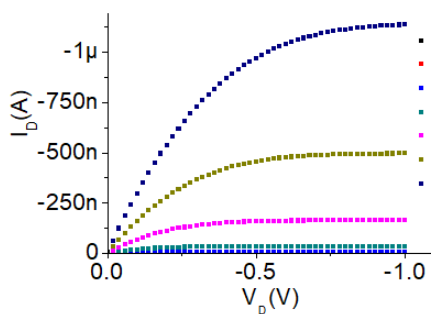
Parylene C [deposited by CVD]

[air-stable, robust, biocompatible and resistant to solvents; can be deposited in very thin films]



Such approach has been demonstrated to be highly reproducible and that different kind of organic semiconductors can be employed, obtaining, in all cases a very high fabrication yield and sufficiently high performances, in terms of mobility and also low threshold voltages.

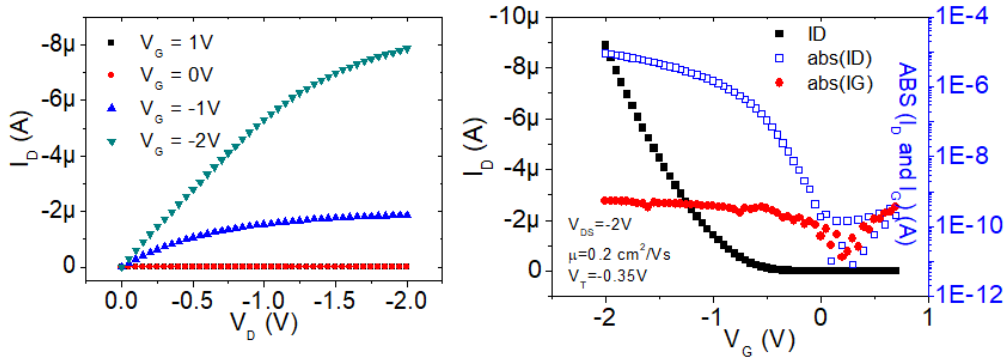
Insulating Structure	Capacitance [F/cm ²]	I _G [A] J _G [A/cm ²]	V _t [V]	μ [cm ² /Vs]	S [mV/dec]	N _t [cm ⁻² eV ⁻¹]	OTFTs Yield [%]
AIOx	3.5 E-6	6 E-6 2.9 E-5	-1.2	3.3 E-3	360	1.1 E14	15%
AIOx + 25nm Parylene	1.3 E-7	4 E-10 1.9 E-9	-0.5	6 E-2	350	4 E12	95%



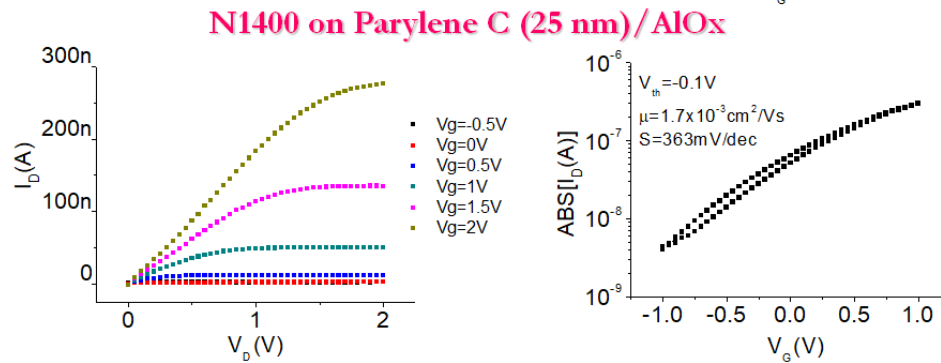
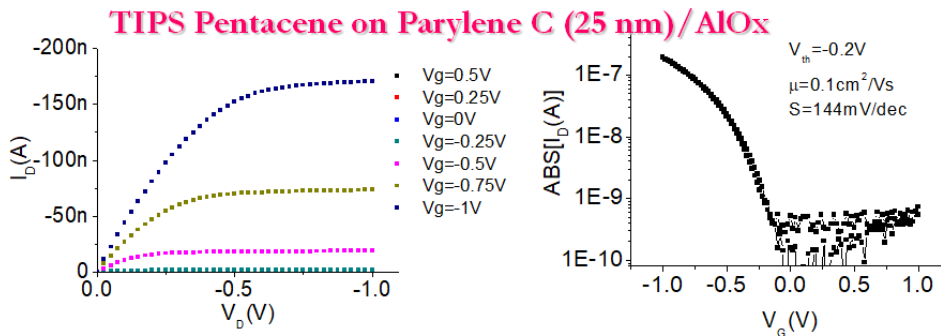
Pentacene

In particular, TIPS pentacene has demonstrated to be a very good material for these kinds of architectures, showing threshold voltages very close to 0 V, and mobility in the range of 0.1-0.5 cm²/Vs.

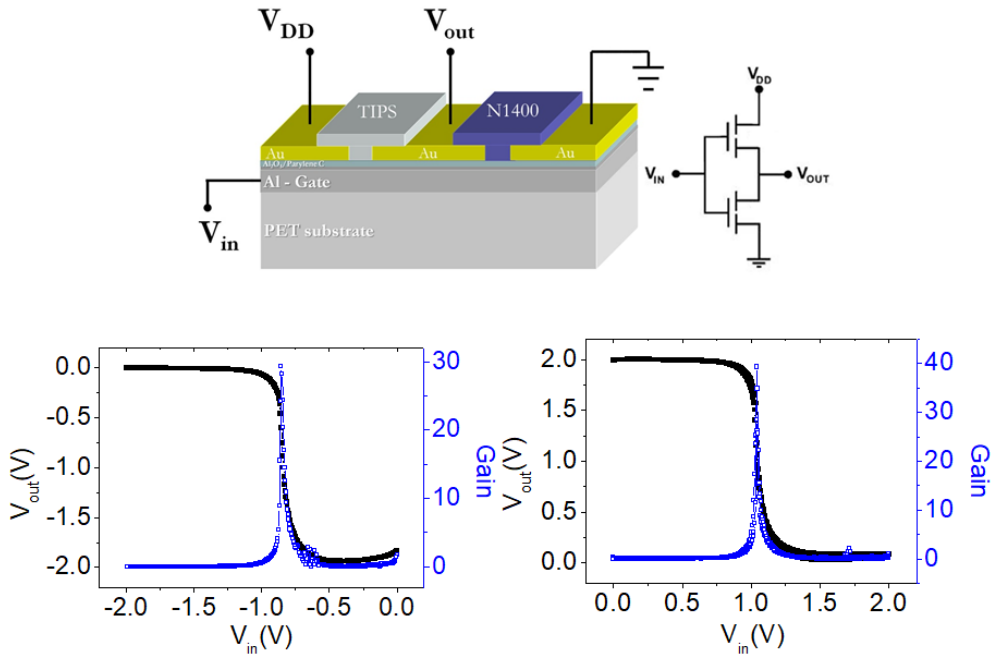
Insulating Structure	Capacitance [F/cm ²]	I _G [A] J _G [A/cm ²]	V _t [V]	μ [cm ² /Vs]	S [mV/dec]	OTFTs Yield [%]
AlOx + Parylene	1.3 E-7	4 E-10 1.9 E-9	-0.2/-0.4	0.3	150	99%



TIPS Pentacene

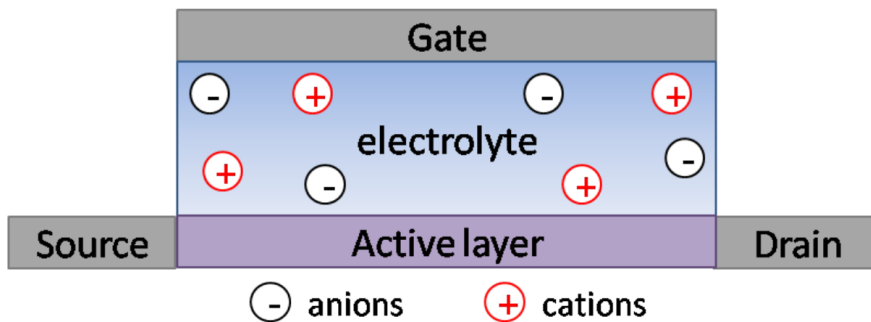


Starting from this architecture also n-type materials as N1400 can be employed for achieving n-type OFETs, and eventually be employed in a simple inverter configuration giving very promising results.



6.1 THE ORGANIC ELECTROCHEMICAL TRANSISTOR

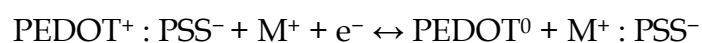
In the past 20 years Organic ElectroChemical Transistors (OECTs), as a subset of Organic Thin Film Transistors (OTFTs), have attracted particular interest for their simple fabrication and low operating voltages. Also, the capability of working in aqueous environments make OECTs suitable for biological and chemical sensing application. The first OECT was reported in 1984 by White and co-workers. In their device the conductivity of a poly(pyrrole) film was modulated by the application of a gate voltage through an electrolyte. Indeed an OECT is made up of two electrodes, source and drain, connected with an active layer (channel) realized with an organic semiconductor, and a third electrode, the gate, separated from the active layer by an electrolyte. In Figure a schematic view of an OECT is showed.



The source-drain current is modulated by electrochemical doping or de-doping of the active layer, mediated by the ionic motion between the electrolyte and the semiconductor film when a gate voltage is applied through the electrolyte. In order to explain in more details the operation principle of such a device, the case in which the active layer of the electrochemical transistor is constituted of PEDOT:PSS first reported in 2002 by Nilsson, will be considered hereafter. PEDOT:PSS is the most commonly used organic polymers for this application and, furthermore, it is the material employed for the realization of OECTs.

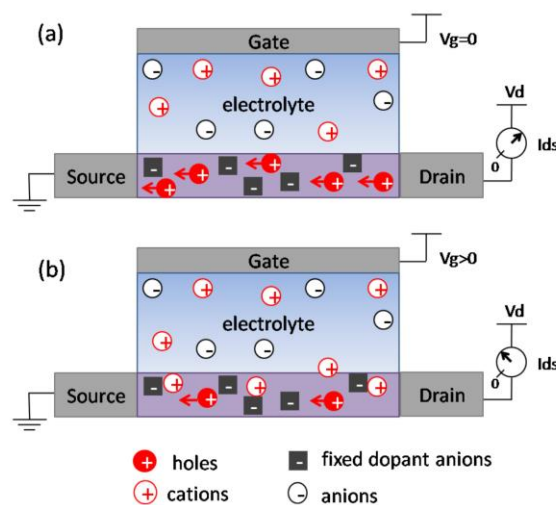
6.1.1 PEDOT:PSS based electrochemical transistors

PEDOT:PSS can be employed as active layer material of a OECT because, as many conjugated polymer systems, it has the ability to conduct not only electrons but also ions. Thus, if in the PEDOT:PSS/electrolyte system there is a surplus of counter ions in the polymeric film, the ions from an aqueous solution enter the polymer film and their conduction in the material increases; in particular, this primarily occurs in the PSS phase and is thus effectively independent on the oxidation state of PEDOT. However, when employed as active layer in OECTs, PEDOT is generally pristinely doped and is therefore in its high conducting, partially oxidized state. From this state the material can either be further oxidized to a more conducting state or reduced to the semi-conducting neutral polymer. The reduction (left to right) and oxidation (right to left) reactions of PEDOT:PSS occur according with the following equation:

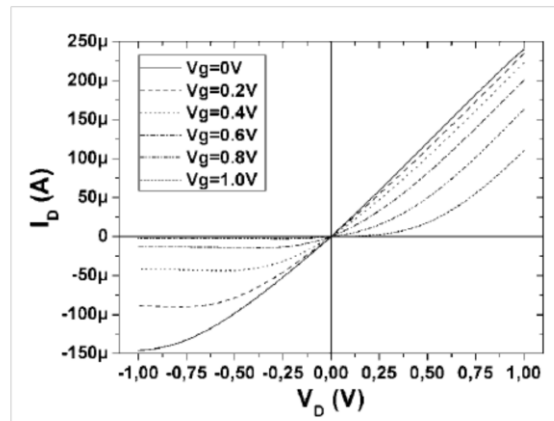


where M^+ represents a cation and e^- is an electron. Despite OECTs can operate in accumulation or depletion mode, most published works refer to the second one. D. A. Bernards and G. G. Malliaras in 2007 proposed a model that describes the behavior of depletion mode OECTs. In this analysis they supposed that the source electrode is

grounded and a voltage V_d is applied to the drain electrode; a current I_{ds} thus flows through the polymeric channel between source and drain contacts. As the gate electrode is positively biased ($V_g > 0$), cations M^+ of the electrolyte enter into PEDOT:PSS film and reduce PEDOT to its neutral state according with the previous equation from left to right, resulting in the de-doping of the channel and, consequently, in the decrease of the I_{ds} current. The model involves two different circuits: an electronic circuit consisting in the holes/electrons transport between source and drain through the active layer, described by the Ohm's Law, and a ionic circuit which accounts for transport of cations and anions through the electrolyte. According with this interpretation, the typical behaviour of a depletion mode OECT ($V_g > 0$), can be explained. In the first quadrant, i.e. when $V_d > 0$ two regimes of behaviour can be distinguished: when $V_d < V_g$ the channel is uniformly de-doped leading to a quadratic dependency of I_{ds} from V_d ; when instead $V_d > V_g$, de-doping occurs only in the channel region where $V(x) < V_g$ leading to a linear I_{ds} vs. V_d behaviour. In the third quadrant ($V_d < 0$) portions of the channel can be completely de-doped when the intrinsic (negative) dopant density is equal to the density of the injected cations; thus, when the drain voltage further decreases towards more negative values, I_{ds} starts to saturate and a channel pinch-off arises leading to the current saturation.



If the gate electrode is grounded or negatively biased, the PEDOT:PSS channel gets reoxidized and a high current flows again between source and drain electrodes. It should be noted that, even if the reduction/oxidation reactions of PEDOT:PSS are reversible, for gate voltages above ca. 2 V an irreversible loss of channel conductivity occurs.



At elevated oxidation potentials, in fact, PEDOT can be oxidized to a non-reversible nonconducting state; such a state is called over-oxidized state and the phenomenon is called overoxidation. Barsh et al. suggested that the overoxidation phenomenon in polythiophene films involves a mechanism that breaks the conjugation of the polymer chain. Even if works about the overoxidation mechanism in PEDOT:PSS films has not been published yet, it is highly probable it is similar to that proposed for polythiophene.

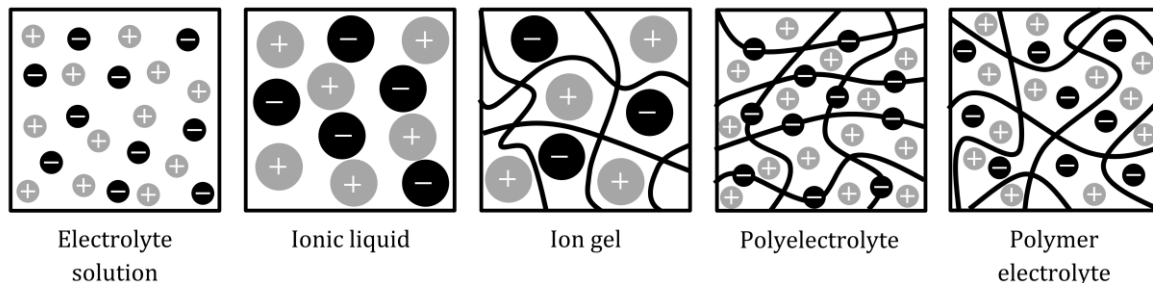
6.2 ELECTROLYTE-GATED ORGANIC FIELD EFFECT TRANSISTOR (EGOFET)

Over the past two decades, OFETs have gained considerable attention owing to their potential as alternatives to conventional inorganic counterparts in low-cost large-area flexible electronic applications. A majority of the OFETs reported to date can only operate well at voltages beyond 20 V. However, implementing low-cost flexible-electronic-applications enforces several requirements that OFETs must comply with including low-operating voltages (in the range of few volts), low-temperature processing, mechanical flexibility and compatibility with flexible substrates, and low-cost robust processing techniques such as printing. Tremendous efforts have been devoted to achieve low-voltage OFETs while maintaining high output current levels which can be accomplished by using a high capacitance gate insulator. The approaches proposed to achieve this include using a high-permittivity (κ) insulator, using a nanometer-thick self-assembled monolayer of organic compound as the gate insulator, or using an electrolyte as gate insulator. However, organic materials normally have low permittivity values and depositing very thin insulator layers is not possible with the low-cost printing techniques. Therefore, we will focus here on the third approach which is using an electrolyte as the gate insulator material. The idea of using electrolyte-gating in transistors is far from new. Plenty of work on electrolyte-gated organic field-effect transistors (EGOFETs) have been previously reported with various electrolyte systems explored such as ionic liquids, ion gels, polymer electrolytes, and polyelectrolytes.

Electrolytes

An electrolyte is any substance that can dissociate into free ions (anions and cations). Applying an electric field across an electrolyte causes the anions and cations to move in opposite directions, thereby conducting electrical current while gradually separating the ions. Depending on their degree of dissociation, electrolytes are considered as either strong (completely or mostly dissociated into free ions) or weak (partially dissociated into free ions). The ionic conductivity level depends on the

concentration of mobile ions. Electrolytes can be found in liquid, solid, and gelled state. Solid or gelled electrolytes are often preferred for use in solid-state devices.



Various types of electrolytes that are commonly used in organic electronics include: electrolyte solutions, ionic liquids, ion gels, polyelectrolytes, and polymer electrolytes.

Electrolyte Solutions

Electrolyte solutions are the most common type of electrolytes, as they basically consist of a salt dissolved in a liquid. Electrolyte solutions are usually suitable for electrochemical experiments. Water is a common solvent, but various organic solvents are sometimes favored due to their electrochemical stability. It is noteworthy to mention that pure water by itself is a weak electrolyte where it dissociates into hydroxide (OH⁻) and hydronium (H₃O⁺) ions, with a concentration of 0.1 μ M under normal conditions.

Ionic Liquids

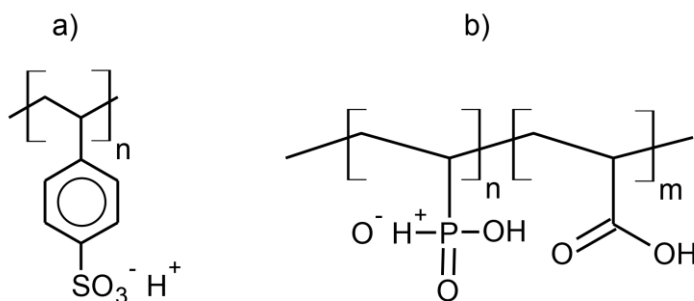
An ionic liquid is a room temperature molten salt consisting of ions and ion pairs with relatively large anions and cations. At least one ion has a delocalized charge and one component is organic, which prevents the formation of a stable crystal lattice. Ionic liquids have many interesting properties such as non-volatility, high ionic conductivity (ca. 0.1 S cm⁻¹), and chemical and thermal stability. They are highly viscous, frequently exhibit low vapor pressure, and have a melting point that is below 100 °C. Such salts that are liquid at near-ambient temperature are important for electric battery applications, and have been used as sealants due to their very low vapor pressure.

Ionic Gels

An ion gel consists of an ionic liquid that is immobilized inside a polymer matrix, e.g. a polyelectrolyte or a block copolymer. Ion gels exhibit easy handling film forming properties of the solid-state combined with the high ionic conductivity of ionic liquids (in the range of 10^{-4} – 10^{-2} S cm^{-1}). Ion gels are used as gate insulators for field effect transistors.

Polyelectrolytes

Polyelectrolytes are polymers with ionisable groups whose molecular backbone bears electrolytic repeat groups. When in contact with a polar solvent such as water, these groups dissociate leaving behind charged polymers chains and oppositely charged counter-ions that are released in the solution. Positively and negatively charged polyelectrolytes are termed polycations and polyanions respectively. In solid dry polyelectrolyte films, charged polymer chains are effectively immobile due to their large size while counter-ions are mobile, which gives rise to ion transport of counter ions. Examples of polyelectrolytes include poly(styrene sulphonic acid) or PSSH and poly(vinyl phosphonic acid-co-acrylic acid) or P(VPA-AA). PSSH and P(VPA-AA) are both anionic polyelectrolytes with typical room temperature ionic conductivity in the range of 10^{-8} S cm^{-1} and 10^{-6} S cm^{-1} , respectively. One of the applications of polyelectrolytes is their use as gate insulators in polyelectrolyte-gated organic field effect transistors due to their remarkable ability to suppressing electrochemical doping of the semiconductor bulk.



Polymer Electrolytes

Polymer electrolytes are solvent-free solid electrolytes consisting of a salt dispersed in

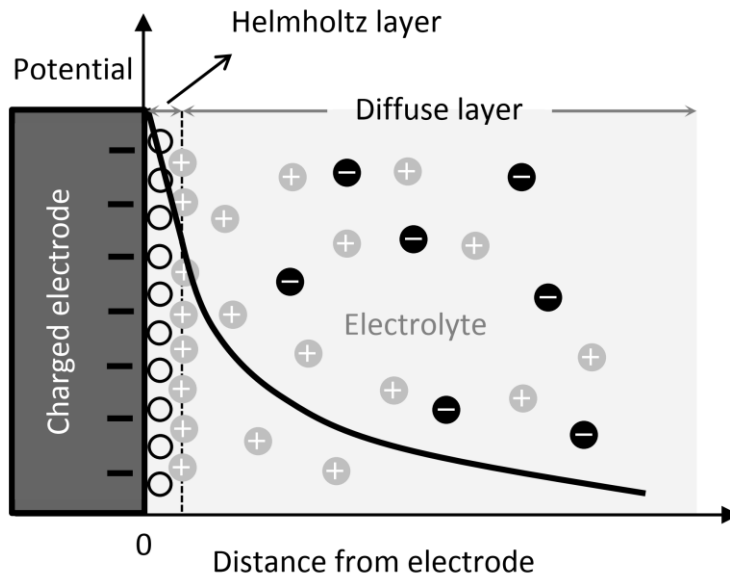
a polar polymer matrix. Both the cations and the anions can be mobile in polymer electrolytes. Typical ionic conductivity is in the range of 10^{-8} to 10^{-4} S cm^{-1} . Polymer electrolytes are used in electrochemical device applications, namely, high energy density rechargeable batteries, fuel cells, supercapacitors, and electrochromic displays.

6.2.1 Ionic Conductivity and Transport

Ionic conduction behavior in electrolytes depends on the concentration and the mobility of the ions present in the electrolyte, where the concentration of ions is determined by the solubility and the degree of dissociation. The ionic motion is governed by two different processes: diffusion caused by a concentration gradient of ions and drift or migration caused by the presence of an external electric field. As to ionic transport, the mechanism is strongly dependent on the electrolyte nature. In electrolytes with low molecular weight solvents, such as polyelectrolytes, the ions are surrounded by solvation shells formed by the solvent molecules. Hence, the ions along with the solvent molecules belonging to the solvation shells are transported as a package through the electrolyte. These ions experience a frictional force proportional to the viscosity of the solvent and the size of the solvated ion, which is the rate limiting factor for ionic mobility at low concentrations. On the other hand, transport of protons in aqueous solutions is done by hydrogen bonds rearrangement according to the Grotthuss mechanism: In aqueous solutions, a proton is immediately hydrated to form a hydronium ion, which subsequently transfers one of its protons to a neighboring water molecule that also transfers the proton to another molecule, and so on. This gives protons the high ionic conductivity in aqueous systems. In electrolytes with high molecular weight solvents such as polymer electrolytes, the polymer matrix which is considered as the solvent is immobile. The ionic motion is strongly coupled to the mobility of the polymer chain segments, where the ions travel across the material by hopping from one site to another. Thus, the ionic conductivity in polymer electrolytes is owed to the flexibility of the polymer chains in disordered regions of their structure. This explains why the ionic conductivity is low in polymers with much crystalline regions where the material is densely packed and does not have sufficient open space to allow for fast ionic transport.

6.2.2 Electric Double Layers

Electrolytes are ion conductors and electron insulators. Upon contact with a charged ionblocking electrode, the electric potential difference between the electrode and the electrolyte gives rise to the formation of a region consisting of two parallel layers of positive and negative charges called the electric double layer (EDL). This is due to the interactions between the ions in the electrolyte and the electrode surface, where the outermost electrode surface holds an excess of electronic charges that are balanced by the redistribution of oppositely charged ions located in the electrolyte close to the electrolyte/electrode interface. The EDL charge distribution is divided into two distinct layers that are described by the Gouy-Chapman-Stern (GCS) model. It consists of a compact Helmholtz layer of ions located close to the electrode surface followed by a diffuse layer extending into the electrolyte bulk. The Helmholtz layer comprises adsorbed dipole oriented solvent molecules and solvated ions, which are assumed to approach the electrode at a distance limited to the radius of the ion itself and a single shell of solvated ions around each ion. Thus, the Helmholtz layer and the electrode are analogous to a parallel plate capacitor separated by a distance of few Ångströms, with the potential drop occurring in a steep manner between the two plates. As to the diffusion layer, it consists of both positively and negatively charged ions with an excess of ions that are oppositely charged compared to the metal electrode. The potential profile in this layer has an exponential decay towards the bulk of the electrolyte. The thickness of the diffuse layer is dependent on the electrode potential and ionic concentration of the electrolyte. The capacitance of the entire double layer is typically in the order of tens of $\mu\text{F cm}^{-2}$

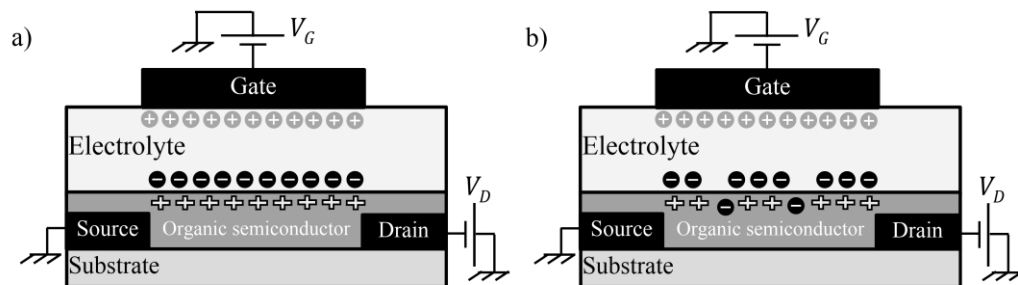


Schematic illustration of the Gouy-Chapman-Stern model of the ionic distribution in an electric double layer. The empty circles represent solvent molecules and the circles with the '+' and '-' signs represent solvated cations and anions respectively.

6.2.3 EGOFET Principle of Operation

An EGOFET differs from a conventional OFET by having an electrolyte as a gate insulator instead of a dielectric layer. The layout of a p-channel EGOFET is shown in Figure. The operation of an EGOFET is quite similar to that of an ordinary OFET with the difference being in terms of the charge polarization characteristics of the gate insulator. Applying a negative potential to the gate electrode will lead to the redistribution of the ions inside the electrolyte where the cations migrate towards the negatively charged gate electrode and the anions towards the semiconductor which induces the accumulation of positive charge carriers (holes) in the semiconductor channel. This results in the formation of two electric double layers (EDLs) at the semiconductor/electrolyte interface (lower EDL) and the electrolyte/gate interface (upper EDL) leaving a charge-neutral bulk in the middle of the electrolyte. After the EDLs are established and steady-state is reached, the driving force for ion migration in the electrolyte bulk is eliminated and the entire applied gate voltage is nearly dropped across the two EDLs with the electric field being very high at the interfaces

and negligible in the charge-neutral electrolyte bulk. The EDLs act as nanometer-thick capacitors, hence they provide the transistor with high interfacial capacitances that enables these devices to operate at low voltages (< 2 V). The total capacitance of the electrolyte is the series equivalent of the two EDLs' capacitances which is dominated by the capacitance of the semiconductor/electrolyte interface which is typically smaller. Thus, the electrolyte capacitance is independent of the gate insulator thickness which enables the use of thicker electrolyte layers while maintaining low-voltage operation. The typical capacitances of electrolyte-gates in thin-film transistors are on the order of ($C_i \sim 1\text{-}10 \mu\text{F cm}^{-2}$) which exceeds the capacitances of conventional high-permittivity dielectrics and that of ultra-thin dielectrics. It is worthwhile noting that it is possible for the ions in the electrolyte to penetrate into the organic semiconductor layer, resulting in the intentional or unintentional electrochemical doping of the semiconductor bulk, which causes the transistor to operate in the electrochemical mode that will slow the switching speed. An EGOFET that undergoes electrochemical doping is no longer an OFET and is referred to as an organic electrochemical transistor instead.



6.2.4 Polyelectrolyte-Gated OFET Characteristics

Electrolyte-gated organic field effect transistors can be classified according to the permeability of the organic semiconductor to the ions in the electrolyte. Transistors that employ permeable semiconductors tend to exhibit electrochemical behavior upon increasing the gate bias which switches their operation mode from field-effect to electrochemical, thus they are termed electrochemical transistors. This potential drawback has been reported in several ion gel-gated and polymer electrolyte-gated

transistors. One way to mitigate this problem is by the use of a polyelectrolyte as the gate insulator material which has been previously demonstrated in several papers. This is attributed to the fact that charged polymer chains in polyelectrolytes are effectively immobile and only the small counter-ions are mobile which prevents the ion penetration into the organic semiconductor bulk. For instance, applying a negative gate bias to an ion-gated OFET causes the mobile cations to move towards the gate leaving bulky polyanions at the semiconductor/electrolyte interface which are less likely to diffuse into the semiconductor. Other advantages of employing polyelectrolyte-gated OFETs include large capacitance value of the EDLs regardless of the gate insulator thickness, low voltage operation (< 1 V), compatibility with printed batteries, delivery of large drive currents, and fast switching times (< 100 μ s). Since the EDLs spontaneously form at the insulator/semiconductor interface upon applying a gate bias, the transistor performance is insensitive to the gate electrode misalignment or to the variations in thickness and roughness of the gate insulator layer which eases the manufacturing requirements and enables robust manufacturing. These features make polyelectrolyte-gated OFETs promising candidates for flexible electronic applications.

7 THE ORGANIC CHARGE-MODULATED FIELD-EFFECT TRANSISTOR

Organic device-based sensors are currently being extensively investigated as key elements in easy-to-use, portable platforms for life science and healthcare. Filling the gap between laboratory environment and real application scenarios poses several challenges that researchers must address in order to meet the requirements for the realization of low-cost and efficient devices for Point-of-Care applications. In this section we report a specific device architecture, namely the Organic Charge-Modulated Field-Effect Transistor (OCMFET), that represents a convenient option for the development of several kinds of electronic biosensors and bio-interfaces.

The basic structure of the OCMFET is reported in Figure 1. The core of the device is a standard OTFT structure, the Organic Field-Effect Transistor (OFET), developed in a bottom-gate/bottom-contact structure. In the OCMFET, the gate of the OFET structure is biased through a control capacitor (also referred as control gate): therefore, no bias is directly imposed (i.e. it is a floating gate) even if its voltage is actually fixed by several concurring effects. The floating gate is insulated from the environment by a dielectric layer, which both acts as the gate insulator and as a protecting layer impeding variations in the charge stored in it. If a part of the floating gate is left exposed, it is possible to influence the charge distribution inside it by an external stimulus, thus allowing the employment of the OCMFET as an extremely sensitive charge sensor.

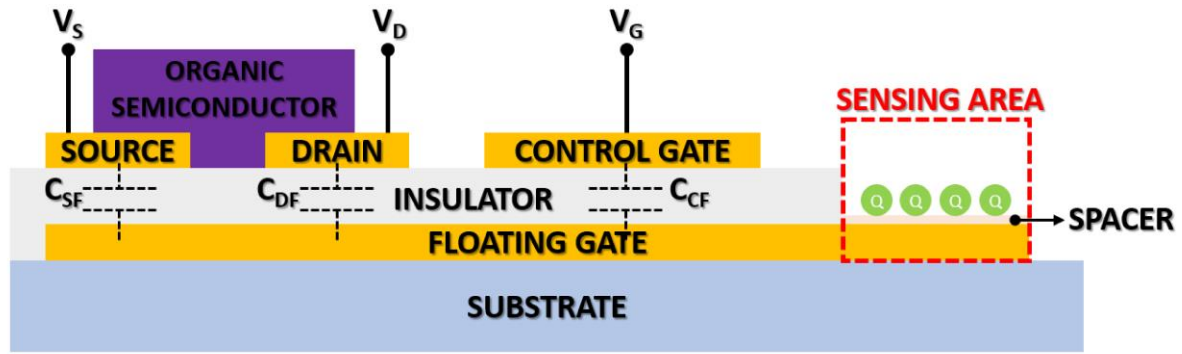


Figure 1: Cross section of a generic OCMFET structure. The OCMFET is a floating gate OTFT with a second gate called control gate that is needed to set the transistor working point. This device can be employed as a charge sensor by exposing the final part of the floating gate (called sensing area) to the measurement environment.

Its working principle has been firstly described by Barbaro et al. using a CMOS version of the device called Charge Modulated FET (CMFET) [18]. The charge inside the floating gate, Q_{TOT} , can be estimated taking into account the different voltage contributions in the device according to Gauss equation:

$$Q_{FG} = C_{CF}(V_{FG} - V_{CG}) + C_{SF}(V_{FG} - V_S) + C_{DF}(V_{FG} - V_D)$$

where CCF, CDF and CSF are, respectively, the control capacitance and the parasitic capacitances related to the overlap between drain and source and the floating gate, V_G , V_D and V_S are the voltages applied to control capacitor, drain and source respectively and V_{FG} is the actual floating gate voltage. This last parameter can be thus written as

$$V_{FG} = \frac{C_{CF}}{C_{CF}+C_{SF}+C_{DF}}V_{CG} + \frac{C_{SF}}{C_{CF}+C_{SF}+C_{DF}}V_S + \frac{C_{DF}}{C_{CF}+C_{SF}+C_{DF}}V_D + \frac{Q_{TOT}}{C_{CF}+C_{SF}+C_{DF}}$$

If a charge Q_S is immobilized on top of the sensing area by interposing an insulating anchoring layer, Q_{TOT} can be written as $Q_0+Q_i(Q_S)$, being Q_0 a constant amount of charge eventually incorporated in the floating gate during fabrication, and $Q_i(Q_S)$ the charge induced in the floating gate by Q_S . When the parasitic capacitances are negligible with respect to the control capacitance, the spacer is thinner than other

insulating layer in the device (thus allowing perfect induction approximation, $Q_i(QS) \approx (-QS)$ and Q_0 is negligible, the last equation can be approximated as

$$V_{FG} = V_G - \frac{Q_S}{C_{CF}}$$

Therefore, the value of the floating gate voltage is linearly related to the amount of charge on the sensing area. Such a variation can be easily transduced as a corresponding variation of the transistor output current. Indeed, the current flowing between source and drain is a function of the floating gate voltage according to the basic characteristic equations of OFETs: for instance, if the device is maintained in the saturation regime ($|V_{DS}| \geq |V_{FG}-V_{TH}|$, being V_{TH} the transistor threshold voltage), the current can be expressed according to the relationship:

$$I_{dsat} = \frac{Z}{2L} \mu C_i (V_g - V_t)^2$$

where μ is the charge carrier mobility, C_i is the capacitance per unit area of the floating gate insulator, Z and L are the transistor's channel width and length respectively. If we

substitute V_{FG} with the approximated relationship the Equation can be written as:

$$I_{dsat} = \frac{Z}{2L} \mu C_i \left(V_g - \left(\frac{Q_S}{C_{CF}} + V_t \right) \right)^2$$

A variation of the floating gate voltage is thus modeled as a shift in the transistor threshold voltage: if the charge QS varies of a quantity ΔQS , the threshold voltage shift is:

$$\Delta V_{Th} = -\frac{Q_S}{C_{TOT}}$$

Applications:

7.1 DNA SENSING

DNA is a negatively-charged molecule, so if a single-stranded oligonucleotide is

employed as a probe and anchored on the sensing area, hybridization with the complementary target sequence can be transduced as an increase of the negative charge immobilized on the sensing area, resulting in a floating gate voltage shift and thus in a variation of the output current of the transistor.

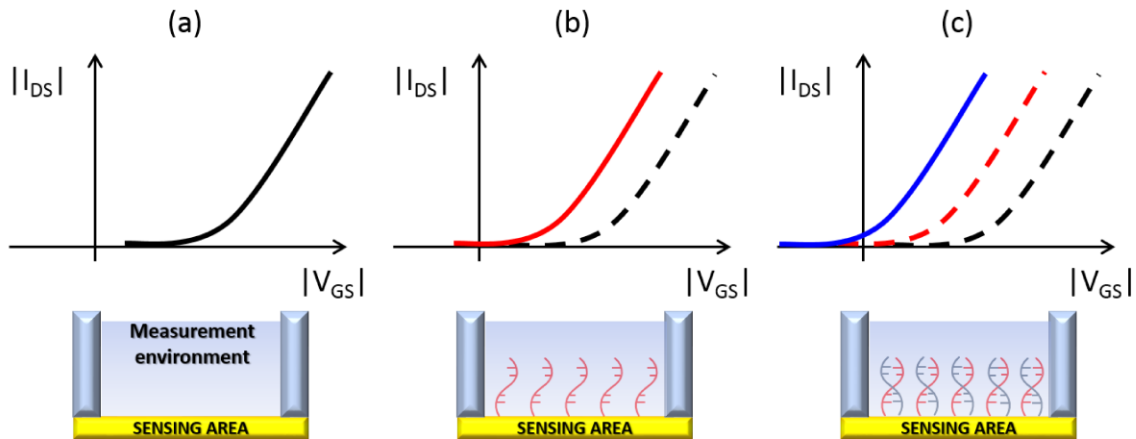


Figure 2: OCMFET as DNA sensor: (a) the transistor transfer characteristic curve before any interaction with oligonucleotides (measurement solution on the sensing area); (b) when single-stranded oligonucleotides are anchored on the sensing area (DNA probe), their negative charge determines a shift in the device threshold voltage; (c) a further shift of the threshold voltage is obtained when probes hybridize with complementary target oligonucleotides, thus determining an increase of the negative charge anchored on the sensing area; this last threshold voltage shift, and the related current variation, represent the detection mechanism for DNA hybridization.

7.2 CELLULAR ELECTRICAL AND pH SENSING

A different application scenario that has gained considerable interest in the last two decades concerns the *in vitro* testing of electrogenic cells cultures. In fact, monitoring the electrical activity of living cells is of great importance in scientific fields such as pharmacology, (neuro)rehabilitation, and computational neuroscience. Recently, *in vitro* approaches involving the use of either microelectrode arrays or ISFET-like electronic devices have been employed for the investigation of fundamental cellular mechanisms and in the disclosing of the insights of the way in which the action potential propagates in 2D and 3D neuronal networks. The OCMFET is a very convenient approach in all the applications where the detection of low charge variations in a liquid environment is involved. Particularly interesting features of this device for this specific application are the absence of a reference electrode during its

operation (thanks to the presence of the control gate) and the elongated shape of the floating gate, which allows separating the active layer (i.e. the organic semiconductor) and the area where the actual sensing occurs (namely the sensing area). These features, together with its high charge sensitivity and relatively high cutoff frequency (up to 100 kHz), make the OCMFET a good candidate for the design of novel electrophysiological/pharmacological tools that can be both reference-less and low-cost, thus potentially having the capability to compete “marketwise” with the already existent and assessed MEA and ISFET technology. In order to meet the specific requirements of the electrophysiological application, a particular kind of OCMFET array (called Micro OCMFET Array - MOA) has been designed and fabricated, and its capability of transducing bio-electrical signals has been thoroughly investigated by using cardio-myocytes cultures. In fact, thanks to the optimal covering of the sensing area and their regular electrical activity in vitro, cardiomyocytes are a very good model to estimate the device sensitivity. As shown in figure 5, the MOA turned out to be capable of reliably monitoring the activity of rat cardiomyocytes in both basal conditions and upon thermal and chemical stimulation, thus confirming the suitability of the OCMFET approach for pharmacological testing.

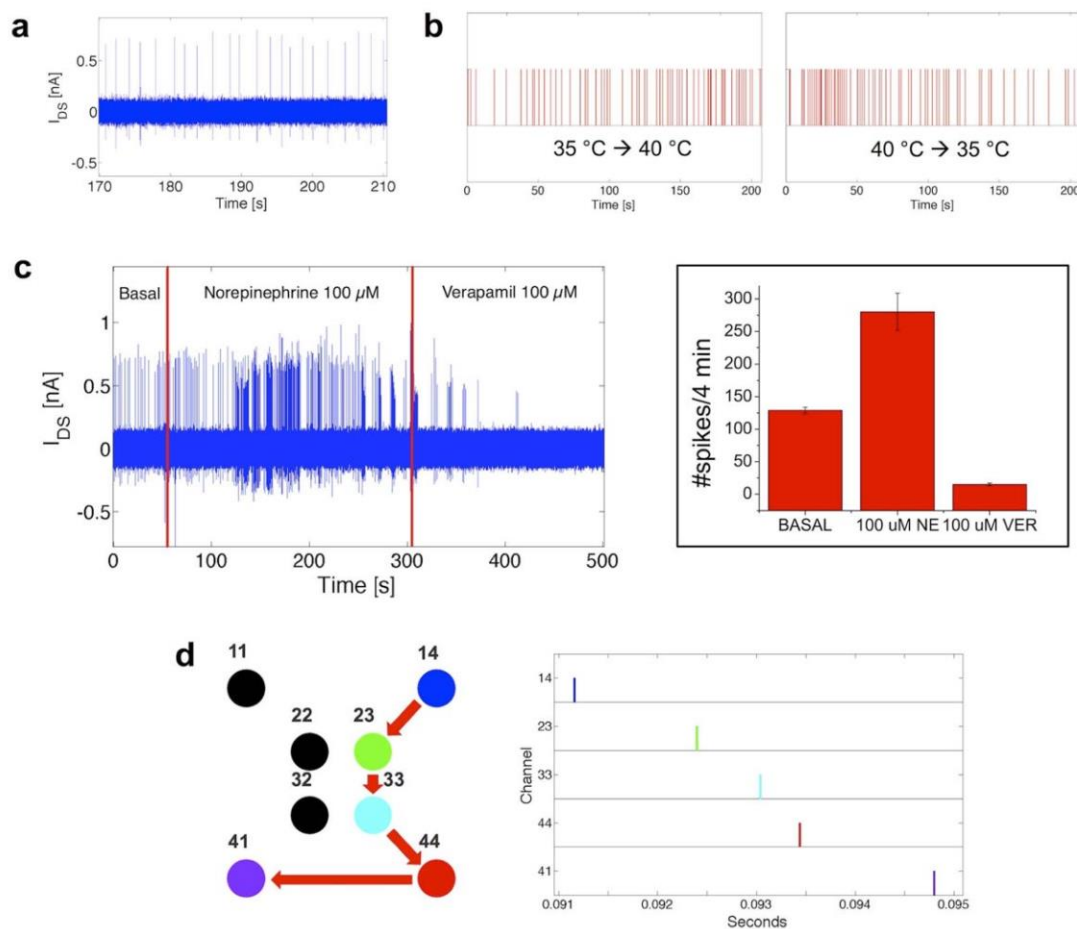


Figure 5: OCMFET validation with rat cardiac myocytes. (a) Basal activity measured with an OCMFET. (b) Raster plots of the thermal modulation of the culture activity. (c) Chemical tuning of the culture's activity. The spontaneous activity was accelerated by means of the addition of 100 mM of Norepinephrine and then suppressed with 100 mM of Verapamil. (c) (inset), Beating frequency modulation (statistics on 5 OCMFETs - average and standard deviation). (d) Multisite recording. The MOA allows to track electrical signals in the culture as shown in the raster plot of the spontaneous activity indicating a propagation of the signal from site 14 to site 41. The culture was maintained 8 days in vitro and measured at 37 °C. Adapted from Scientific Reports volume 5, Article number: 8807 (2015) [32].

Another important parameter when dealing with cell cultures is the cellular metabolic activity. In fact, the pH of the medium where the cells are cultured influences the cells activity and, on the contrary, variations of cellular metabolic activity (either physiological or induced by means of chemical/electrical stimulation) causes relative pH variations of the medium. Thanks to its versatility, the OCMFET can be easily turned into a pH sensor by properly modify the sensing area. To this purpose, a simple

pH-sensitive membrane, consisting in an oxygen plasma-activated Parylene C thin layer, has been employed. The transduction principle, as previously explained, is related to a variation of the transistor threshold voltage induced by the (pH-dependent) charge immobilized onto the sensing area. As shown in figure, such an OCMFET turned out to be a very sensitive pH sensor, thanks to the intrinsic charge amplification given by the peculiar structure of the device.

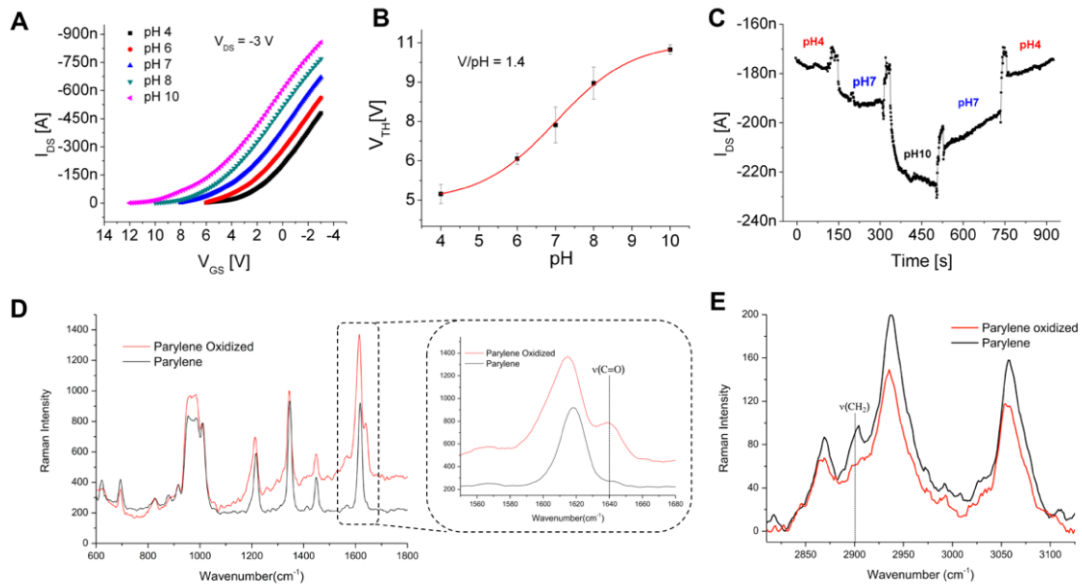
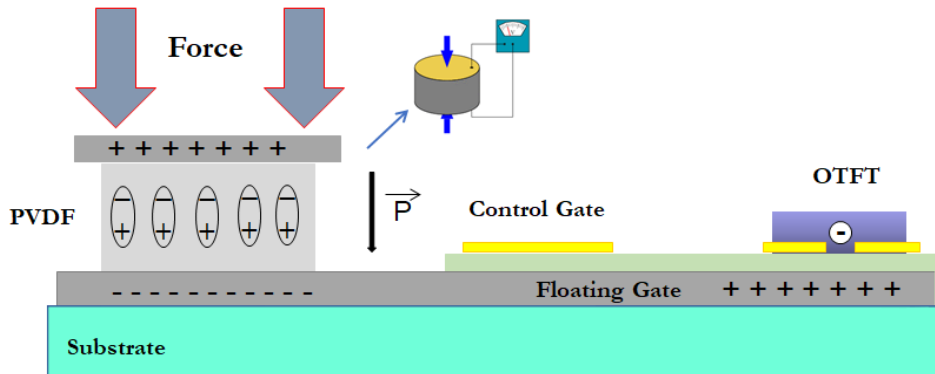


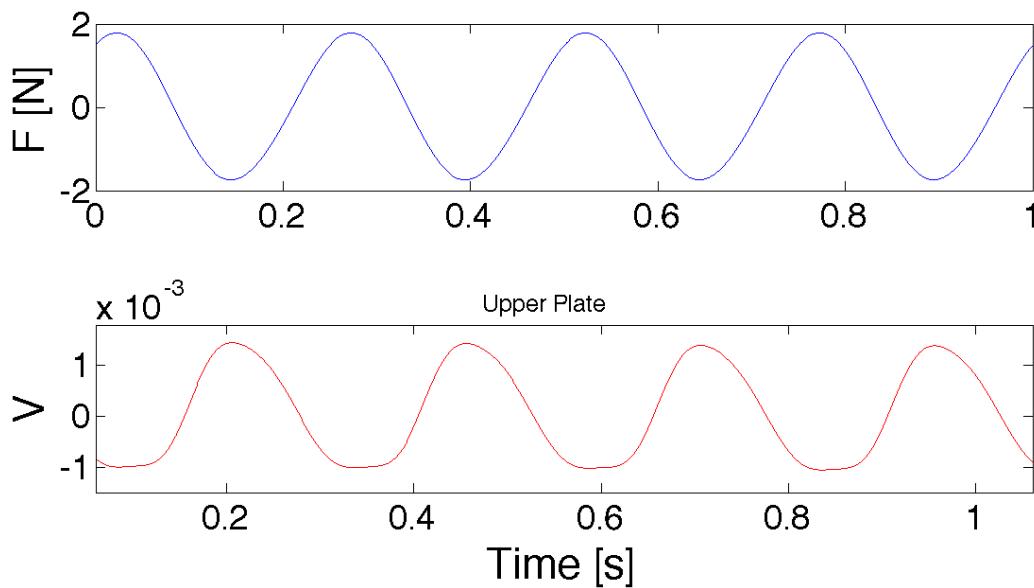
Figure 6: Characterization of an OCMFET for pH sensing. a) Transfer characteristics performed while the sensing area is exposed to buffer solutions at different pH. It is noticeable the gradual switching on of the transistor going from pH 4 to pH 10 due to the shift of the threshold voltage to a more positive value. b) Device calibration. The V_{TH} has been extrapolated from the trans-chars (three chars for each pH point) and plotted against the pH value as mean and standard deviation. The device shows a typical sigmoidal behavior and a relatively wide linear region (from pH 6 to pH 8). c) I_{DS} VS Time of another OCMFET device. As it can be noticed, the device (despite the current drift, which is mainly due to the bias stress) showed a fast response and a reproducible behavior. d) Raman spectra of pristine Parylene C (black) and plasma activated Parylene C (red). A silicon wafer has been employed as the carrier substrate. The additional band at 1640 cm^{-1} has been assigned to the vibration of the C=O stretching of the carboxyl group. (E) The vibration at 2900 cm^{-1} , related to the CH_2 stretching, decreased after the oxidation process with the related increase of the band at 1640 cm^{-1} [34]. Reprinted from *Organic Electronics*, 48, A. Spanu, F. Viola, S. Lai, P. Cosseddu, P. C. Ricci, A. Bonfiglio, A reference-less pH sensor based on an organic field effect transistor with tunable sensitivity, 188-193, Copyright (2017), with permission from Elsevier.

7.3 PRESSURE AND TEMPERATURE SENSING – ARTIFICIAL SKIN

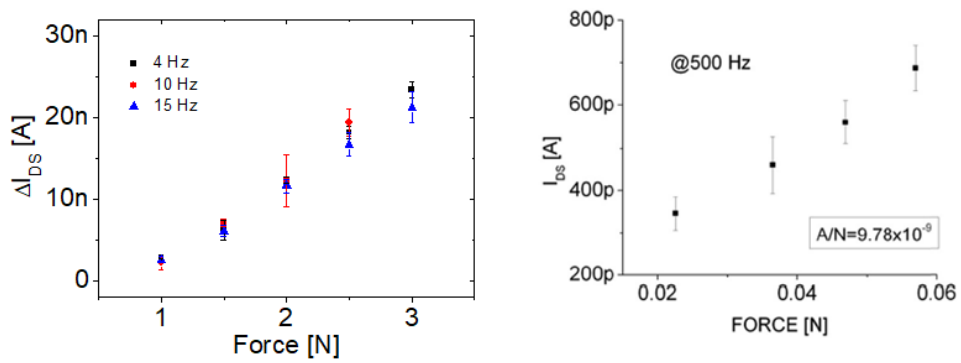
A different approach can be employed for the fabrication of tactile transducers. In this case the sensing area of the OCMFET can be treated with a piezo(pyro)-electric material, see the following figure.



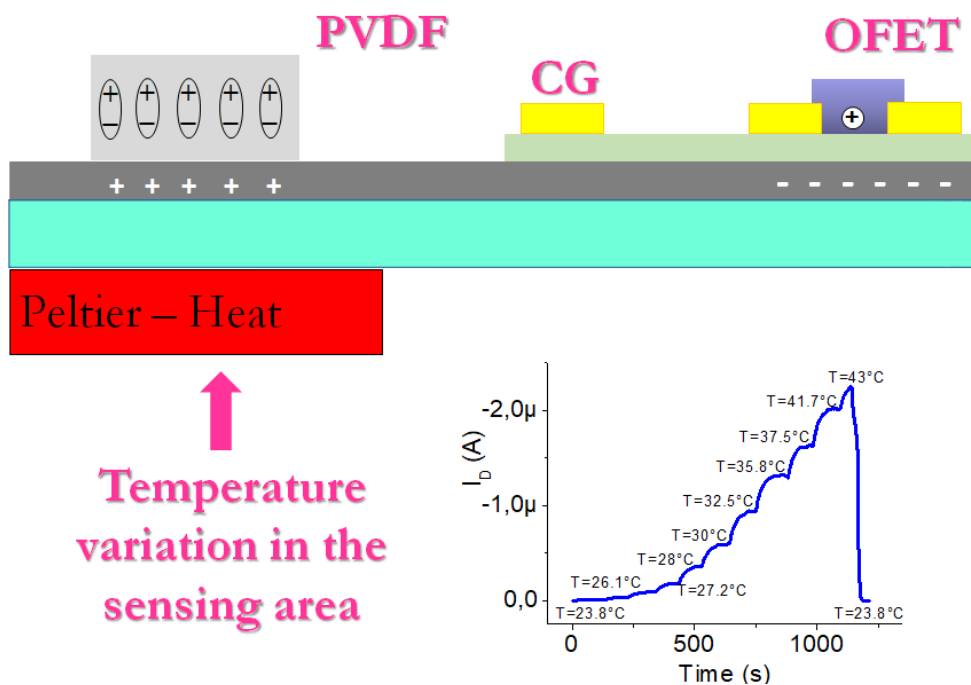
In this particular case, a piezoelectric polymer, namely poly(vinylidene fluoride) (PVDF) was used. The working principle is very easy, if pressure is applied on the sensing area, a charge separation will be induced in the PVDF film, thus leading to a charge redistribution in the floating gate. In other words, this process will induce a variation of the carriers concentration in the active channel, leading to a variation of the output current.



Such phenomenon was employed for the fabrication of force sensors, capable to detect forces as small as 20 mN even at relatively high frequency (500 Hz).



Interestingly enough, such polymer is also pyro-electric, meaning that a similar response can be also obtained when a temperature variation is induced on the PVDF film.



This approach is very interesting because it demonstrate that it is possible, by using a single technology to fabricate at the same time one sensing element capable at the same time to monitor both applied forces and temperature variations, as our tactile transducers are able to do.

8 EFFECT OF MECHANICAL DEFORMATION IN ORGANIC FETs

One of the biggest issues in the fabrication of flexible/wearable devices is that they should be able to withstand continuous mechanical deformation. It is a common thought that conjugated polymer-based devices can be employed for the fabrication of highly flexible electronics. However, despite the intrinsic mechanical flexibility of the most common semiconducting polymers (when deposited in thin films), their electrical stability over continuous mechanical deformation is still a big issue. In fact, there are several reports that demonstrate a pronounced variation of charge transport properties in OTFTs during mechanical stress. Among the possible explanations for the observed variation of the electrical performances in organic semiconductor-based devices during mechanical deformation, it has to be considered at first that the active layer morphological and/or structural properties of the polycrystalline semiconductor film could be severely affected by the applied mechanical stress. Indeed, at the micro-scale, a mechanical stress could lead to a change of the distance between domains in the polycrystalline semiconductor thin film, whereas, at the nano-scale, it could also be possible to induce a variation of the lateral spacing between the molecules, thus affecting the π stacking in the film. In both cases, the immediate consequence should be a variation of the hopping probability for charge carriers, thus leading to a change in the measured carriers mobility.

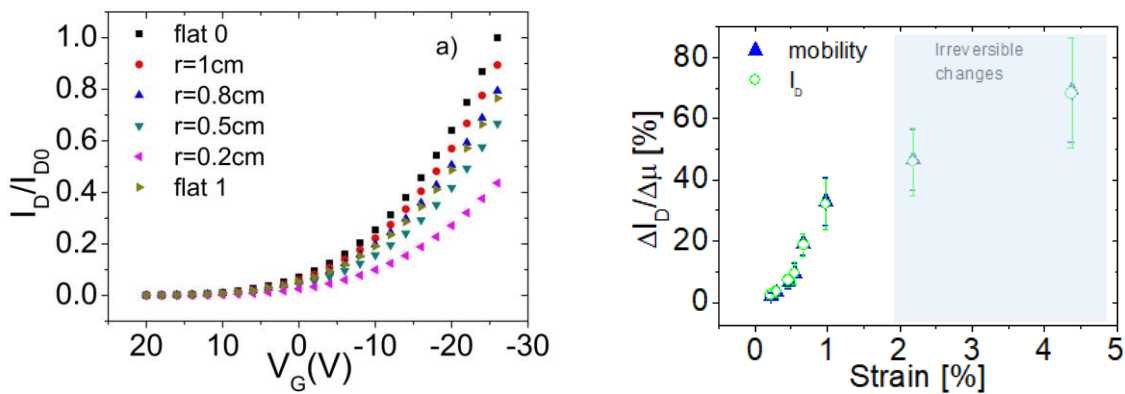
The aforementioned effects have been clearly observed in Pentacene thin films. Pentacene is undoubtedly the most common organic semiconductor, and it has been employed for a large number of different organic sensing applications. Because of its widespread use in organic electronics, the study of its morphological properties is of great interest in the field.

First of all it has to be reminded that by applying a uniaxial deformation to a thin film, induces a surface strain which depends on the applied bending radius, but also on the thickness of the employed substrate.

$$\text{Strain} = \left(\frac{d_f + d_s}{2 * R} \right) \frac{(1 + 2\eta + \chi\eta^2)}{(1 + \eta)(1 + \chi\eta)} \quad \longrightarrow \quad \text{Strain} = \left(\frac{d_f}{2 * R} \right)$$

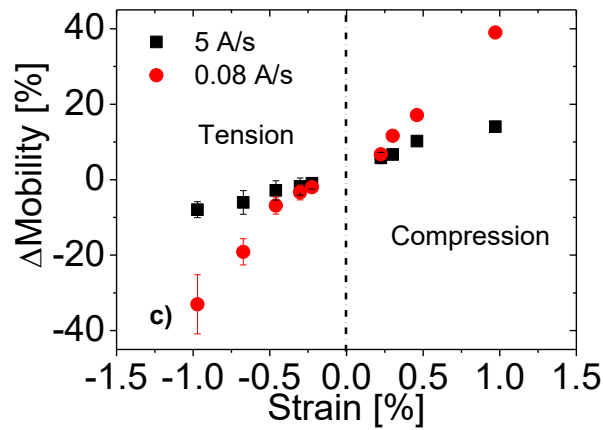
In which d_l and d_s are the thicknesses of the layer and of the substrate respectively, η is d_l/d_s , χ is the ratio between the Young moduli of the layer and of substrate ($\chi = Y_l/Y_s$) and R is the bending radius.

The influence of surface strain on different kinds of organic semiconductors have been widely studied. And it has been demonstrated that by increasing the surface strain, generally a decrease of the output current can be observed as follows.

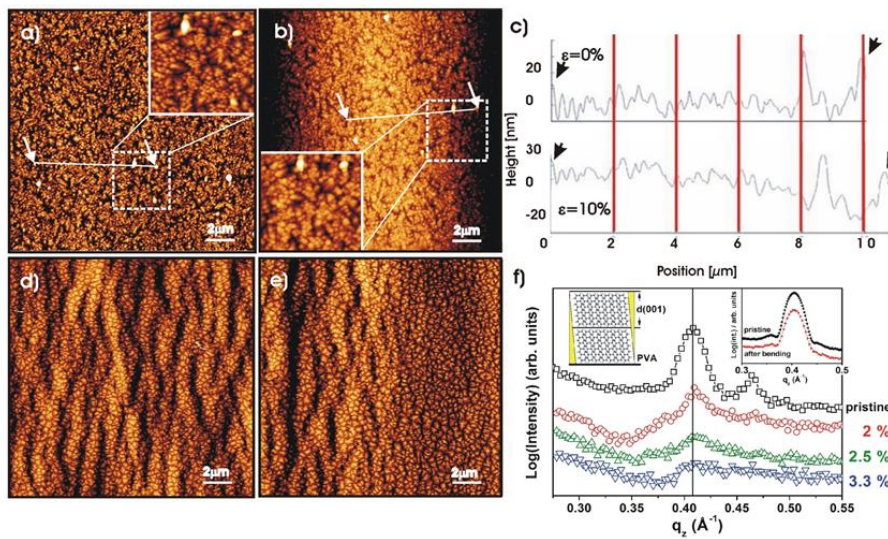


It is worth noting that within a certain range of applied strain, up to 2% the response is linear, reproducible and fully reversible. Moreover current variation is strictly related to mobility variation in the measured transistor, meaning that such effect is related to charge transport mechanism variations induced by the mechanical deformation. Second of all, 2% seems to be the critical surface strain that such devices are able to withstand, after such value, the response is not reversible any more.

The reason why the mobility changes during mechanical stress can be correlated to the fact that during bending, the morphology of the polycrystalline film changes. In particular, when tension is applied the domains distance increases, thus increasing the barrier for hopping, and reducing the mobility. Whereas, when compression is applied the distance between domains decreases thus leading to an increase of mobility.



Such effect was demonstrated by recent studie, where AFM imgaes and XRD analysin showed that no strcutral defomration in induced by such small applied surface strain, whereas, on the contrary, a clear, reversible, modification of the active layer morphology can be observed.



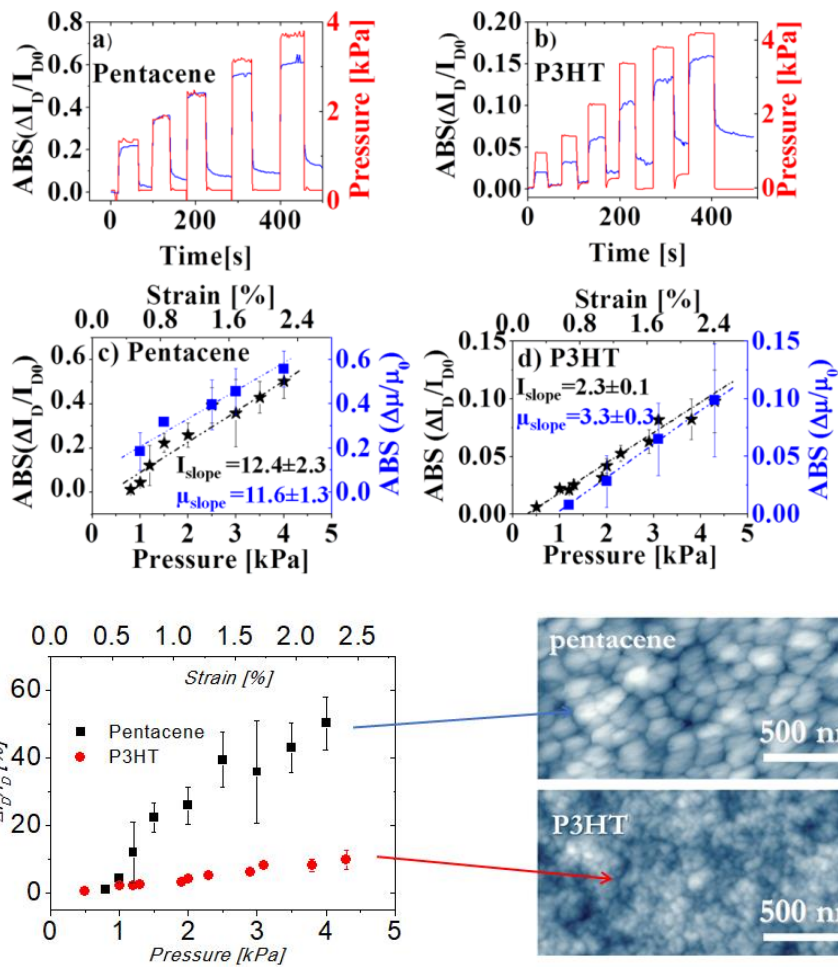
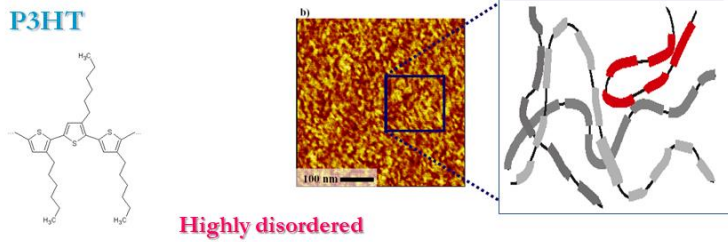
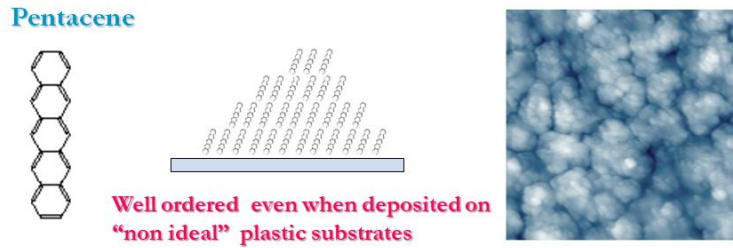
Response is more related to MORPHOLOGICAL CHANGES

Pentacene film properties are not permanently affected by mechanical deformation

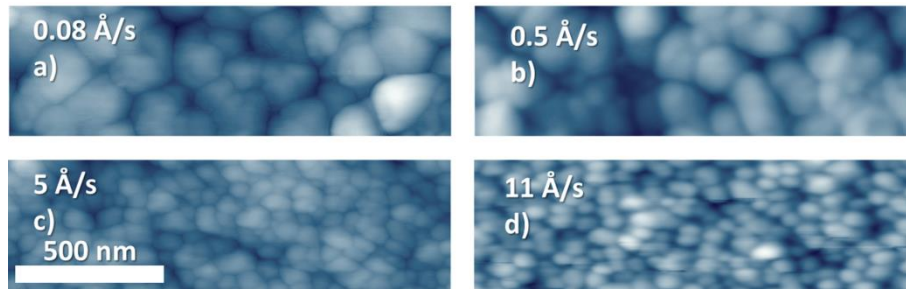
Moreoevr it was also noticed that after 2% of surface strain some cracks starts forming and propagating only in the electrodes regions, which seems to be the cause for the observed failure of the devices in this range of deformations.

Considering that all these effects are related to morphological changes in the active layer, one can think that by changing material, with different morphological features,

more intentionally changing the morphology of the active layer, by changing the deposition technique.



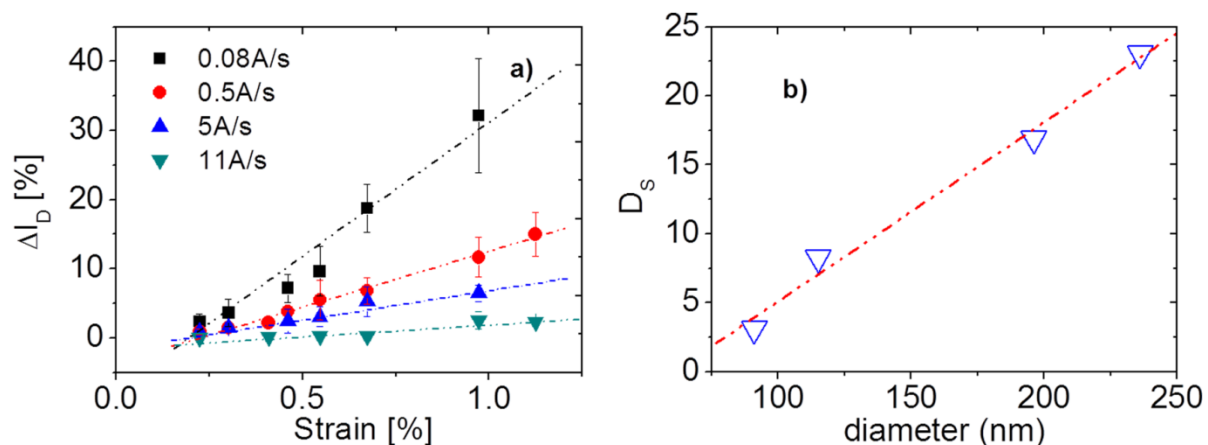
In particular, the response of this organic semiconductor to mechanical stress has been correlated to different morphologies of the Pentacene thin film, which can be obtained by simply varying its deposition rate. In fact, as can be observed in Figure, an increase in the deposition rate leads to a visible decrease of the average grain dimension into the deposited film.



AFM micrographs of different Pentacene films, deposited at different deposition rates

Interestingly enough, it has also been found that such morphological features strongly influenced the response of the devices to mechanical deformation. As can be observed in the following figure, increasing the applied mechanical strain on the active layer, leads to a clear decrease of the devices output current. This phenomenon has been observed in all the different sets of devices. It is very important to highlight that within this range of mechanical stress, the current variation is linear (with respect to the applied strain), fully reversible and reproducible, meaning that such an approach could potentially be used for the fabrication of reliable flexible strain sensors. Moreover, it can also be observed that as the average dimension of the pentacene grains diminishes, the response to mechanical deformation, although still present, diminishes as well.

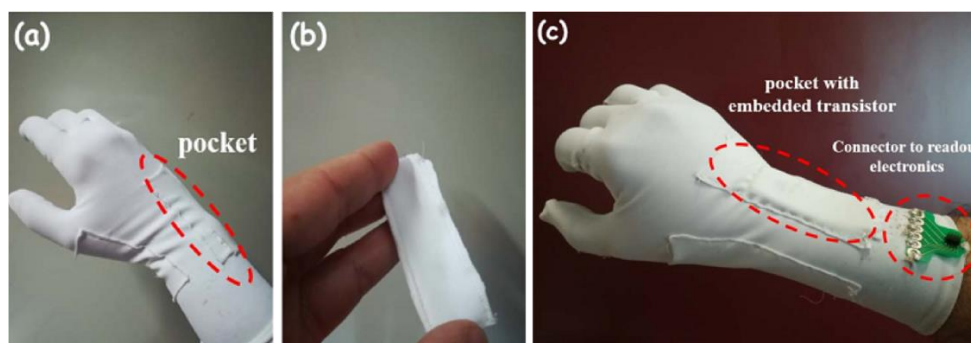
In other words, the sensitivity to mechanical deformation in such systems could be very nicely controlled by simply tuning the intrinsic morphological feature of the active layer, so that highly sensitive devices can be fabricated using semiconductors with higher grain dimensions, whereas almost insensitive devices can be obtained by simply making them smaller.



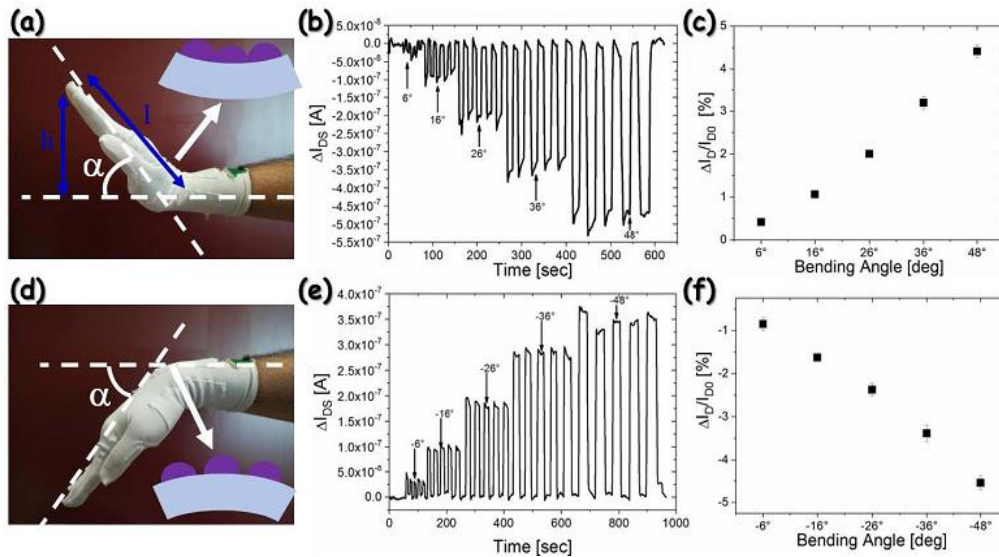
Sensitivity variation vs strain (a) in the four different sets of devices and correlation between sensitivity and grain dimensions (b)

The interesting point here is that highly sensitive strain sensors can be easily fabricated onto flexible plastic substrates, and easily integrated into clothes for the realization of smart wearable mechanical sensors. Using this idea, a fabrication process for the realization of a sensorized glove that can be used for monitoring the wrist movements has recently been developed.

This “smart glove” was fabricated using elastane (Lycra®). A small pocket was fabricated on the glove in correspondence of the wrist in order to accommodate the strain sensors. The OFET is further embedded into a Lycra® pouch to prevent any damage during insertion/extraction in the glove pocket. Interestingly enough, this makes the glove re-usable, while OFET sensors may be easily substituted if damaged. Different angle values, from 6° to 48°, were considered, in order to evaluate different kind of applications in the field of occupational health, such as the monitoring of hands motion of workers of assembly lines.



Pictures of the sensing glove: (a) the glove without sensors, where the position of the pocket is highlighted; (b) the Lycra® pouch where the OFET sensor is inserted; (c) glove provided with sensor (inserted in the pocket) and connector.



a and d) Setup for sensor test upon wrist flexion and extension, (b and e) absolute current variation recorded in real-time for a device biased in the saturation regime upon the application of different extent of wrist flexion and extension; (c and f) average percentage current variation as a function of the given deformation.

9 SOLAR CELLS

Many solar technologies exist with varying degrees of development, and organic solar cells are one of the newer classes of these technologies. The most commercially available solar cell technologies can be divided into two main groups: crystalline and multicrystalline silicon and inorganic thin films. After these two main groups, there are several emerging technologies that have not yet seen broad commercial availability but are still being heavily investigated in the laboratory for future application, including GaAs, concentrator, dye-sensitized, and organic thin-film solar cells.

9.1 CRYSTALLINE AND MULTICRYSTALLINE SILICON

Solar cells based on crystalline and multicrystalline silicon are by far the most developed and produced of all the solar cell technologies and currently account for ~80% of the solar cell market. Despite the fact that silicon is not the most convenient material for the fabrication of photovoltaic devices, it still represents the driving force as silicon based electronics was already largely developed when the first photovoltaic concepts were developed. In inorganic solar cells, a photon is absorbed to generate a free hole and electron that are separated and collected to generate current. Recombination of the carriers before collection, which leads to losses, can be reduced by using high-purity silicon and by applying processing techniques and device structures made possible by the deep understanding of the physics in silicon. Furthermore, the optical absorption spectrum of silicon is well matched to the solar spectrum for solar cells based on a single material. While there are concerns about the supply of silicon wafers going into the future, the widespread availability of silicon from the integrate circuit industry has also contributed to the success of silicon solar cells. Power conversion efficiencies, which define the percent of incoming light power converted into electrical power, up to 25% and 20.4% have been demonstrated in crystalline and multicrystalline silicon solar cells, respectively.

While silicon is by far the leading solar cell technology, there are still many areas for improvement either with advances in silicon or with other material systems. First, high-purity silicon is generally expensive and slow to grow. Moreover, silicon is an indirect band-gap semiconductor, therefore it has a weaker absorption compared to

other semiconductors, thicker layers of silicon are generally required compared to other materials. For these and other reasons, the silicon alone accounts for nearly 50% of the cost of a completed solar module. To circumvent some of these limitations and potentially achieve lower costs per produced power, technologies are also being developed that can use less material either by having thinner active layers based on thin films or smaller active layers with light from a large area concentrated onto the small cell.

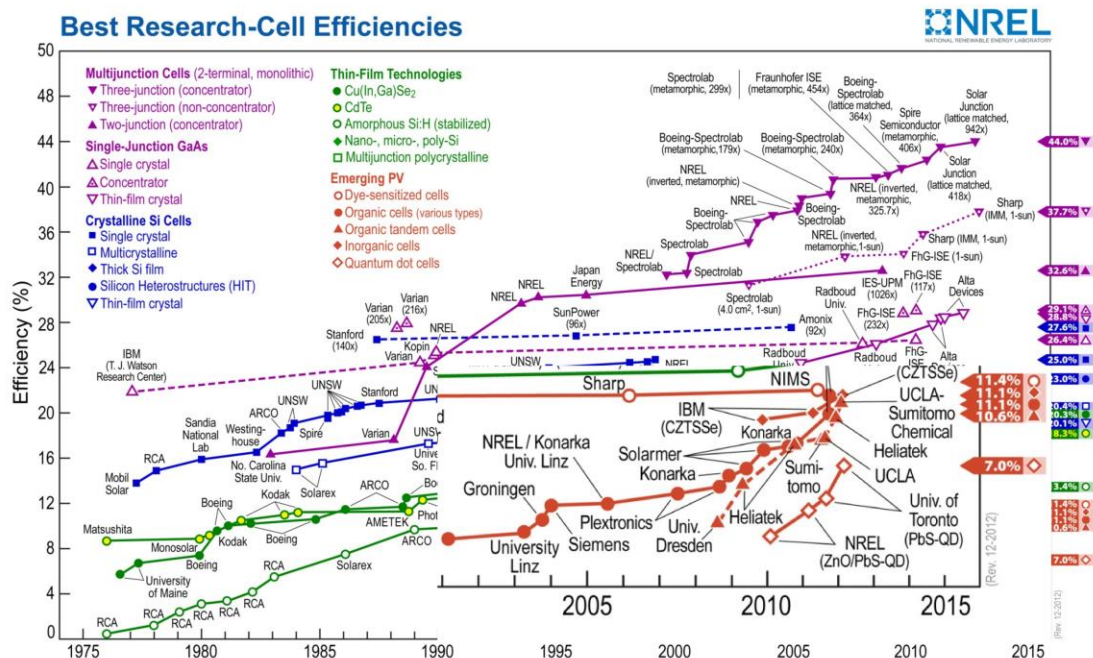
9.2 INORGANIC THIN FILM

Inorganic thin-film solar cells are the basis for nearly all of the presently available commercial solar cells that are not based on crystalline and multicrystalline silicon. Thin-film solar cells attempt to reduce the expensive cost of wafers in silicon cells by using thin films of semiconductors that are usually deposited onto a supporting substrate. The active layers are only a few microns thick but can still absorb significant amounts of light because of strong absorption in the materials. More impurities in the semiconductors can be tolerated since charges have a shorter distance to travel through the thin films. Deposition and processing of thin-film materials also uses lower temperatures compared to silicon. Lower active material volume, purity, and processing temperatures can all lead to lower cost per area for thin-film solar cells, though it generally comes with a tradeoff of efficiency relative to crystalline and monocrystalline silicon. The net effect is a cost per Watt that is competitive with silicon. The leading material platforms for inorganic thin-film cells are amorphous silicon (a-Si), Cu(InGa)Se₂ (CIGS), and CdTe with highest efficiencies of 10.1%, 19.4%, and 16.7%, respectively.

9.3 EMERGING TECHNOLOGIES

Numerous other solar cell technologies exist that are still not widely available commercially. The highest efficiencies have been demonstrated in cells based on GaAs for both single and multijunction devices. Multijunction solar cells use multiple layers that are tailored to more efficiently convert different portions of the solar spectrum based on the band gap of the layers. However, GaAs solar cells have generally been

limited to space applications because of their higher cost. The high cost of high efficiency cells can potentially be offset by concentrating a large area of sunlight onto a solar cell with a small area. Concentration can produce a large amount of power with only a small amount of semiconductor. Furthermore, higher efficiencies can be obtained under concentrated light compared to the standard one sun illumination. Efficiencies of 41.6% have been obtained in multijunction solar cells under concentrated sunlight. However, concentrator systems are more complex because of the additional hardware for focusing light, tracking of the sun, and cooling the cell. Two other technologies that have been garnering significant attention are based on organic materials.



Dye-sensitized solar cells use an organic dye coating a porous electrode with high surface area to absorb light. Efficiencies of up to 11% have been achieved for dye-sensitized solar cells; however, the use of a liquid electrolyte in the cells is presently a source of reliability issues. Another organic technology is thin-film solar cells based on solid-state organic semiconductors. Organic semiconductors can have their chemical and electrical properties tailored in numerous ways by modifying the chemical structures and can allow for new processing methods. Organics have great potential for light-weight, flexible devices fabricated with high-throughput processes from low-cost materials in a variety of colors. However, organic semiconductors are

still a relatively young field, and the highest efficiencies are only around 8% for the very best organic thin-film cells.

9.4 WORKING PRINCIPLE

When light shines on a semiconductor (band gap E_g) some of the photons having an energy higher than the band gap of the material are absorbed from (energy $h\nu \geq E_g$), in this case, an electron-hole pair is generated, the other photons (energy $h\nu < E_g$) freely pass through the material. Let's call this electron-hole pair exciton. The two charge carriers are not free to move, on the contrary they are bound together by a coulomb attraction force that generally varies from material to material.

In order to obtain a current, such charges must be separated. This can be done by means of an electric field which can be applied or intrinsically be present due to the device architecture.

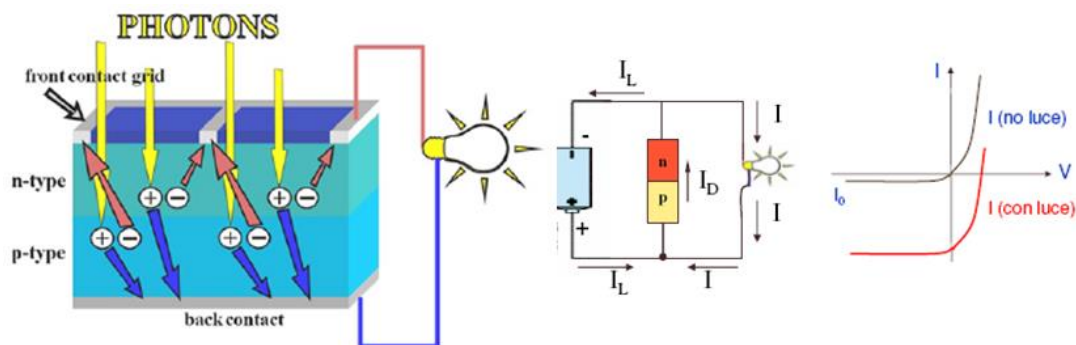
Among the different approaches that can be employed to get this separation done, the employment of heterojunction, a p-n junction is still one of the most used one. In this case the interface potential locally created by the p-n junction is enough to break the exciton and create two free charges, one electron and one hole. Such charges will then be transferred separately in the two device regions and eventually reach the external circuit.

If there is no light shining on the solar cell, the behavior is identical to what is seen in the normal p-n junction

When light is shining on the device, we have two current contributions,

- dark current density J_D
- photoinduced current density J_L

this phenomenon can be modeled as a current generator, in parallel with the diode



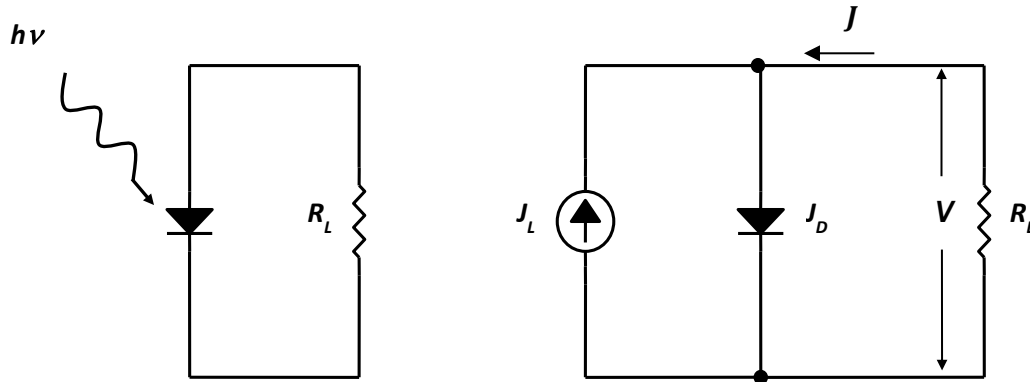
Total current density J is the difference between the dark current J_D and photogenerated current J_L :

$$J = J_D - J_L$$

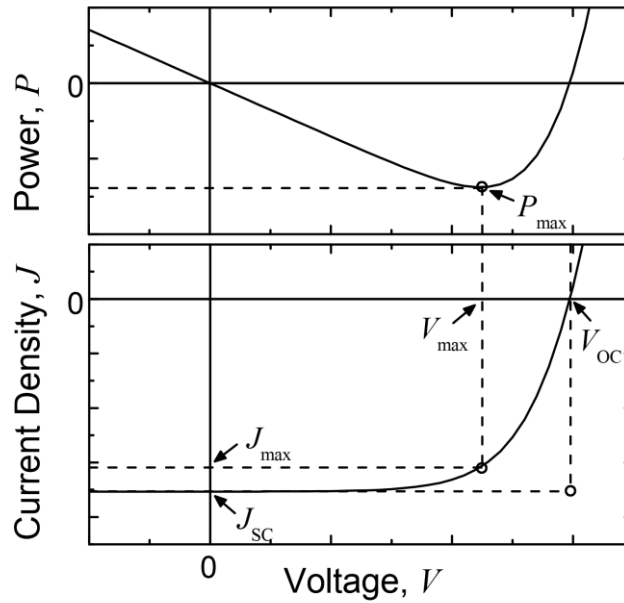
$$J_D = J_0 \left[e^{qV / \eta KT} - 1 \right]$$

$$J_L(\lambda) = J_n(\lambda) + J_p(\lambda) + J_{dr}(\lambda)$$

where $J_n(\lambda)$ and $J_p(\lambda)$ two contribution to the current in the two regions n and p whereas $J_{dr}(\lambda)$ takes into account the charges generated in the depletion region



When measured in the dark, the current-density vs. voltage (J - V) characteristics of most efficient inorganic and organic solar cells resemble the exponential response of a diode with high current in forward bias and small current in reverse bias. Shining light on a device generates a photocurrent in the cell in addition to the diode behavior, and the J - V characteristic under illumination is ideally the superposition of the dark characteristic and the photocurrent. The J - V characteristics of an ideal device can be described by the Shockley equation with an additional photocurrent term. Note that, the photogenerated current is an inverse current that has to be subtracted from the diode current.

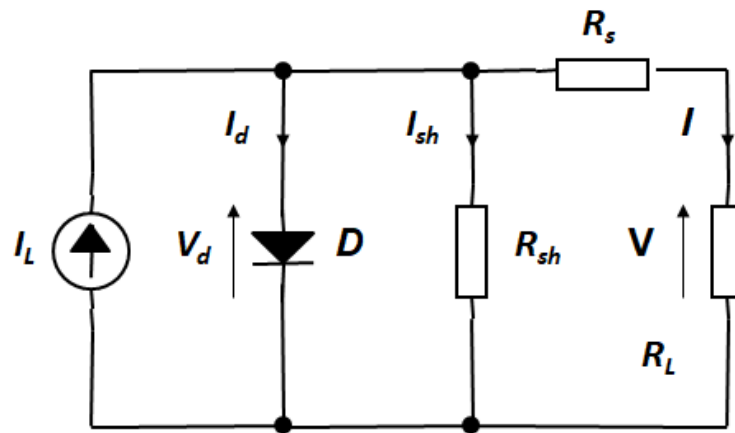


The previous Figure depicts the J - V plot for an ideal solar cell in the region of power generation. Power density, the product of voltage and current density, versus voltage is also plotted, and negative power indicates power generation.

We should also take into account some possible parasitic effects that could affect the performances of a solar cell device.

- Series resistance, it is a resistance in series with the two electrodes and it is generally due to ohmic drops at the contacts
- Parallel resistance (*shunt*) R_{sh} short circuits or leakage current through the device due to defects. In other words, some defects can create a low resistance path throughout the cell.

If we take these two effects into account the real model becomes the following one:

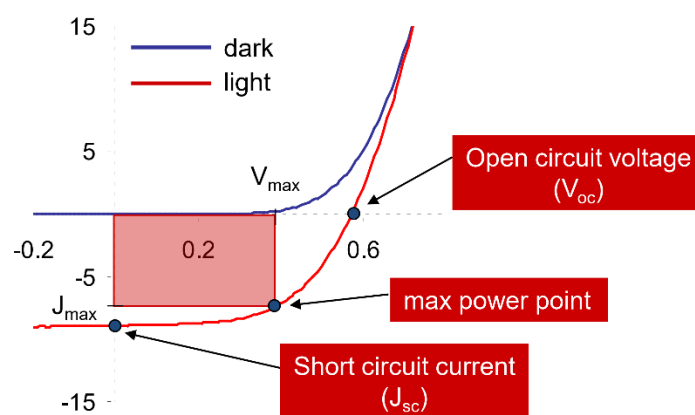


And the current expression changes into the following:

$$I = \frac{I_L - V/R_{sh}}{1 + R_s/R_{sh}} - \frac{I_0}{1 + R_s/R_{sh}} \left[e^{\frac{q(V+R_s I)}{\eta K T}} - 1 \right]$$

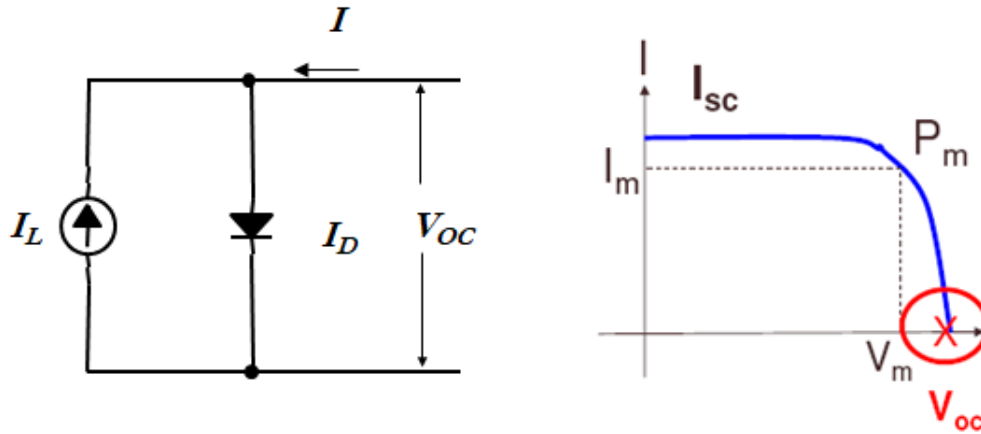
Where, I_0 diode reverse current, η ideality factor, q electron charge I_L photogenerated current.

The most discussed performance parameters that can be found from the J-V curve of a device under a known illumination source are open-circuit voltage (VOC), short-circuit current density (JSC), fill factor (FF), and power conversion efficiency (η).



9.5 OPEN-CIRCUIT VOLTAGE

The open-circuit voltage V_{OC} is the voltage across the solar cell when $J = 0$, which is the same as the device being open-circuited. Because $J = 0$ and power is the product of current and voltage, no power is actually produced at this voltage. However, the V_{OC} marks the boundary for voltages at which power can be produced.



$$V_{OC} = \frac{\eta KT}{q} \ln\left(\frac{I_L}{I_0} + 1\right)$$

$$V_{OC} = \frac{\eta KT}{q} \ln\left(\frac{I_L - V_{OC} / R_{sh}}{I_0} + 1\right)$$

9.6 SHORT-CIRCUIT CURRENT

Similar to V_{OC} , the short-circuit current density J_{SC} is the current density when $V = 0$, which is the same conditions as the two electrodes of the cell being short-circuited together. Again, there is no power produced at this point, but the J_{SC} does mark the onset of power generation. In ideal devices, the J_{SC} will be the same as the photocurrent density J_{pl} . Although J_{SC} is technically a negative number with the conventions used J_{SC} values will focus primarily on the magnitude of the value and be treated as a positive number, *e.g.*, a higher J_{SC} corresponds to a higher J_{pl} .

$$I_{sc} = \underbrace{\frac{I_L}{1 + \frac{R_S}{R_{sh}}}}_{I_L - I_{sh}} - \underbrace{\frac{I_o / \phi_{PL}}{1 + \frac{R_S}{R_{sh}}} \left(e^{\frac{IR_S}{\eta kT/q}} - 1 \right)}_{I_D}$$

In other words, we can split the current into two contributions:

- Photogenerated current (excitons separated per second) minus the current in the shunt R_{sh} (I_{sh})
- Current flowing in the diode D (I_D)

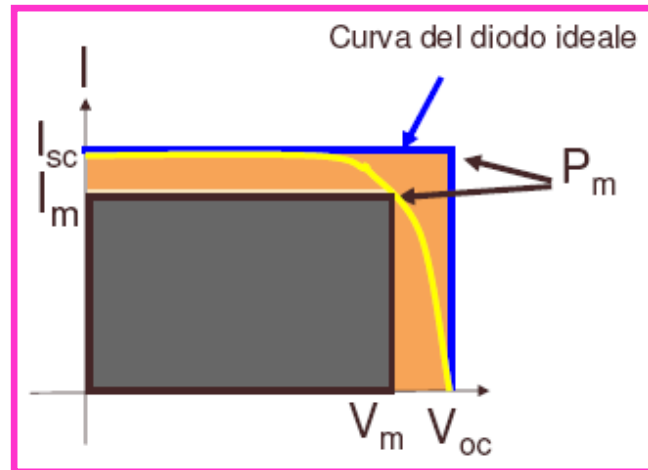
$$I_{sc} = I_L - I_{sh} - I_D$$

Where, I_{sc} is the highest current that can be obtained by a solar cell

9.7 FILL-FACTOR

While V_{OC} and J_{SC} mark the boundaries of power production in a solar cell, the maximum power density produced P_{max} occurs at the voltage V_{max} and current-density J_{max} where the product of J and V is at a minimum (or maximum in absolute value), as shown in Figure. Because of the diode behavior and additional resistance and recombination losses, $|J_{max}|$ and V_{max} are always less than $|J_{SC}|$ and V_{OC} , respectively. The fill factor FF describes these differences and can be represented as the ratio between the area given by the maximum power rectangle and the area of the rectangle given by V_{OC} and I_{SC} , and it is defined as:

$$FF = I_m V_m / I_{sc} V_{oc}$$



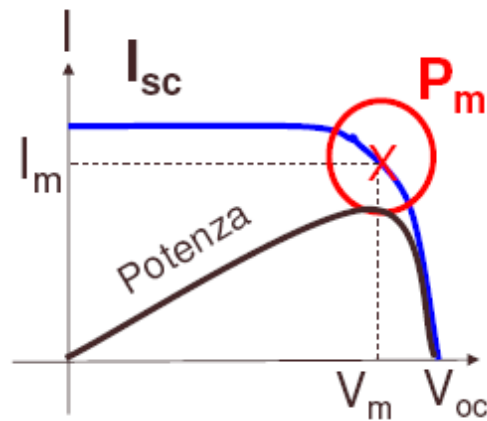
The higher the FF the more the solar cell can be approximated to a constant current generator with the maximum given voltage. In other words, the higher the FF the higher produced power.

9.8 POWER CONVERSION EFFICIENCY

The most discussed performance parameter of a solar cell is the power conversion efficiency η and is defined as the percentage of incident irradiance IL (light power per unit area) that is converted into output power. Because the point where the cell operates on the J - V curve changes depending on the load, the output power depends on the load. For consistency, the maximum output power is used for calculating efficiency. In equation form, efficiency is written

$$\eta = P_{\max} / P_{\text{inc}}$$

Where $P_{\max} = I_m V_m$ maximum power given by the device P_{inc} incoming power, due to incoming radiation



The power given by the cell increases with voltage until the P_m point, afterwards it decreases. Considering also the FF:

$$\eta = I_{sc}V_{oc}FF/P_{inc}$$

This form clearly shows that FF, J_{SC} , and V_{OC} all have direct effects on η . Furthermore, the area used to calculate J can affect η and should include inactive areas that are integral to the solar cell, such as grids and interconnects, when calculating efficiency for large area devices or modules. Power conversion efficiency is important since it determines how effectively the space occupied by a solar cell is being used and how much area must be covered with solar cells to produce a given amount of power. Power conversion efficiency is also very dependent on the power and spectrum of the light source since solar cells do not absorb and convert photons to electrons at all wavelengths with the same efficiency. To draw comparisons between various solar cells, a standard spectrum must be chosen for the calculation of η . Although the spectrum of the sunlight at the earth's surface varies with location, cloud coverage, and other factors, the AM1.5 G spectrum is the most commonly used standard spectrum for measuring and comparing the performance of photovoltaics that are intended for outdoor use. Because of difficulties recreating this exact spectrum in the laboratory with standard lamps, power conversion efficiency measurements must often be corrected based on the external quantum efficiency.

9.9 SPECTRAL RESPONSE

Conversion efficiency between incoming photons into current considering the dependance of I_{sc} from incoming radiation (which varies with the wavelength)

$$SR(\lambda) = \frac{I_{sc}(\lambda)}{\phi(\lambda)}$$

where ϕ light intensity per Area (W/m^2), I_{sc} short circuit current

9.10 EXTERNAL QUANTUM EFFICIENCY

The external quantum efficiency (EQE) of a device is the fraction of incident photons converted into current and depends on wavelength. One reason for the wavelength dependence is that the absorption in the active layers is a function of wavelength. Another reason, especially in inorganic solar cells, is that the location where a photon is absorbed in a device can also affect the probability of the resulting charges being collected or recombining and being lost. The short-circuit current density expected under a light source can be estimated from the EQE and the spectral irradiance of the light source by integrating the product of the EQE and the photon flux density. For the standard AM1.5 G spectrum, the calculation is:

$$EQE = \frac{\text{numero di elettroni nel circuito esterno}}{\text{numero di fotoni incidenti}}$$

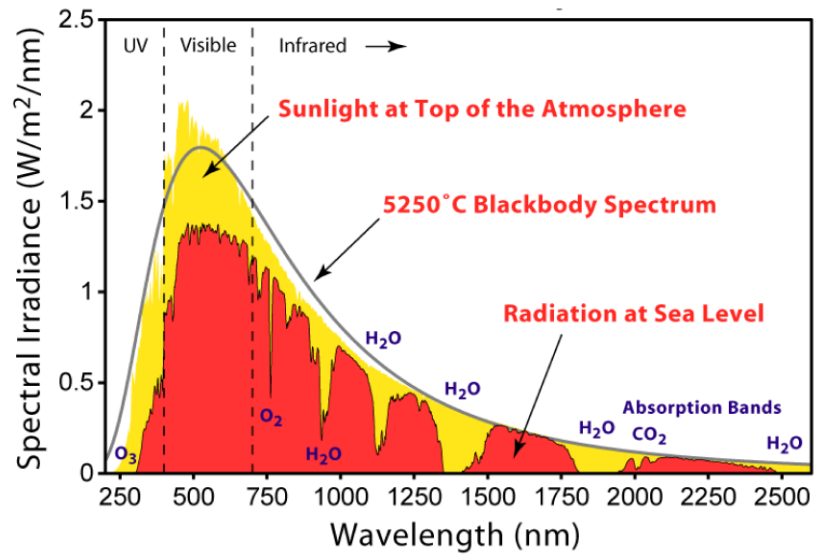
If the spectral response is known, EQE can be derived as follows, considering that $E_p = hc/\lambda$

$$EQE(\lambda) = SR(\lambda) \cdot \frac{hc}{q\lambda}$$

To certify reliable comparison of different solar cells standard test conditions are used. Thereby, incident solar power density (P_o) standards have been defined. National American Society for Testing Materials (ASTM) standard E948 and International Electrotechnical Commission (IEC) standard 60904-1 specifies a set of common test conditions and methods to measure the electrical performance of photovoltaic cells. They are named the Standard Testing Conditions (STC) and are defined as follows:

1. Temperature of the device under test (DUT) is to be $25^\circ \pm 1^\circ C$;
2. Spectral distribution of the light is to be $AM1.5 \pm 25\%$;
3. Irradiance measured at the plane of the solar cell is to be $1 \text{ sun} \pm 2\%$

The spectrum standard is the AM1.5 which can be approached by commercial solar simulators. AM is the air mass coefficient defined by direct optical path length through the Earth's atmosphere, expressed as a ratio relative to the path length at the zenith. AM1.5 atmosphere thickness corresponds to a solar zenith angle of $z = 48.19^\circ$. Therefore, AM1.5 is useful to represent the overall yearly average for mid-latitudes.



10 ORGANIC SOLAR CELLS

Thin-film solar cells based on organic semiconductors are interesting for several reasons. For one, the electrical and chemical properties of organic semiconductors can be tailored by modifying the chemical structure of the compounds in endless combinations. Though specific design rules are still under investigation, the potential for tailoring molecules to different applications is great. Furthermore, the organic molecules have the potential to be cheaply synthesized without significant concern on the limit of raw materials. Next, organic semiconductors can be deposited in a number of low temperature and high-throughput ways, such as evaporation and solution processing, that can lower manufacturing costs. Because organic materials can have high absorption coefficients, a layer of only a few hundred nanometers is often enough to absorb a large fraction of light in the material's absorption spectrum. The use of such thin layers reduces the amount of active material needed and also makes light-weight and flexible devices possible. For these and other reasons, organic solar cells have gained significant attention.

The working principle of organic solar cells is basically the same of the inorganic ones. However, a very important difference must be taken into account.

At this point, it is worthwhile to note that, in contrast to inorganic semiconductors, the term donor and the term acceptor are used in relation to organic solar cells. Thus, a donor can describe a molecule (material) which transfers an electron to another molecule. Therefore, an acceptor can describe a molecule (material) which receives an electron from another molecule. Another important difference of organic versus inorganic semiconductors is the existence of the exciton. The exciton is an electron-hole pair, where electron and hole are bound by Coulomb force:

$$F_C = \frac{1}{4\pi\epsilon\epsilon_0} \frac{q^2}{r^2}$$

where r is the distance between the two charges q , ϵ_0 is the vacuum permittivity and ϵ the permittivity of the organic medium.

In organic semiconductors the formed excitons are Frenkel type, whereas in inorganic semiconductors (like crystalline silicon) they usually are Wannier Mott-type. The latter

have a small binding energy, in the range of 1 to 40 meV, and are often thermally dissociated at room temperature, which is not the case in a Frenkel exciton where the binding energy is ten times greater (up to 300 meV). Due to the high dielectric constant the Wannier Mott exciton has a radius larger than the lattice spacing; in contrast, Frenkel excitons tend to be small, of the same order as the size of the unit cell because of the low dielectric constant values found in organic semiconductors. This aspect is of essential importance to describe the operation of organic solar cells, as discussed below.

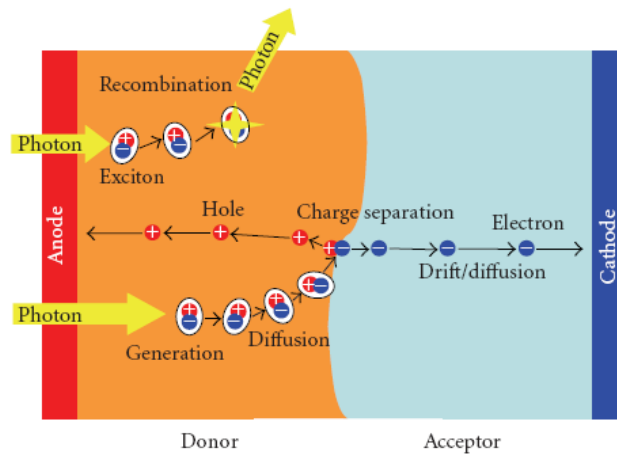
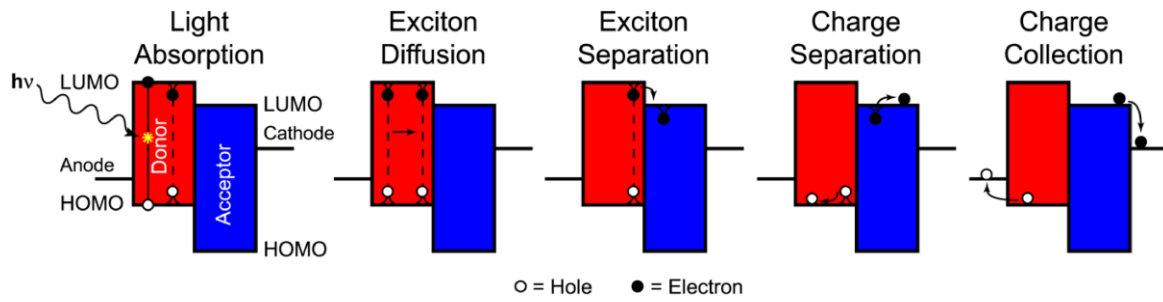
Due to the low dielectric constant permittivity in organic materials (~ 3) photoexcitation leads to a strongly bound exciton, which needs (in the case of solar cells) to be dissociated into free electrons and holes (carriers).

Therefore, excitons in an OSC require a very high electrical field in order to get separated. Such field can be localized in the electrode/semiconductor interface or in a bulk heterojunction between donor and acceptor materials. However, due to the very high concentration of trap sites, which is not the case in inorganic SCs, the recombination process is very active.

Once the exciton is dissociated, electron and hole, diffuse up to the corresponding electrodes, where they are collected and giving rise to an electric current. Exciton dissociation is energetically favourable when the energy of binding exciton (EEX) is larger than the difference between ionization potential of the donor (IPD) and the electron affinity of the acceptor (EAA).

$$E_B^{exc} > IP_D - EA_A$$

If the difference is not sufficient the exciton will recombine (geminate recombination) without contributing to the photocurrent. Exciton dissociation can also occur at the organic semiconductor/metal interfaces or in presence of impurities (e.g. oxygen). Organic solar cells are generally fabricated in thin film form of donor (D) and acceptor (A) materials, with suitable energy levels matching, between two electrodes. One electrode must be transparent to allow the incident light reaching the photoactive materials. The conversion of the photon energy into free charge carriers in an organic solar cell could be explained in the follow simplified steps



C

10.1 PHOTON ABSORPTION

This step is similar to that in inorganic photovoltaic devices. And, absorption can occur either in the electron donor (p-type) material or the electron acceptor (n-type) material. The first step in the photovoltaic process consists in the absorption of the light. In most organic solar cell only a small percentage of the incident light is absorbed. Principal reasons are:

- Thickness of photoactive materials: the organic layer is too thin. Low charge carrier mobilities and the low exciton diffusion lengths require layer thickness between 20 and 100 nm. Fortunately, the high optical absorption coefficients (e.g. $> 10^5 \text{ cm}^{-1}$) of organic semiconductors allow that organic solar cells could work with a layer thickness of a few tens of nanometres.
- Semiconductor bandgap too high with typically values about 2 eV. Besides the high absorption coefficient, only a small portion of the incident light is absorbed because of higher bandgap values.

When the electron is excited by the light absorption an exciton is created. For most

organic semiconductors permittivity values (ϵ) lies between 1 and 6 which is quite low compared to the permittivity of inorganic semiconductors (as for instance silicon) which exhibits $\epsilon = 12$. Excitons in inorganic semiconductors are usually of Wannier-Mott type. Their radius is in most cases larger than the lattice spacing and the charges are quasi-free. In contrast, the attractive force between electrons and holes in organic solids, where the exciton is initially localised in one molecule, is much higher and the binding energy is comparably strong. Such strongly bound excitons are called Frenkel excitons

Moreover, in order to absorb the 77% of the incoming solar radiation a semiconductor should have a band gap in the range of 1.1 eV (1100 nm) however the most of organic semiconductors have a band gap around 2.0 eV (600 nm) therefore, the absorption is only around 30%. However, organic materials have much higher absorption coefficients. This means that the device thicknesses can be on the order of ~ 100 nm, as opposed to $\sim 10 - 100$ μm . The spectral response (and, thus, bandgap) will be defined by the molecular absorption modes

10.2 EXCITON DIFFUSION

An exciton is bound electron-hole pair that has a lifetime of ~ 300 ps in common organic semiconductors. This means that it is able to move in space for ~ 10 nm prior to recombination. Because the exciton is charge neutral, it does not respond to any electric fields present in the device, and explore space in a manner similar to that of random walk diffusion. Generally, it requires > 0.3 eV of energy to separate the exciton into two free charge carriers. Therefore, reaching the donor-acceptor interface can be crucial.

Imagine to have a dissociation center at a certain position, the photogenerated excitons should travel into the material in order to reach such point. If the distance is much higher than the diffusion length, recombination process is highly probable, therefore no charge collection can be obtained

The excitonic nature of organic solar cells make them unique relative to inorganic solar cells. The nature of the exciton is related directly to the dielectric constant of the

material. Recall from Coulomb's Law that the force (F) between two charges (q_i) separated by (r) in a medium with dielectric constant (ϵ) can be written as the following

$$F = \frac{q_1 q_2}{4\pi \epsilon \epsilon_0 r^2}$$

Because the dielectric constant of organic semiconductors are ~4x smaller than inorganic semiconductors, the binding force between the electron and hole is greater.

10.3 CHARGE SEPARATION

If the exciton reaches a location in the device where charge transfer will lower the energy of the system, it will transfer the charge. This charge transfer occurs most usefully at the p-type/n-type interface. That is way the p-type material is called the "electron donor" and the n-type material is called the "electron acceptor". In the schematic above, the hole will remain in the electron donor phase and transfer the electron to the electron acceptor phase. This is because the electron wishes to move farther from free vacuum and the hole wishes to move closer to free vacuum.

10.4 CHARGE TRANSPORT

Charges will move through the device due to a combination of a drift (i.e., due to the electric field within the OPV) and diffusion (i.e., because of concentration gradients in the device) currents. Here, we wish to move the hole and the electron through the device without having the charges recombine. There are two classes of recombination.

1. Geminate recombination is where the hole and electron that formed the original exciton recombine after splitting.
2. Non-geminate recombination is where an electron or hole recombines with entities that are not the opposite charge that formed the exciton

Non-geminate recombination can occur for a variety of reasons. For example, the following could occur.

1. A charge could recombine with the large amount of electrons or holes at either of the electrodes.

2. An electron could recombine with a hole that was not part of its excitonic pair.
3. A hole could recombine with an electron that was in a deep level trap.

10.5 CHARGE COLLECTION

If there is a large energy barrier to overcome between the transport level of the semiconducting phase and the work function of the metal contact, there will be a high series resistance in the device. Therefore, we would prefer if the work function energy level of the anode matched the HOMO energy level of the p-type material and the work function energy level of the cathode matched the LUMO energy level of the n-type material.

Sometimes interfacial modifying layers are added to make these junctions more level with respect to energy.

10.6 ARCHITECTURES FOR ORGANIC SOLAR CELLS

Among the many different configuration employed for the fabrication of organic solar cells (OSCs) we will focus our attention on the following three: i) singlayer structure; ii) double layer structure; iii) bulk heterojunction structure.

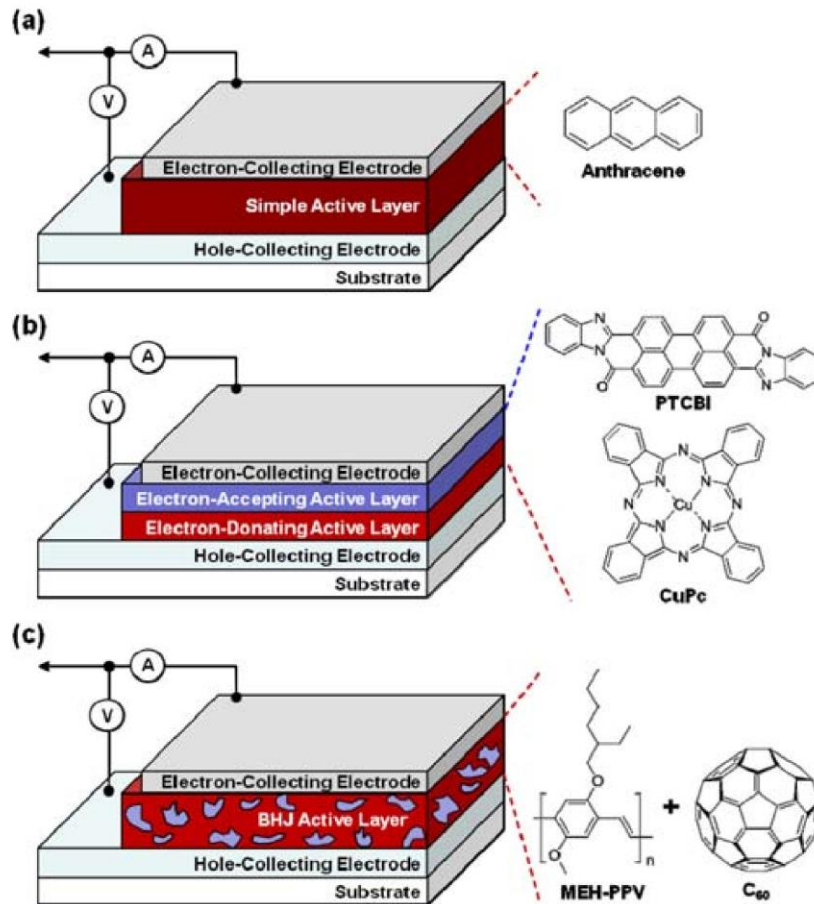
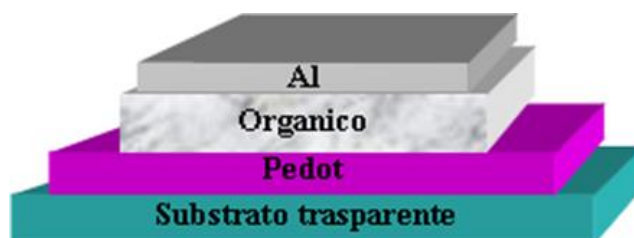


Fig. 1. Three representative device structures for organic solar cells: (a) single active layer, (b) double active layer (p-n junction bilayer), (c) bulk heterojunction active layer. The chemical structures in each device structure show materials that were first used for corresponding device structures.

Single layer structure

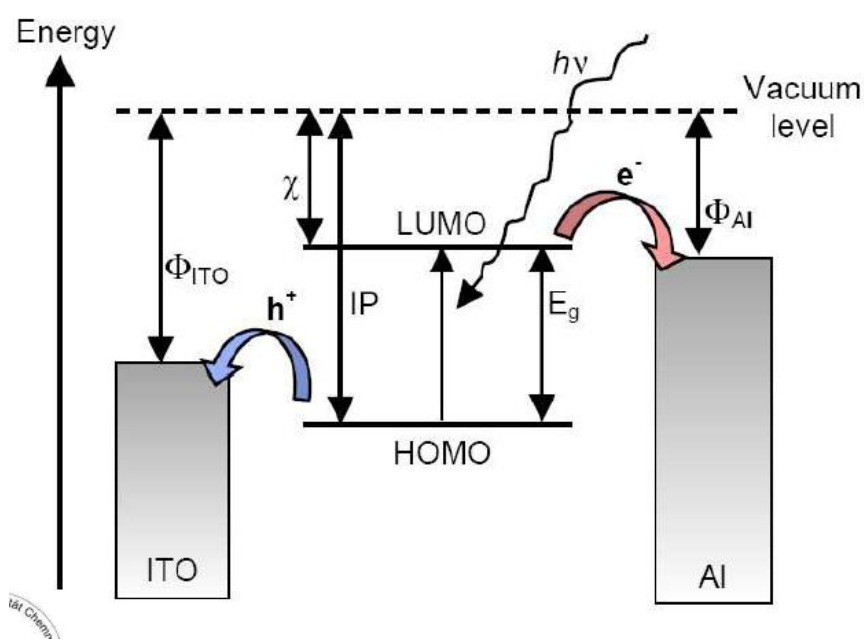
Single layer structures consist of only one semiconductor material between two electrodes. Single layer cells are often referred to as Schottky type devices or Schottky diodes since charge separation occurs at the rectifying (Schottky) junction with one electrode. The other electrode interface is supposed to be of ohmic contact. Holes are generally collected through a high WF, transparent material, typically PEDOT or ITO (Cathode) whereas electrons are collected by means of a low WF material

Aluminum or Calcium (Anode). In this case when an exciton is formed it has to diffuse and reach one of the two electrodes in order for charge separation to happen. If the exciton reach the low WF electrode, electron will find more convenient to be trasferred into it.



It can also happe that the exciton diffuses and reach the high WF electrode, thus allowing one electron the be trasferred into the OS, i.e. a a hole moves from the OS to the metal electrodes breaking the exciton. In this way free charge carriers are generated.

Such structure is simple but the absorption is usually low using a single type of molecule, moreover, since both positive and negative charges travel through the same material, recombination losses are generally high.



Bilayer cell.

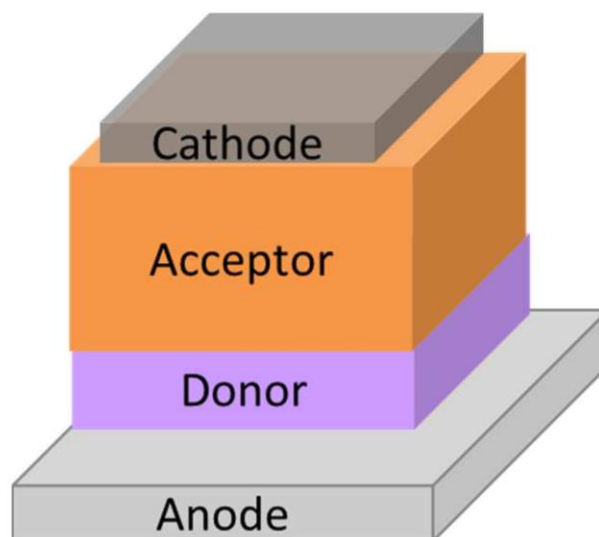
In this case the active layer is made by the deposition of two different films, typically one with low IE and one with a higher IE

- The energetic difference between IE and EA must be sufficiently high to allow charge separation and avoid recombination
- The two materials must have a complementary absorption spectrum, in order to maximise the photogeneration of excitons

It can be done in two ways

- Thermal deposition of two small molecules films
- Deposition of two layers of solution processable materials (orthogonal solvent!!)

This structure benefits from the separated charge transport layers that ensure connectivity with the correct electrode and give the separated charge carriers only little chance to recombine with its counterpart. The principal drawback is the small interface area that allows only excitons to reach it and get dissociated. This architecture has an important limitation which relates to the exciton diffusion length in the organic materials. The exciton diffusion length is dependent on the exciton lifetime and is in the range of 10–40 nm

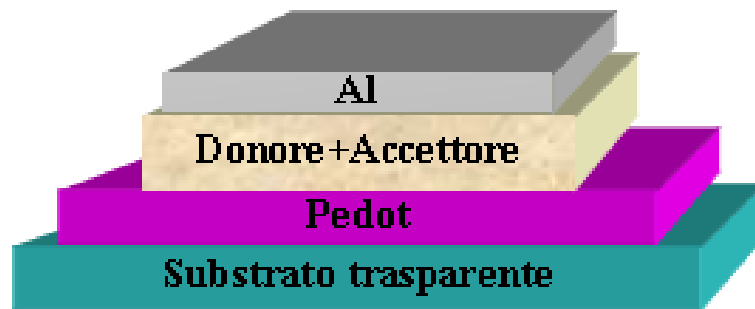


Bulk Heterojunction cell. A mixture of donor and acceptor materials is sandwiched between anode and cathode. The strong point of this type is the large interface area,

allowing high molecular mixing and, therefore, most excitons can reach the D/A interface. This accounts for the intrinsically low exciton diffusion lengths and allows for more generated excitons to be separated into free charge carriers. However, the charges have to be transported to the electrodes via closed and short percolation pathways. Otherwise transport losses by trapping or recombination may occur. Hence, the connectivity with the correct electrode is the big weak point of this structure. As a result, the photocurrent is usually higher in bulk heterojunction than in heterojunction solar cells.

Such mixed layer can be obtained in two ways:

- Coevaporation of the two molecules
- Blend of two solution processable molecules (same solvent)



• Limited exciton diffusion length
➤ “Bulk heterojunction” concept

F. Yang, et. al. *Nature Materials* 4 (2005)

The main idea in this case is to maximise the interface between donor and acceptor molecules, do that exciton dissociation probability can be dramatically increased. On the other hand it i also very important to have a percolating path of the two molecular

species, required for the generated free carriers to be able to reach the cathode and the anode.

Hereafter, a summary of the recent results obtained with the different OSCs configurations is given.

TABLE 1: Best in class solar cells: small molecule-based solar cells.

Donor	Acceptor	η	V_{oc}	FF	IPCE	Reference
CuPc	C60	5.7%	1.0 V	59%	NA	Xue et al. [4]
CuPc	C60	5.0%	0.6 V	60%	64%	Xue et al. [6]
MeO-TPD, ZnPc (stacked)	C60	3.8%	1.0 V	47%	NA	Drechsel et al. [51]
CuPc	C60	3.5%	0.5 V	46%	NA	Uchida et al. [46]
DCV5T	C60	3.4%	1.0 V	49%	52%	Schulze et al. [49]
CuPc	PTCBI	2.7%	0.5 V	58%	NA	Yang et al. [44, 45]
SubPc	C60	2.1%	1.0 V	57%	NA	Mutolo et al. [47]
MeO-TPD, ZnPc	C60	2.1%	0.5 V	37%	NA	Drechsel et al. [51]
TDCV-TPA	C60	1.9%	1.2 V	28%	NA	Cravino et al. [50]
Pentacene on PET	C60	1.6%	0.3 V	48%	30%	Pandey and Nunzi [52]
SnPc	C60	1.0%	0.4 V	50%	21%	Rand et al. [48]

TABLE 3: Best in class solar cells: polymer-polymer (bilayer) solar cells.

Donor	Acceptor	η	V_{oc}	FF	IPCE	Reference
PPV	BBL	1.5%	1.1 V	50%	62%	Alam and Jenekhe [96]
MDMO-PPV:PF1CVTP	PF1CVTP	1.4%	1.4 V	34%	52%	Koetse et al. [95]
M3EH-PPV	CN-Ether-PPV	1.3%	1.3 V	31%	29%	Kietzke et al. [97]
MEH-PPV	BBL	1.1%	0.9 V	47%	52%	Alam and Jenekhe [96]
M3EH-PPV	CN-PPV-PPE	0.6%	1.5 V	23%	23%	Kietzke et al. [97]

TABLE 2: Best in class solar cells: polymer-polymer (blend) solar cells.

Donor	Acceptor	η	V_{oc}	FF	IPCE	Reference
M3EH-PPV	CN-Ether-PPV	1.7%	1.4 V	35%	31%	Kietzke et al. [92]
MDMO-PPV	PF1CVTP	1.5%	1.4 V	37%	42%	Koetse et al. [95]
M3EH-PPV	CN-Ether-PPV	1.0%	1.0 V	25%	24%	Breeze et al. [12]

TABLE 3: Best in class solar cells: polymer-polymer (bilayer) solar cells.

Donor	Acceptor	η	V_{oc}	FF	IPCE	Reference
PPV	BBL	1.5%	1.1 V	50%	62%	Alam and Jenekhe [96]
MDMO-PPV:PF1CVTP	PF1CVTP	1.4%	1.4 V	34%	52%	Koetse et al. [95]
M3EH-PPV	CN-Ether-PPV	1.3%	1.3 V	31%	29%	Kietzke et al. [97]
MEH-PPV	BBL	1.1%	0.9 V	47%	52%	Alam and Jenekhe [96]
M3EH-PPV	CN-PPV-PPE	0.6%	1.5 V	23%	23%	Kietzke et al. [97]

TABLE 4: Best in class solar cells: blends of polymers and fullerene derivatives.

Donor	Acceptor	η	V_{oc}	FF	IPCE	Reference
P3HT	PCBM	5.0%	0.6 V	68%	NA	Ma et al. [114]
P3HT	PCBM	4.9%	0.6 V	54%	NA	Reyes-Reyes et al. [5]
P3HT	PCBM	4.4%	0.9 V	67%	63%	Li et al. [115]
MDMO-PPV	PC ₇₁ BM	3.0%	0.8 V	51%	66%	Wienk et al. [17]
MDMO-PPV on PET	PCBM	3.0%	0.8 V	49%	NA	Al-Ibrahim et al. [116]